# NEURAL RESPONSES TO INJURY: PREVENTION, PROTECTION, AND REPAIR
# Annual Technical Report - Revised
# 1995


**Submitted by**

**Nicolas G. Bazan, M.D., Ph.D.**
**Project Director**


**Period Covered: 20 September, 1994, through 19 September, 1995**


**Cooperative Agreement DAMD17-93-V-3013**


**between**

**United States Army Medical Research and Development Command**
**(Walter Reed Army Institute of Research)**

**and**


**Louisiana State University Medical Center**
**Neuroscience Center of Excellence**


**Volume 2 of 8**

**Revised 1/96**



## Repair and Regeneration of Peripheral Nerve Damage


Project Directors:
Roger Beuerman, Ph.D.
David Kline, M.D.
Austin Sumner, M.D.

# DISCLAIMER NOTICE


**THIS DOCUMENT IS BEST QUALITY AVAILABLE. THE COPY FURNISHED TO DTIC CONTAINED A SIGNIFICANT NUMBER OF PAGES WHICH DO NOT REPRODUCE LEGIBLY.**

# TABLE OF CONTENTS

# INTRODUCTION

The overall focus of this project has been to understand the cellular and molecular biology of neuroma formation as a complication of damage and repair to peripheral nerves. As part of this, a secondary focus has been to establish *in vitro* models of cell lines of fibroblasts from peripheral nerves that can be used to uncover the molecular mechanisms of peripheral nerve fibroblast response to damage and also to their interaction with cell signaling molecules that may be present in the repair process. A third objective has been to understand the origin of pain that accompanies neuroma formation. It has not been known how the cellular developments affect the physiology of the entrapped nerve endings. Electrophysiological and immunohistochemical studies have been carried out on human neuroma tissue to determine how the ion channels change as the neuroma develops.

Peripheral nerve injuries are amongst the most common of injuries that are seen not only in the armed forces where they have a crippling affect on personnel, but also in the general population. In as much as 30 to 40% of patients the outcome of repair is often unsatisfactory and it is characterized by a reduction and a loss of motor function and sensory capability, the origin of this complication to repair, as well as to injury, is the accumulation of cells and extracellular matrix at the site of injury in what is usually called a neuroma. In this study it is hypothesized that the exaggerated healing response is very similar to a fibrotic mechanism that may be seen elsewhere in the body. However, this is complicated by the local cellular environment which may compartmentalize changes, particular cell signaling molecules and cell interactions that are unique to the peripheral nerve, but in this regard it is suggested that growth factors and cytokines are probably of primary importance in this process. It is also hypothesized that the cellular involvement could be altered in order to

provide more normal healing with better functional recovery.

To accomplish these objectives we have worked simultaneously at several different levels. The first has been to understand the cellular mechanisms that may be operating in the mature human peripheral nerve neuroma. This is summarized in the first part of the report, Sections I and II. However, the work from humans indicates that the only growth factor family that is found in any regularity or in large amounts has been basic fibroblast growth factor, as well as the FGF receptor 1. Although extensive searching for a number of other growth factors was carried out, these were found in barely detectable amounts using Western blots or were not found at all. These family of growth factors include acidic fibroblast growth factor, platelet derived growth factor beta beta, transforming growth factor beta 1, as well as important cytokines such as IL-1 and tumor necrosis factor $\alpha$. The absence of either interleukin 1 and tumor necrosis factor $\alpha$ suggests that the mature peripheral neuroma is not characterized as a continuing inflammatory process. It is interesting, however, that the neuroma may be characterized as a poorly vascularized, encapsulated fibrous matrix and this matrix may be slightly acidic and hypoxic due to the lack of vascularity. Associated with this suggestion that the neuroma, which develops uniquely in the proximal part of the nerve stump, is a complex interaction of several cell types including the outgrowing neurites. The work then proceeds with developing a model of the human neuroma in the rhesus monkey. This work has proceeded this past year and the analysis of this tissue has not been completed, however, it is clear that basic fibroblast growth factor is found in the monkey neuroma in abundance as well and also that there is an increase in fibroblast growth factor in the developing neuroma which is in Sections III and IV. Basic fibroblast growth factor receptor, as well as fibroblast growth factor has now been localized in the fibroblast using

double-labeling immunofluorescence, as well as electron microscopic studies. However, there is still a doubt as to the presence of fibroblast growth factor in Schwann cells and that work is continuing.

Next, a question regarding the origin of the cells forming in neuroma was raised, as it has been unclear as to the origin of these cells. Although fibroblasts have many cell and molecular characteristics in common, their precise reaction to stimuli changes depending on the environment and their origin. Thus, in Section V work is under way to determine if fibroblasts and Schwann cells can migrate from proximal nerve into a neuroma and where these locate. This work is continuing with the added feature to determine whether the labeled cells are Schwann cells or fibroblasts and the relative contribution of each and their localization at longer times following the induction of an experimental neuroma.

In Section VI, part of the work has characterized the type of injury that occurs either proximal or distal to the molecular genetic affects or the affects on early immediate gene expression depending on whether or not the injury is either close or more distal from the dorsal root, ganglion, and the spinal cord. As there are many injuries associated with the brachial plexus which often lead to neuromas and it was found experimentally that a brachial plexus injury by root avulsion such as may occur in motor vehicle accidents is more likely to cause a widespread change in the nervous system in early immediate gene expression.

In Section VII, work that is under way and that is potentially very productive has used early passage fibroblasts from human peripheral nerve neuromas. One of the challenges has been to scale up production of cells so that large amounts of fibroblasts and Schwann cells will be available for more experiments done on tissue culture cells and to preserve these cell lines. It is found that by passage five after the culturing of human neuromas, the

contribution of Schwann cells is essentially nonexistent and the cells are more than 96% fibroblasts. In examining the role of TNF$\alpha$ in the IL-1 on these cells, it has been found that these are capable of acting individually and synergistically to increase the level of mitogen-activated protein kinase (MAPK) which may be one of the early inflammatory mechanisms by which fibroblast proliferation is increased and may contribute to the developing neuroma. However, there is interest to understand the localization of inflammatory cells in the early stages after neuroma production as these cells may, in fact, become localized within the more confined space of the proximal nerve stump and have a potentially much greater affect on cell proliferation. This assay also gives us a way to test the level of stimulation and the inhibition of stimulation of fibroblasts that could be obtained from antimetabolites, interferon, or minoxidil which may be potentially useful to inhibit neuroma production in the patient.

The work on opioid receptors in Section VIII, was a particular opportunity to study an important advancing area in our understanding of the peripheral localization of opioid receptors. Due to the availability of human neuroma tissue which is both painful and nonpainful, and monkey primate experimental neuromas, this type of analysis was an important opportunity to shed some light on this field with growing interest. It is unclear at the moment if peripheral opioid receptors are functional and how they would function to decrease pain in a neuroma. The work that has been carried out has studied both the mu and delta receptor using antibodies provided to us by Dr. Elde at the University of Minnesota. It was shown that both human neuromas, as well as experimental primate neuromas were positive for these two types of opioid receptors. This has been an advancement from previous work using experimental rat neuromas. However, in double labeling studies it was clear that the localization of these receptors did not exactly correspond with the localization

of the neural tissue in a neuroma. It is felt that the next stage for this would be to study these at an EM level to try to co-localize these cells and to determine exactly what type of cell that they are on, either fibroblast or Schwann cell.

Next, in Section IX , work on sodium channels and human neuromas has proceeded on two levels. One is electrophysiology of sodium channels which has suggested that these have an increased activity, and the other has been a productive study using specific antibodies to sodium channels. Radioimmunoassays, in addition, has confirmed the increased channel density which may, taken together, suggest that this work will uncover the physiological basis of the painful human neuroma. In the appreciation of the painful state of neuroma, however, both the central nervous system, as well as the peripheral nervous system are affected.

In Section X, the study is underway to understand how the input at the level of the thalamus is changing in painful neuroma and that this is involved in the transmission of pain through the thalamus leading to the pain state.

A number of publications have come out of this work and several are in progress. The publication by England, et al has been accepted and is in press in Neurology. We have been asked to contribute a special section on our work on cytokines and peripheral nerve fibroblasts for a special edition of International Neurochemistry on the subject of "Cytokines and the Nervous System" which will be published later this year. In addition, we have been invited to speak about some of this work at one of the most prestigious gatherings of surgeons and scientists, the Sunderland Society, which specifically discusses the complications of peripheral nerve surgery and the problems of neuroma.

# I. Summary of Human and Monkey Neuroma Data

A neuroma is a disorganized mass of connective tissue and axons that causes unsatisfactory peripheral nerve regeneration and often pain (Fig. 1). The cellular mechanisms leading to the exaggerated and haphazard fibroblastic proliferation and extracellular matrix production characteristic of neuromas are unknown. Growth factors could be important in the cellular stimulation that leads to neuroma formation and growth. Initially, the purpose of this project was to determine the nature of the cell-signaling environment in the human neuroma. We removed 23 neuroma samples from 12 patients (ages 21-57 years); specimens were either assayed for the presence of growth factors and their receptors or prepared for tissue culture. Methods included Western blots (foreskin fibroblasts or the specific growth factor were used as controls) and the polymerase chain reaction (PCR). Basic fibroblast growth factor (bFGF) was present in the largest amount (62 $\pm$ 0.11% of control, mean $\pm$ SE) and was found in samples from all 12 patients, as well as in neuroma cell cultures (Figs. 2 and 3). The bFGF receptor was found in small amounts in 7/12 patients (Fig. 4). Platelet-derived growth factor-BB (PDGFbb) was present in small amounts in samples from 5/12 patients. Epidermal growth factor and its receptor were present only in cultured neuroma cells. PCR demonstrated messages (mRNA) for transforming growth factor and its receptor in tissue-cultured cells in 4/12 patients. The results suggest an important role for fibroblast growth factor in cell-signaling within the neuroma. These signals appear to be essential for the proliferation of connective tissue seen in most neuromas.

The immediate goal for year two was to determine how similar two potential models of human neuroma based in the monkey were to the humans. These models were blunt section and a 10 cm crush of tibial nerve in rhesus monkey.

# II. Primate Model of Neuroma

### Fibroblast growth factor

Previous studies of human neuromas using quantitative Western blot analysis of growth factor and growth factor receptors indicated that basic fibroblast growth factor (bFGF) and its receptor (bFGFr) were prominent in the long-term neuroma. An important goal of the second year work was to examine the monkey models of neuromas, both blunt nerve section and crush, to determine how the cell-signaling characteristics compare with the human neuroma. In addition, other studies examined the role of bFGF in human peripheral nerve fibroblasts.

The monkey studies of neuroma formation utilized prepared monkeys from 2 weeks to 12 months with either a crush or blunt section. At the present time, tissue has been studied from 3, 6, and 12 month nerves. It appears as if the blunt section is more appropriate than the 10 cm crush, since the blunt section has a much greater regenerative capacity. At time of sacrifice, these animals underwent electrophysiological studies for functional continuity. bFGF, epidermal growth factor (EGF), platelet-derived growth factor (PDGF), and the associated receptors were examined by Western blots, as well as immunohistochemistry. The distinct advantage of the monkey model is that normal nerve is also available. As with the human neuromas, the 18-24Kd bands of the bFGF were prominent at 3-12 months. This suggests a strong similarity with the long-term human neuroma, as in this case EGF, EGFr, PDGFbb, and the receptor, as well as tumor necrosis factor-$\alpha$, were not prominent in the Western blot analysis.

### Low affinity nerve growth factor receptor

Nerve growth factor (NGF) and its low affinity receptor (NGFr) have recently been

detected in the distal segment of the sciatic nerve 6 hours to 14 days after transection. However, neuromas are hypothesized to require the presence of neural tissue and, at least fibroblasts, if not Schwann, in the early stages of development. However, a translocation of NGF or another growth factor could significantly modulate the immediate cell-signaling environment of these cells.

A study was carried out using immunohistochemistry to determine the cellular localization of low affinity NGFr, FGFr-1, growth-associated protein (GAP-43), and bFGF in developing monkey neuromas after blunt section. Two weeks after blunt section, NGFr in the proximal adjacent segment was found primarily in the perineural tissues and less intensely in the endoneurium. In both monkey and human, NGFr was found in Schwann sheaths surrounding masses of axons. Immunoreactivity was more intense in 12-month monkey specimens and long-term human neuromas. Proximal segments of the neuroma, merging into more normal nerve, showed even staining for GAP-43; however, the thin fibers of the neuroma were poorly stained. bFGF and FGFr-1 showed less intense staining when compared to proximal segments at 3 months. These results suggest that the increase in NGFr, the decrease in GAP-43, and the change in distribution of bFGF may have a role in the balance of cellular conditions sustaining the fibrous growth associated with the neuroma.

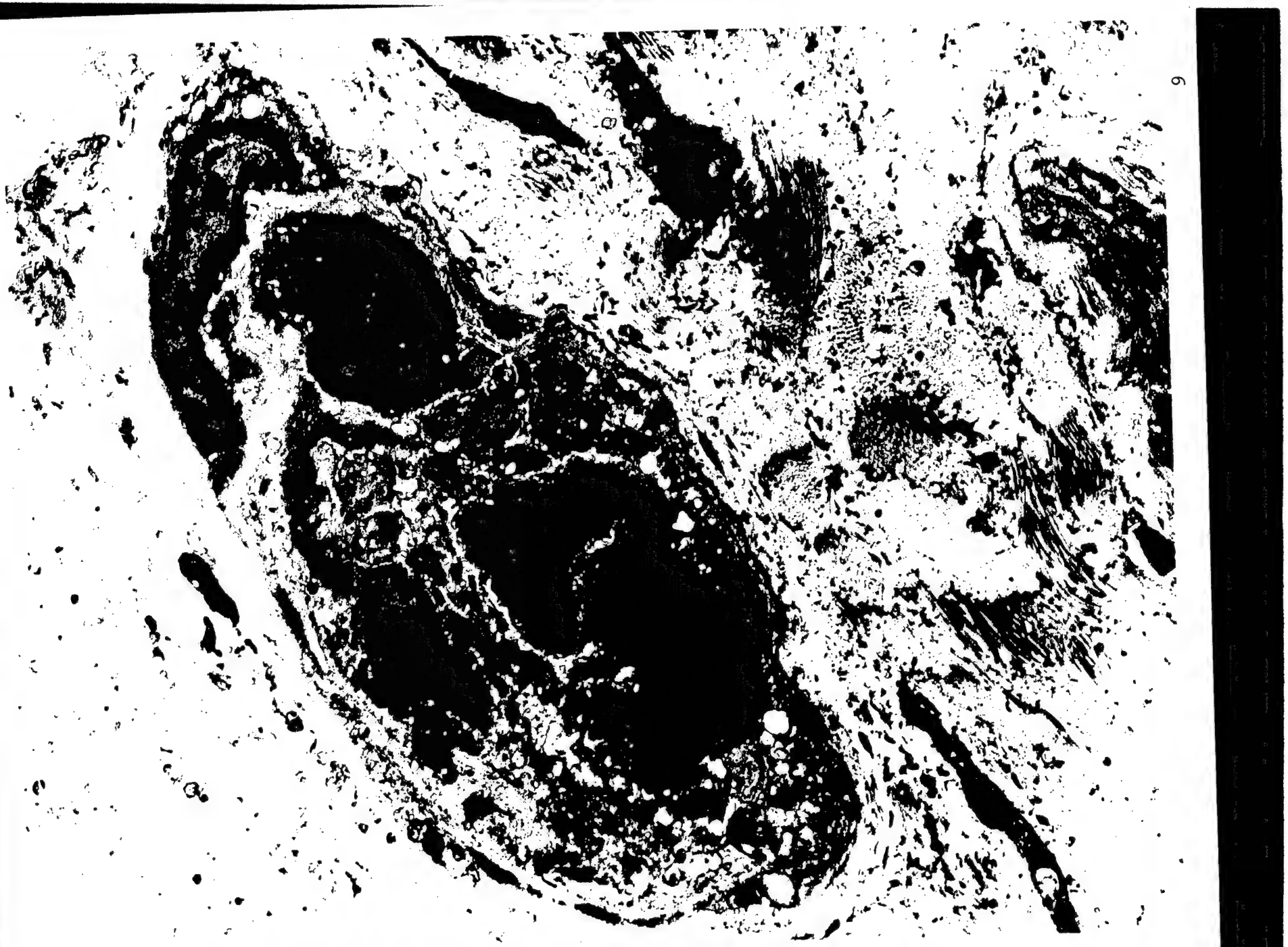

Figure 1

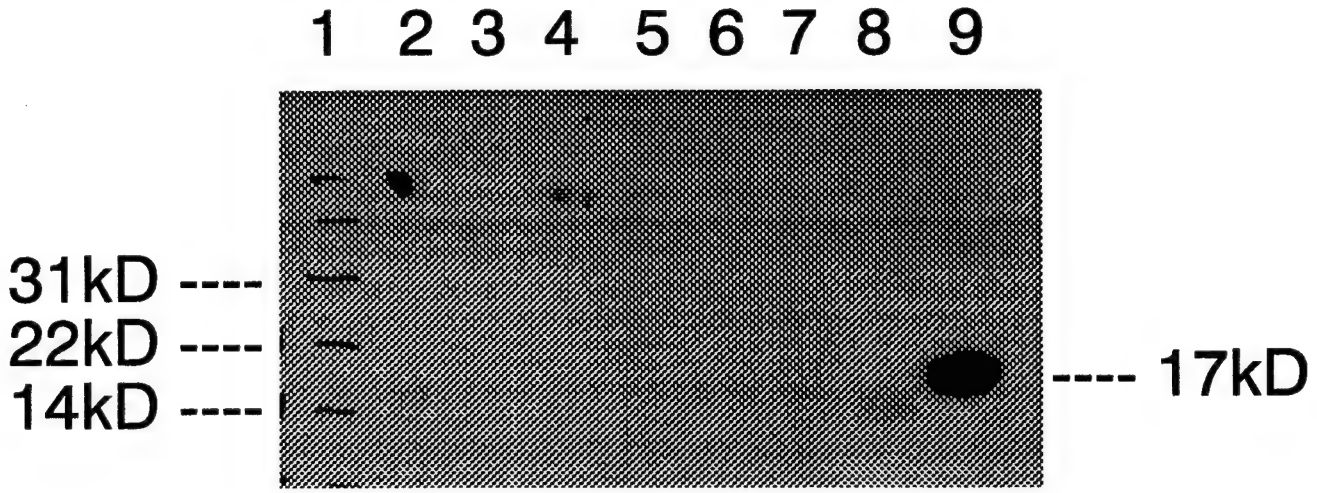


Figure [2]: Western blot of Tumor Necrosis Factor alpha (TNFa) of human neuroma tissues using 1ug/ml of monoclonal mouse anti human TNFa antibody (UBI). No TNFa was detected in all the samples.

1. Markers; 2. C5; 3. C6; 4. C7; 5. D; 6. E;
7. B1; 8. B2; 9. 500ng of human TNFa.


Figure 3: Western blot of bFGF of human neuroma tissues using 1$\mu$g/ml of monoclonal mouse anti-human bFGF antibody (Transduction Laboratories). The 18kD component of bFGF was present in all samples.
Lanes C-5, C-6, and C-7 represent human neuroma tissues as do E, B1, and B2. The lane marked D is from the foreskin fibroblast homogenate.

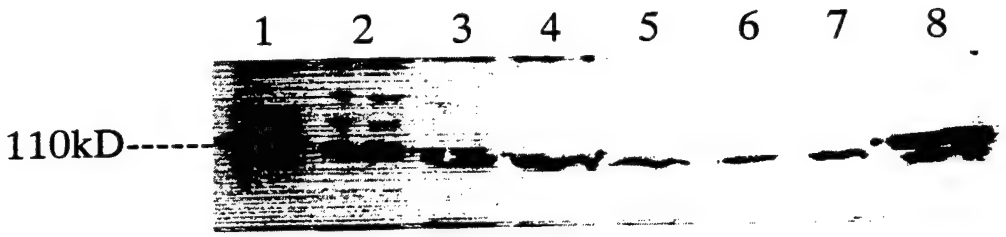


Figure 4: Western blot of FGFR (I) of neuroma tissues using 1$\mu$g/ml of monoclonal antibody against human FGFR (■) (Transduction Laboratories).
Lanes 1 and 8 are fibroblast cell culture from neuroma tissue; lanes 2 to 7 are neuroma tissue samples.

# III. Immunolocalization and Quantitation of Basic Fibroblast Growth Factor and Fibroblast Growth Factor Receptor-1 in Cells of Peripheral Nerve Neuromas


## Summary

The purpose of this study was to determine the involvement of basic fibroblast growth factor (bFGF) and fibroblast growth factor receptor-1 (FGFR-1) in the formation of human peripheral nerve neuromas. Previous studies have shown that bFGF is the most abundant growth factor in surgical specimens of human neuromas. Immunocytochemical localization of bFGF and FGFR-1 in cultured fibroblasts at passage 5 and 6 from neuromas was examined at light and electron microscopic levels. Double leveling studies confirmed the difference in localization between the growth factor and its receptor. Subcellular localization of the growth factor and receptor were studied by electron microscopy showing that gold particles (15 nm diameter), bound to an antibody against bFGF, localized mainly in the cytoplasm. However, in a similar fashion, gold particles for FGFR-1 localized primarily along the cell membrane and showed regularity in the spacing of about 1.3 $\mu$m average distance between gold particles. Quantitation of FGF membrane receptor was analyzed using flow cytometry. The number of the receptor was about 5600/cell. The results of this study have contributed to the understanding of the formation of peripheral nerve neuromas.



**Key words:** peripheral nerve neuroma, basic FGF, FGF receptor, immunolocalization


## Introduction

Fibroblast growth factor (FGF) comprises a family of heparin-binding polypeptide

mitogens. To date, at least seven members have been identified from both normal and tumor tissues. In addition to their mitogenic activity towards a wide variety of cell types, FGF influence cellular differentiation, promote neuron survival and neurite outgrowth, participate in angiogenesis, and play an important role in tissue repair. Peripheral nerve neuroma often form after injury or surgical repair of the involved peripheral nerves. Fibroblasts are the primary cellular elements in the formation of a neuroma. However, there is little information about precise localization of bFGF and FGFR-1 in fibroblasts in formation of neuroma. The aim of this study was to clarify localization of bFGF and FGFR-1 in fibroblasts from peripheral nerve neuroma using specific antibodies directed against bFGF and FGFR-1 at light and electron microscopy levels.

## Materials and Methods

### Primary Culture of Human Peripheral Nerve Neuroma

The peripheral nerve neuroma tissue was obtained at the time of surgical correction and placed in saline. The patients were all males, average age was 25.2 years (14-38). Tissue culture was established immediately after the tissue was cleaned of epineural connective and cut into 1 $mm^3$ explants, which were attached to a T 25 flask and incubated with 5% $CO_2$, 95% air at 36°C. Cultures were maintained in Dulbecco's Modified Eagles Medium (D-MEM) plus 20% fetal bovine serum (FBS) and 1% antibiotic-antimycotic (Gibco). Confluent cells were passaged (a total of 14 days) into T 75 flasks containing 10% FBS and 1% antibiotic-antimycotic in D-MEM. After passage 4-5 times, the cells were used for immunocytochemical testing. To avoid potential interference from cell signaling factors and receptors present in FBS, the culture medium was replaced with serum-free D-MEM 12-

24 hr before the addition of the primary antibody. This step could be omitted, however, without a significant loss of sensitivity because the concentration of factor and receptor in inactivated FBS is very low.

**Antibodies**

**Anti-fibroblast growth factor-Basic.** Rabbit polyclonal IgG (Sigma), FGF(R)VBS6): mouse monoclonal IgG (Santa Cruz Biotechnology, Inc.). Anti-rabbit and anti-mouse IgG peroxidase conjugate and anti-mouse IgG FITC conjugate, anti-rabbit IgG TRITC conjugate, anti-mouse IgG R-Phycoerythrin conjugate (Sigma). Colloidal gold particle (15 nm diameter)-goat anti-rabbit and goat anti-mouse IgG (BBI International). Anti-NGF-receptor, human monoclonal antibody to human nerve growth factor-receptor (NGF-receptor)(Genzyme).

**Indirect Immunocytochemistry**

**Light microscopy.** Immunostaining was performed using a three-stage avidin-biotin complex (ABC) technique. Briefly, the cells were passaged into multi-well glass chamber slides (Nunc). Confluent monolayer cell were fixed with 4% paraformaldehyde/0.1M phosphate buffered saline (PBS pH 7.4) for 40 min at room temperature (RT). After washing with PBS, slides were treated with 0.3% hydrogen peroxide in methanol for 10 min at RT to remove intrinsic peroxidase activity. Washed again with PBS, the slides were incubated with 5% normal goat serum diluted with PBS for 30 min at RT, then covered with primary antibody diluted with PBS containing 1% bovine serum albumin (BSA, Sigma) (anti-bFGF 1:100, anti-FGFR-1 1:60) overnight at 4°C in a humidified chamber. After washing the slides were incubated with secondary antibody diluted with PBS (1:200) for 30 min at 37°C. After additional washes, immunostaining was performed using an avidin-biotin

complex (ABC) kit (Vector Laboratories) for 30 min at 37°C under light microscopic examination. For controls, the primary antibody was replaced with PBS.

**Light microscopy-double labeling.** The cells were passaged into multi-well glass chamber slides (Nunc). Confluent monolayer cells were fixed with 2% paraformaldehyde/0.1 M PBS pH 7.4 for 30 min at RT, washed with PBS and incubated with a 5% solution of normal goat serum in PBS for 1 hr at RT. The cells were incubated overnight with the primary antibody. Anti-bFGF and anti FGFR-1 were diluted with PBS/0.3% BSA, 0.1% triton X-100 (Mallinckrodt, Inc.) at 4°C and the same concentration as above. Antibody binding was detected by incubating the slides with fluorescein (FITC and TRITC) conjugated secondary antibodies diluted with PBS for 1 hr at RT. After a final wash with PBS, the slides were examined using an axioplan fluorescence microscope. In the controls, the primary antibody was replaced with PBS.

**Electron microscopic localization.** Cells were grown in multi-well plastic chamber slides (Nunc, Inc.). They were fixed with 4% paraformaldehyde in 0.1 M PBS for 40 min at RT and then washed and treated with PBS plus 0.1% saponin and 5% normal goat serum for 30 min at RT. Afterwards they were incubated overnight with the primary antibody diluted with PBS containing 1% BSA (anti-bFGF 1:100, anti-FGFR-1 1:60) at 4°C. After washing with PBS, the slides were treated with colloidal gold particle (15 nm diameter-conjugated anti-mouse IgG or anti-rabbit IgG (diluted 1:100 with PBS containing 0.1% BSA) for 1 hr at RT. After another wash with PBS and distilled water, silver enhancement was added (British Bio Cell) for 8 min. After a final wash, the slides were fixed with 2% glutaraldehyde for 10 min, treated with 0.2% osmium tetroxide, enblock mordanted with 1% urynal acetate buffer (pH 5.0), dehydrated through a graded series of ethyl alcohol,

embedded in Epon, and examined with a Zeiss EM 104A transmission electron microscope.

**Flow cytometry.** Cells were cultured in plastic tissue culture T125 flasks (Corning Scientific Products, Corning, NY). Confluent monolayer cells were harvested using trypsinization. Pellets were washed with ice-cold red-free HANK's balanced salt solution two times and resuspended in D-PBS (pH 7.4) containing 0.1% sodium azide (to prevent receptor internalization) at a concentration of $5x10^5$ cells per 100 $\mu$l sample. The number of cells was determined by trypan blue exclusion. The suspensions were incubated with the primary antibody (2$\mu$l anti-FGFR-1 per 100 $\mu$l sample) for 30 min at 4°C. After incubation, the cells were washed three times with D-PBS containing 0.1% sodium azide and 2% (w/v) BSA and incubated with the secondary antibody (anti-mouse IgG R-Phycoerythrin conjugated, 1:40 in PBS) for 30 min at 4°C. After a final wash x 3 (D-PBS with 2% BSA and 0.1% sodium azide) the cells were maintained in 500 $\mu$l D-PBS at 4°C in light-proof containers until analyzed by flow cytometry.

## Results

The antibody for FGFR-1 was found to be localized in the cytoplasm in human neuroma cells at passage 506 (Figs. 1, 3). Fibroblasts were positively stained with bFGF under light microscopy (Figs. 3, 4). In double-label immunofluorescence studies, in fibroblasts it was shown that, while bFGF is localized to the nucleus, receptor staining was more concentrated in the cytoplasm (Figs 5, 6). Further, subcellular localization of bFGF was examined by electron microscopy using the pre-embedding immunogold labeling technique. Gold particles (15 nm diameter) binding to bFGF were shown to localize mainly in the cytoplasm (Figs. 9-12). An interesting finding was the failure of S-100 protein to

clearly distinguish fibroblasts from Schwann cells (Figs. 7, 8).

Monoclonal anti-fibroblast growth factor receptor-1, human IgG was used to recognized to FGFR-1 and observed with light microscopy (Fig. 4). Fibroblasts also expressed FGFR-1 in double-label immunofluorescence test. Unlike bFGF, the nucleus was not stained for FGFR-1 (Fig. 5). Further, FGFR-1 was examined by electron microscopy using a pre-embedding immunogold labeling technique.

Gold particles binding to FGFR-1 were shown to localized along the internal side of the cell membrane where they had a spacing of about 1.3 $\mu$m.

Quantitation of the FGF membrane receptor was performed by flow cytometry using Quantum Simply Cellular Microbeads as a standard (Fig. 13). The inherent autofluorescence of unstained fibroblasts is presented in Fig. 14. The fluorescence calibration was based on dye-loaded microbeads. The soluble R-Phycoerythrin per bead ranged from 10 (peak B) to $1.2 \times 10^5$ (peak F). Fluorescence intensity versus cell count for stained fibroblasts was plotted in Figs. 15 and 16. The Density of FGFR-1 was calculated to be about 5600/each cell.

## Discussion

In the normal nerve, an important function of Schwann cells and endoneurium is to isolate axons from the surrounding tissues. When a nerve trunk is damaged, regrowing axons leave the nerve trunk through the defect. The perineurial cells such as fibroblasts enclose small numbers of myelinated or unmyelinated axons, leading to the formation of a nodule, bulb or neuroma that consist mainly of fibroblasts and Schwann cells **(Underland, 1988)**. High percentages of fibroblasts in culture can be obtained from neuroma tissue

because fibroblasts divide well in vitro and rapidly outnumber other cell types. **Scarpini et al.** reported that the percentage of adult Schwann cells identified by the S-100 protein decreased rapidly from about 90% at day 1 to about 50% at day 7 because fibroblasts replicate faster than Schwann cells in culture. In the present study, primary cell cultures from peripheral nerve neuromas were passaged 4-5 times. Under these conditions, the number of Schwann cells relative to the abundance of fibroblasts was very small. In this way, a highly purified population of fibroblasts was obtained for use in our study. In culture, Schwann cells can be distinguished from fibroblasts by morphology and immunology. Nerve growth factor (NGF) receptor has been previously established as a marker for Schwann cells (**Scarpini, 1988**). We employed a specific monoclonal antibody against the NGF receptor to examine the cultured cells and found positively stained Schwann cells to be scarce.

The present immunocytochemistry study revealed that both bFGF and FGFR-1 were localized in cultured fibroblasts obtained from peripheral nerve neuroma. The bFGF was distributed throughout the cytoplasm as well as the nucleus. This cytoplasmic localization of bFGF is consistent with the previous immunohistochemical report on the localization of bFGF in cultured human epidermoid carcinoma cells. The production of bFGF by fibroblasts has also been reported in vitro (**Yabu, 1993; Moscatelli, 1986; Story, 1989**) and fibroblasts are thus considered to have the potency to produce bFGF.

## References

Duran, D.R. and Werner, L.S.T. (1992) A naturally occurring secreted form of fibroblast growth factor (FGF) receptor 1 binds basic FGF in preference over acidic FGF. *J Biol Chem* **267**, 16076-16080.

Hughes, S.E. and Hall, P.A. (1993) Immunolocalization of fibroblast growth factor receptor 1 and its ligands in human tissues. *Lab Invest* **69**, 173-182.

Lopez, J.G., Beuerman, R.W., and et al. (1992) EGF cell surface receptor quantitation on ocular cells by an immunocytochemical flow cytometry technique. *Invest Ophthalmol Vis Sci* **33**, 2053-2062.

Lucocq, J. (1994) Quantitation of gold labelling and antigens in immunolabelled ultrathin sections. *J Anat* **184**, 1-13.

Morrison, R.S., Yamaguchi, F., and et al. (1994) Basic fibroblast growth factor and fibroblast growth factor receptor 1 are implicated in the growth of human astrocytomas. *J Neuro-oncology* **18**, 207-216.

Suzui, H., Takahas, M., and et al. (1994) Immunohistochemical study for basic fibroblast growth factor and fibroblast growth factor receptor 1 in pituitary adenomas. *Neurosci Lett* **171**, 192-196.

Ueba, T., Takahashi, J.A., and et al. (1994) Expression of fibroblast growth factor receptor-1 in human glioma and meningioma tissues. *Neurosurgery* **34**, 221-226.

Yabu, M., Shimomura, Y, and et al. (1993) Immunohistochemical localization of basic fibroblast growth factor in the healing stage of mouse gastric ulcer. *Histochemistry* **100**, 409-413.

Fig.1. Cultured cells from human neuroma tissues: positive staining with FGFR-1 (VBS6).

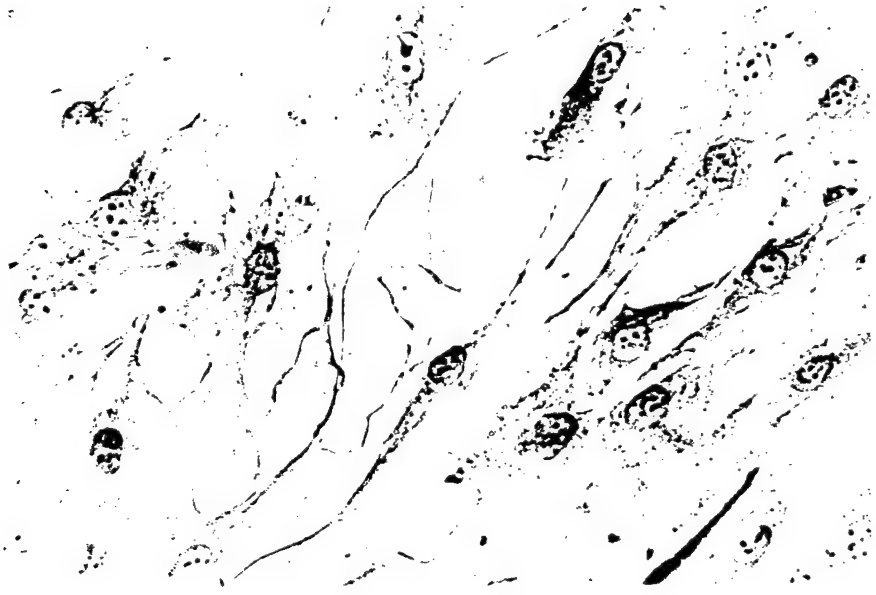

Fig.2. Cultured cells from human neuroma tissues: negative control for FGFR-1.(no primary antibody)

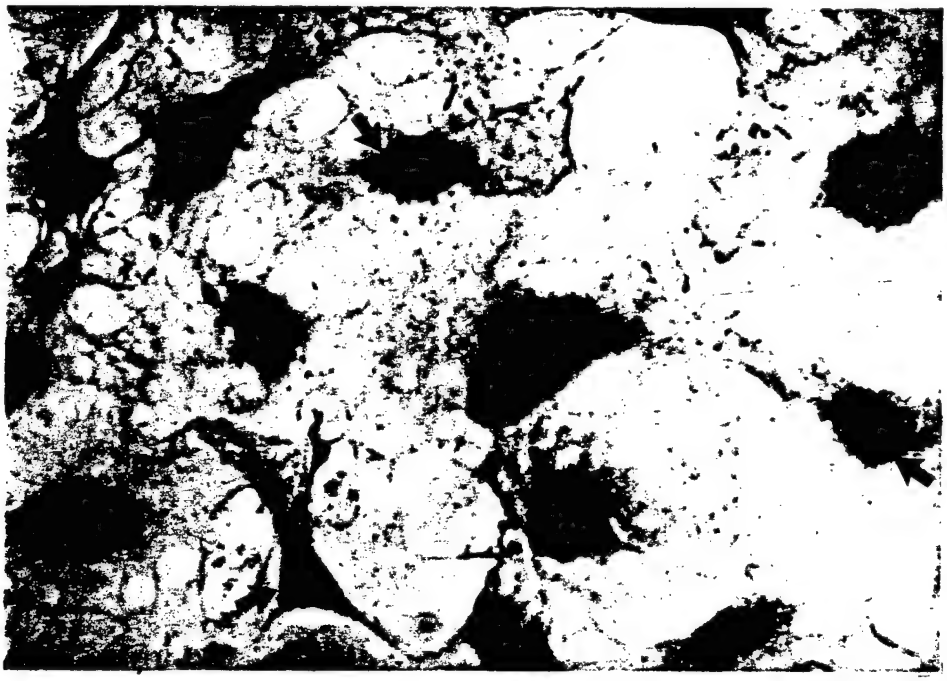

**Fig 3. Cultured cells from human neuroma tissues: positive staining with bFGF. ( AEC kit stain)**

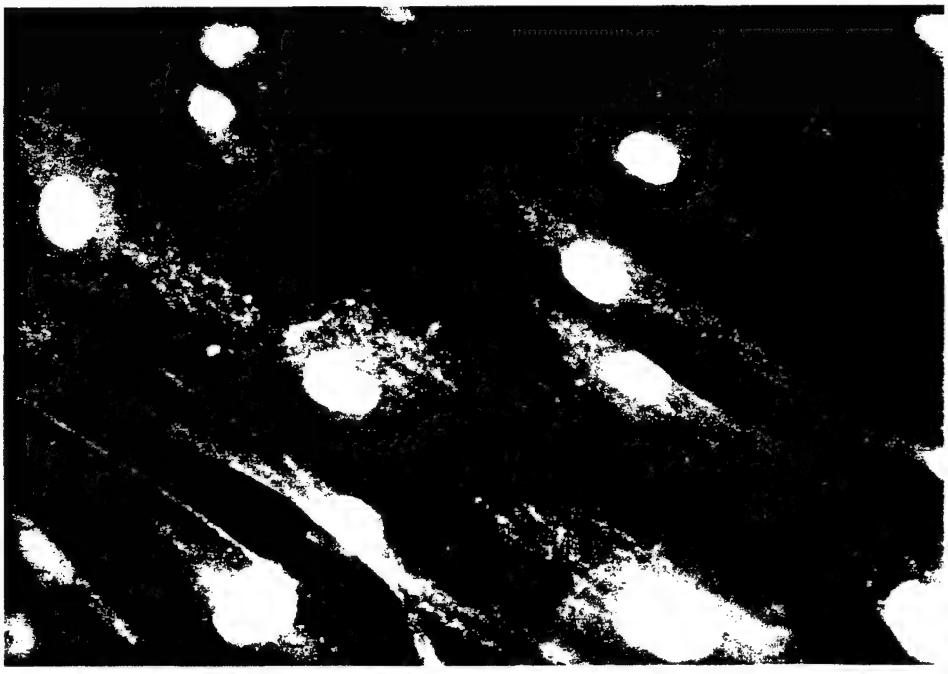

**Fig 4. Cultured cells from human neuroma tissues: positive TRITC immunofluorescent staining for bFGF.**

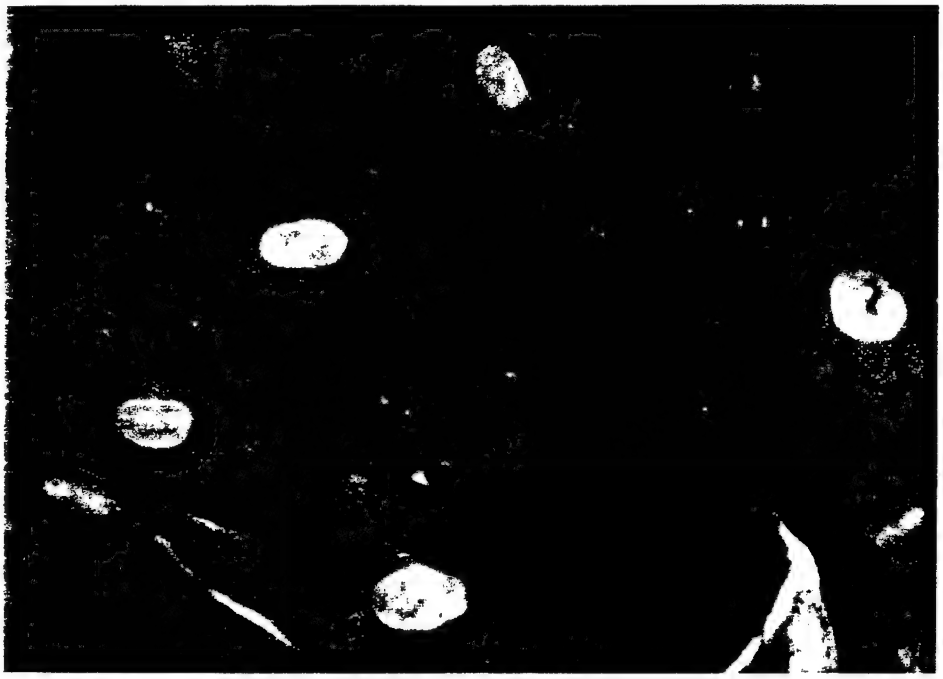

**Fig 5. Cultured cells from human neuroma tissues: Double labeling immunofluorescent-positive staining of cells expressing bFGF with FITC.**

**Fig 6. Cultured cells from human neuroma tissues: Double labeling immunofluorescent-positive staining of cells expressing FGFR-1 with TRITC.**

Fig.7. Cells of human neuroma tissues cultured: positive staining show Schwann cell expressing NGF-R .

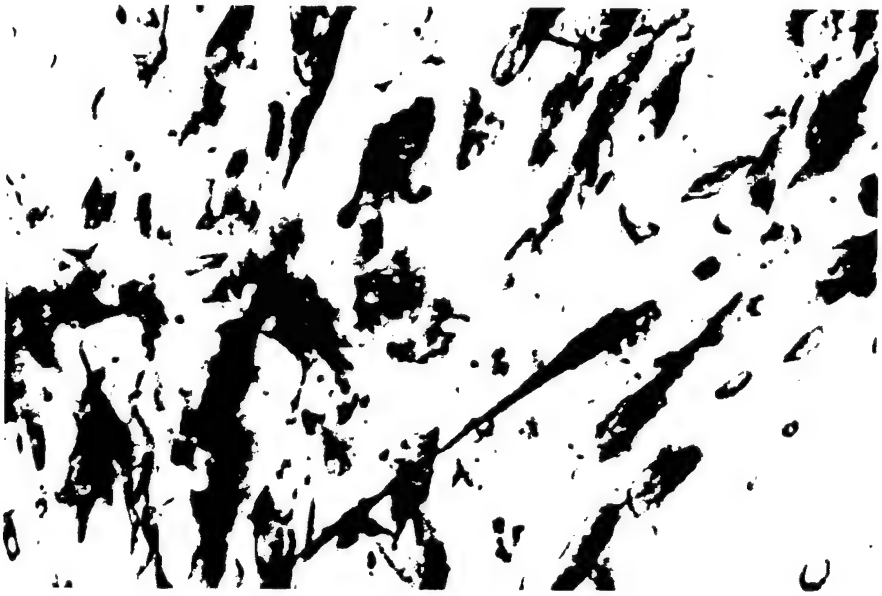

Fig.8. Cultured cells from human neuroma tissues : positive staining show cells expressing S-100 protein.(Anti-S100)(sigma)

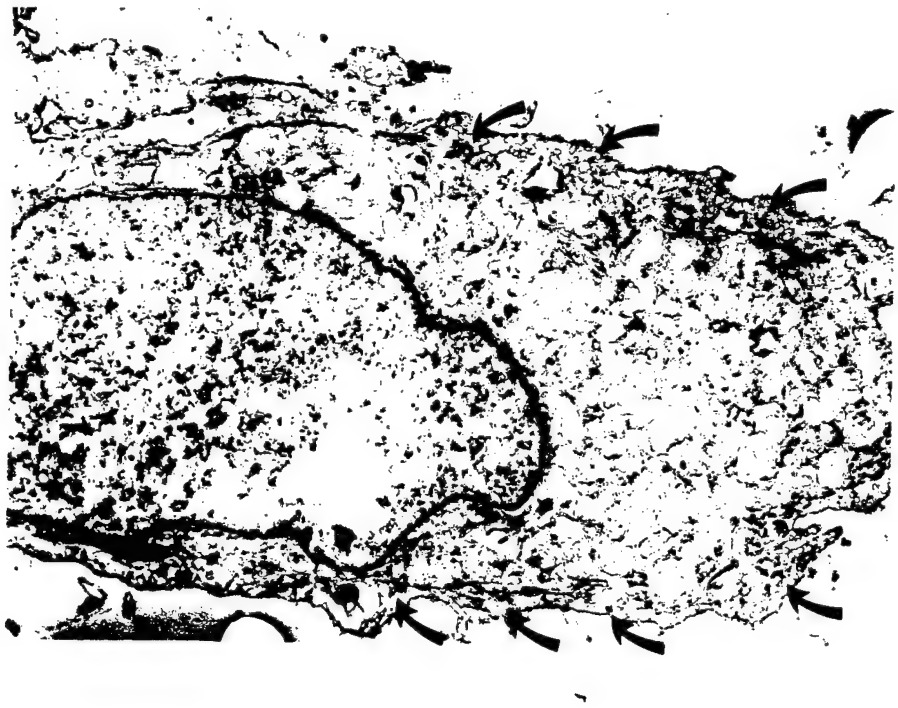

**Fig 9. Cultured cells from human neuroma tissues: Electron micrograph showing the localization of FGFR-1 along the fibroblasts membrane using 15 nM gold particle.**

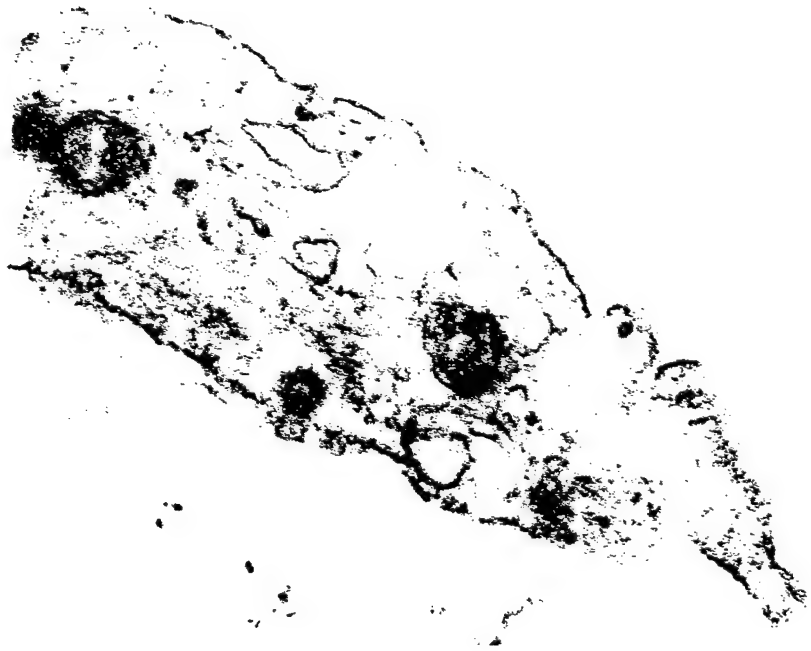

**Fig 10. Cultured cells from human neuroma tissues: Electron micrograph showing negative staining for FGFR-1 (no primary antibody).**

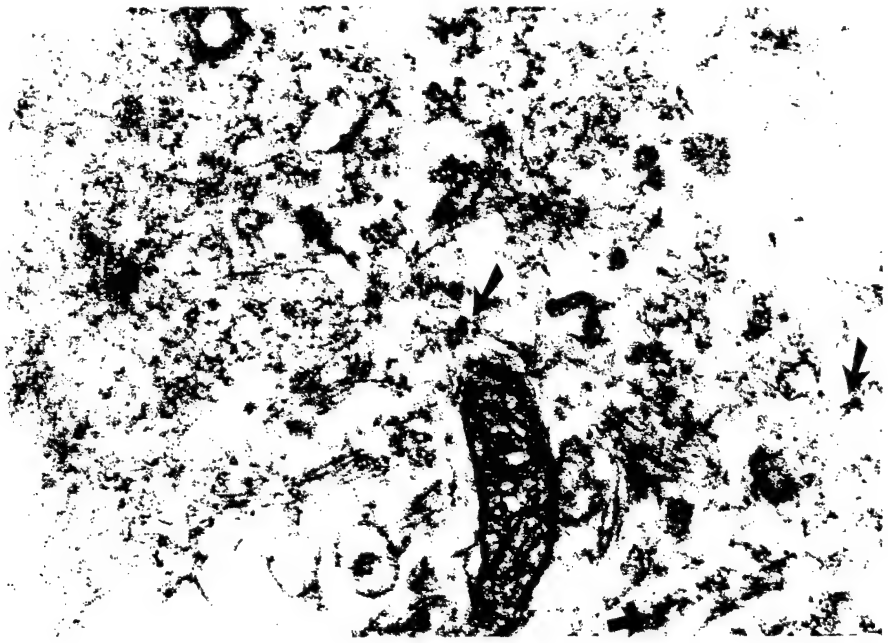

**Fig 11. Cultured cells from human neuroma tissues: Electron micrograph showing the localization of bFGF in the cytoplasm of fibroblasts using 15 nM gold particle.**

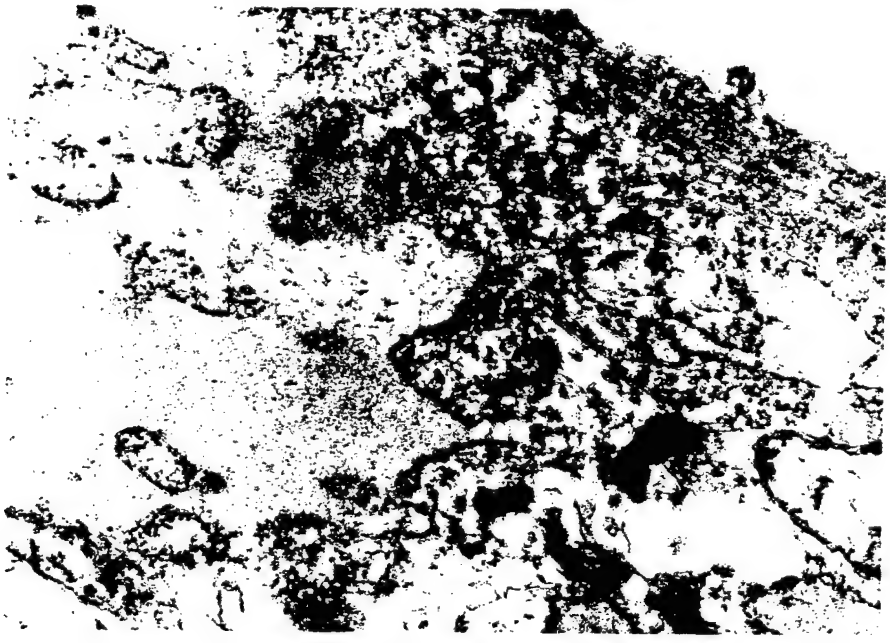

**Fig 12. Cultured cells from humam neuroma tissues: Electron micrograph showing negative staining for bFGF (no primary antibody).**

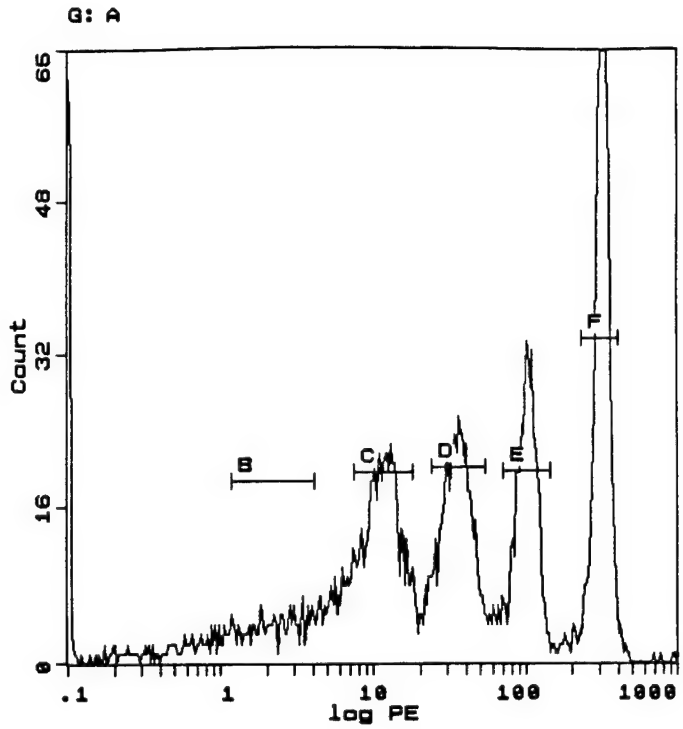


Fig.13. Flow cytometric analysis of FGFR-1 quantitation. Plot of the log of fluorescence versus cell count for unstained cultured neuroma cells for fluorescein (578 + 15 nm pass band). An increase of channel represents increase

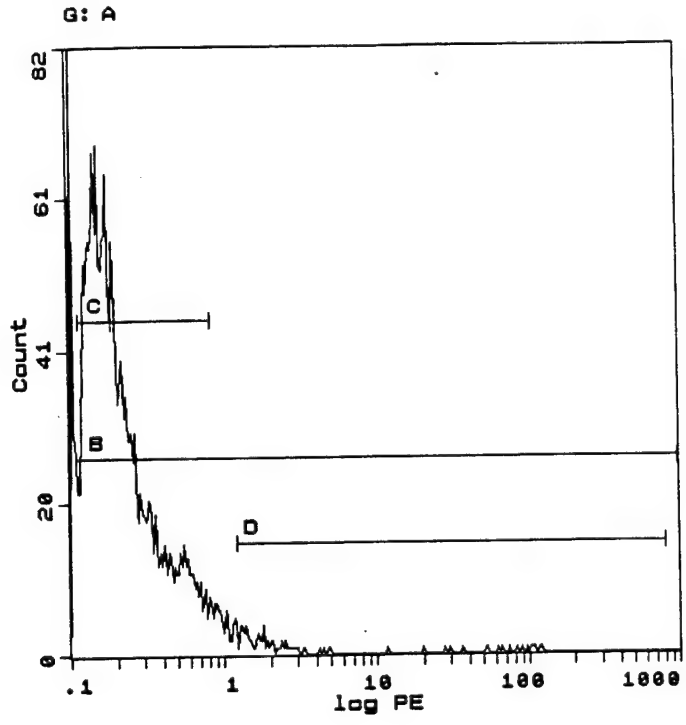


Fig.14. Plot of log fluorescence versus cell count for unstained cultured neuroma cells only after being added to the second

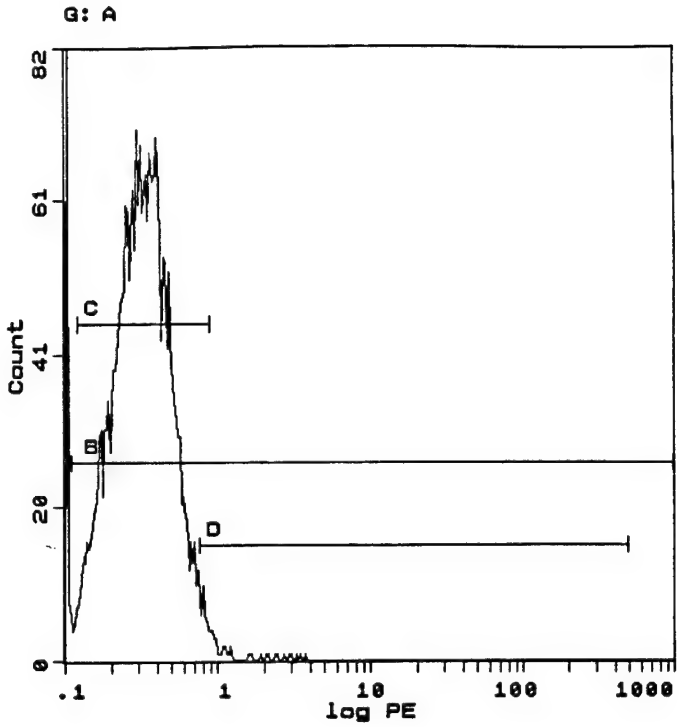


Fig.15. Single parameter frequency distribution for a population of cultured neuroma cells incubated with anti-FGFR-1 monoclonal antibody and subsequently stained with PE, calculated FGFR-1 density is about 5600/cell.

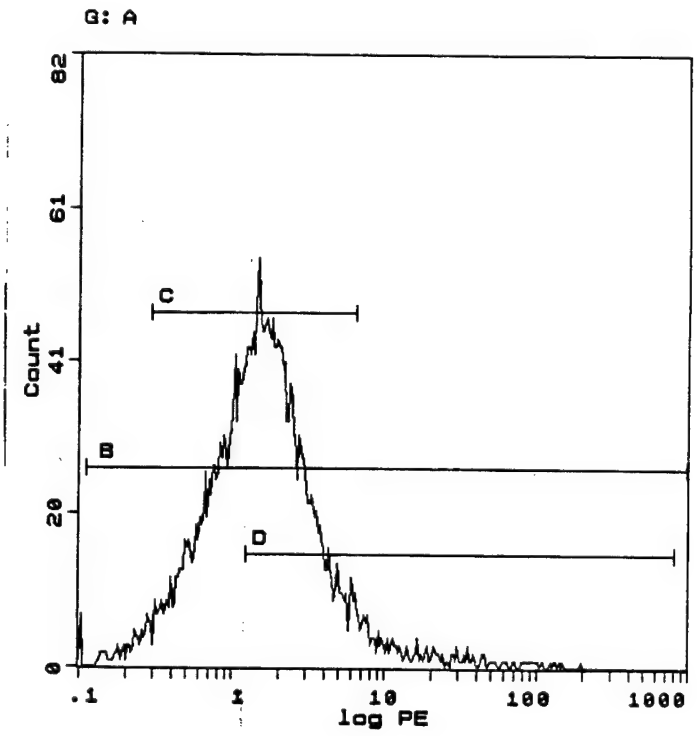


Fig 16. Flow cytometric analysis of FGFR-1 quantitation. Single parameter frequency distribution for a population of neuroma cells stained by R-Phycoerythrin. This channel represents an increase in the fluorescence due to receptor binding. Calculated FGFR-1 density is about 5600/cell.

# IV. Increase in Basic Fibroblast Growth Factor and Fibroblast Growth Factor Receptor-1 Following Sciatic Nerve Injury and Neuroma Formation


## Summary

Neurosurgical practice has indicated that severed nerve ends that have the endoneurium sealed with a bipolar coagulator or that are buried in muscle are less likely to produce a neuroma, compared with nerve ends that are ligated or untreated. A neuroma can be formed within two weeks in rat after the sciatic nerve injury (Carlton et al., 1991). These experiments were undertaken to investigate the activity of basic fibroblast factor (bFGF) and FGF receptor-1 in neuroma development. The sciatic nerves of adult rats were severed below the sciatic nerve notch and severed ends were treated in one of four ways: 1) buried in muscle; 2) perineurium and endoneurium sealed with a bipolar coagulator; 3) perineurium tied with #6 suture; and 4) no treatment. Nerves were harvested at 2, 4, 8, and 16 days after surgery. A section (0.5 mm) was removed from the proximal severed end of each nerve and total proteins were extracted. The results of Western blot analysis showed increased amounts of bFGF and FGF receptor-1 beginning 2 days after surgery, compared with normal controls. Nerves that had been treated with the bipolar coagulator or buried in muscle yield less bFGF and FGF receptor-1 than the nerves that were ligated or the nerves that were not treated. This study provides evidence that increased activation of bFGF and FGF receptor-1 are associated with neuroma formation from the very early stages of nerve response to injury.


## Background

Neuroma is the common pathology associated with peripheral nerve injury. In this condition, accumulation of collagen and extracellular matrix form a barrier that the regenerating axons can not penetrate and forming a bulb-like enlargement or neuroma (Sunderland, 1988). While the mechanism of neuroma development is not clear, some growth factors are considered to be involved in the process. Basic fibroblast growth factor (bFGF) is a pluripotent polypeptide involved in various biological activities, including angiogenesis, mitogenesis, cellular differentiation, and repair of tissue injury (Gospodarowicz et al., 1987). The bFGF have been shown to promote fibroblast proliferation (Goldsmith et al., 1991; Doumit et al., 1993). FGFs mediate their biological responses by binding to and activating specific cell surface receptors (Burgess and Maciag 1989). Four different fibroblast growth factor receptors (FGFR-1 to FGFR-4) have been identified. Except for the FGFR-4 which binds only to aFGF, all other three receptors bind to both aFGF and bFGF (Yazaki et al., 1994). In this study, we investigate the expression of bFGF and FGFR-1 after the nerve injury and possible roles in the neuroma formation in rat.

## Methods

Sprague-Dawley rats (male 270 to 330 gram) were anesthetized by intraperitoneal injection of ketamine. The sciatic nerves on both sides were isolated and severed 1 cm below the sciatic notch. The severed ends were treated in one of four ways (Fig 1):

1) buried in the muscles;

2) perineurium and endoneurium sealed with a bipolar coagulator;

3) perineurium tied with #6 suture;

4) no treatment.

The incisions were closed by layers. Nerves were harvested at 2, 4, 8, and 16 days after surgery. A section (0.5 mm) was removed from the proximal severed end of each nerve. Tissue samples were homogenized in hot 1% SDS and 10mM Tris pH 7.4. Total proteins were determined using BCA method. The proteins were electrophoresed and transferred on to nitrocellulose membrane. The membrane was incubated in turn in the primary antibody, then in the secondary antibody-HRP conjugated after washing. Specific antigens were detected using ECL method.

**Results and Discussion**

The Western blot analysis showed increased FGFR-1 and bFGF at 2 days after surgery in comparison with the normal control. This increase lasted to the later days (4, 8 and 16 days after the nerve injury). While all nerve ends showed increase of the expression of bFGF and FGFR-1, the nerve ends with ligation or no treatment showed higher expression than the nerve ends sealed with a bipolar coagulator or buried in the muscles. Fig. 2 and Fig. 3 show the results of the Western blot of bFGF and FGFR-1 from the rat 4 days postoperatively. Fig. 4 and Fig. 5 are the results of Western blot of the bFGF and FGFR-1 from the rats 16 days postoperatively.

The expression of the bFGF and FGFR-1 was higher in all the proximal cut ends of the sciatic nerve in comparison with the normal nerve. The expression of the bFGF and FGFR-1 was also higher in the proximal severed sciatic nerve ends that were ligated or not treated than the nerve ends treated with bipolar coagulator or buried in the muscles. The bFGF is a pluripotent polypeptide which has been proved to promote the fibroblast proliferation (Goldsmith et al., 1991; Doumit et al., 1993). The fibroblast proliferation plays

an important role in the neuroma formation. After nerve injury, the expression of the FGFR-1 and bFGF is a response which may be necessary to the repair of the lesioned nerve. For reasons that are still unclear, however, excessive expression of FGFR or FGF, or overgrowth of the fibroblast appears to be involved in the formation of the neuroma. Therefore, the amount and length of time of expression of FGF and FGFR may be important in the nerve repair and the neuroma formation. In the current study, the group with nerve ligated expressed higher amounts of FGFR-1 and bFGF, which might be the results of the stimulation of the nerve tissues by the suture. The neurosurgical practice of sealing nerve ends with a bipolar coagulator or burying in muscle is less likely to produce a neuroma (Dellon and Mackinnon, 1986; Kline and Hudson, 1995). The current study showed that the expression of bFGF and FGFR-1 in the groups with the nerve ends sealed with a bipolar coagulator or buried in muscle was less than the groups with the nerve ends ligated or not treated. The neuroma can be formed within two weeks in the rat (Carlton et al., 1991). This study may suggest that the bFGF and FGFR-1 play a significant role in the neuroma formation from the early stage of nerve repair after injury.

## References


Burgess, W.H., Maciag, T. (1989) The heparin-binding (fibroblast) growth factor family of proteins. *Annu Rev Biochem*, 575-606.

Carlton, S.M., Dougherty, P.M., Pover, C.M., and Coggeshall, R.E. (1991) Neuroma formation and numbers of axons in a rat model of experimental peripheral neuropathy. *Neurosci Lett* **131**, 88-92.

Dellon, A.L. and Mackinnon, S. (1986) Treatment of the painful neuroma by neuroma resection and muscle implantation. *Plast Reconstr Surg* **77**, 427-436.

Doumit, M.E., Cook, D.R., and Merkel, R.A. (1993) Fibroblast growth factor, epidermal growth factor, insulin-like growth factors, and platelet-derived growth factor-bb stimulate proliferation of clonally derived porcine myogenic satellite cells. *J Cell Physiol* **157**, 326-332.

Kline, D.G. and Hudson, A.R. (1995) Pain of Nerve Origin. In DG Kline and AR Hudson (eds.), *Nerve Injuries*, Vol. 20, W.B. Saunders Company, Philadelphia, pp. 513-523.

Sunderland, S. (1988) Nerve and Nerve Injury, 2nd ed, Churchill Livingston, New York, pp. 180-193.

Yazaki, N., Hosoi, Y., Kawabata, K., Miyake, A., Minami, M., Satoh, M., Ohta, M., Kawasaki, T., and Itoh, N. (1994) Differential expression patterns of mRNAs for members of the fibroblast growth factor receptor family, FGFR-1, FGFR-4, in rat brain. *J Neurosci Res* **37**, 445-452.

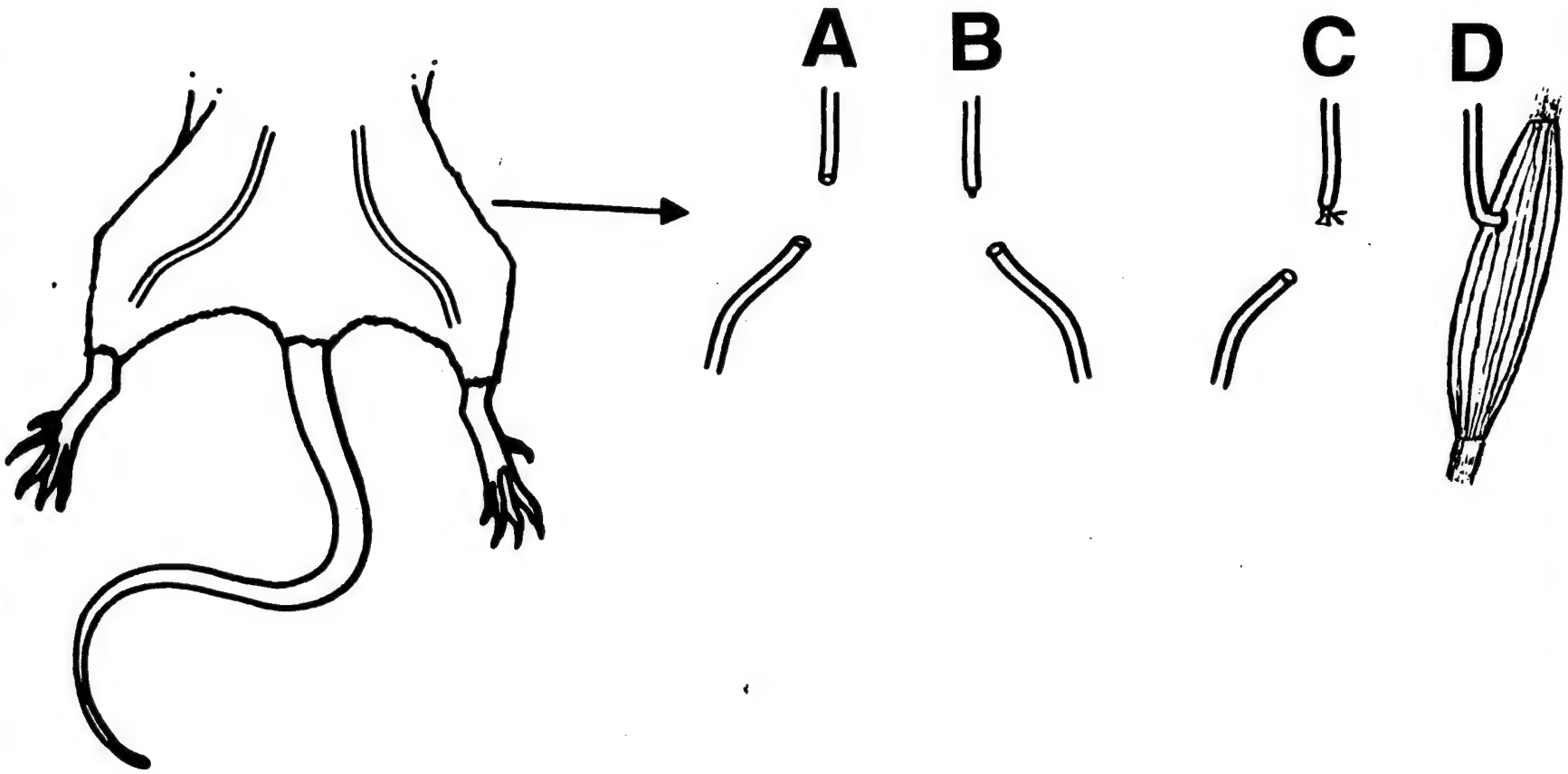


**Fig 1. Schematic illustration depicts the method by which the severed proximal sciatic nerve were treated. A. No treatment; B. Sealed by a bipolar coagulator; C. Ligated with a #6 suture and D. Buried in a muscle.**

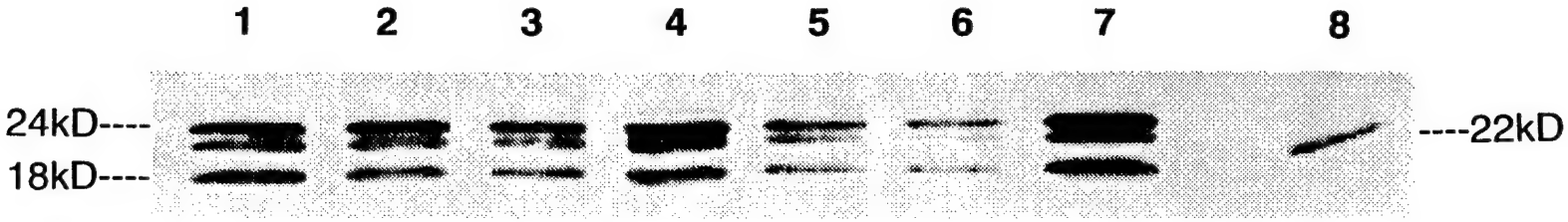




**Fig 2. Western blot of bFGF of the proximal ends of sciatic nerves obtained 4 days postoperatively.**

**1. Nerves with no treatment**

**2. and 5. Nerves buried in muscle**

**3. and 6. Nerves sealed with a bipolar coagulator**

**4. and 7. Nerves tied with #6 suture**

**8. Normal control**

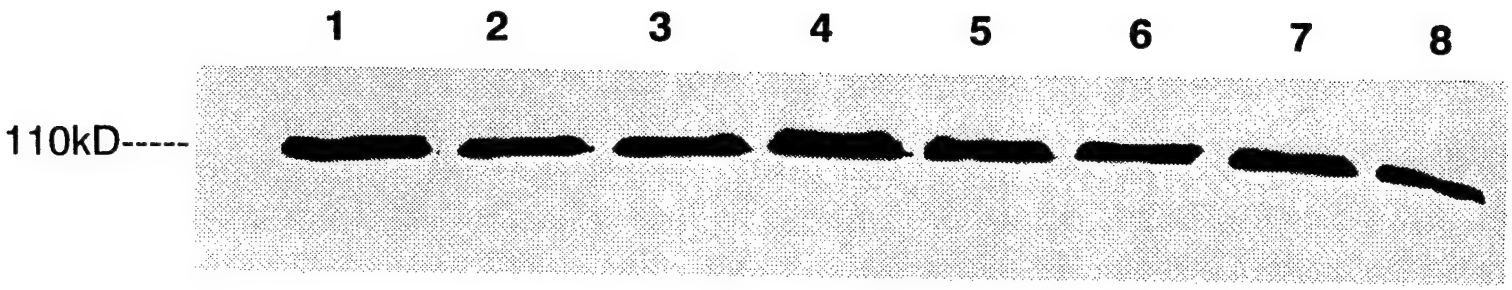


**Fig 3. Western blot of FGFR-1 of the proximal ends of sciatic nerves obtained 4 days postoperatively.**
**1. and 4. Nerves tied with #6 suture**
**2. and 5. Nerves sealed with a bipolar coagulator**
**3. and 6. Nerves buried in muscle**
**7. Nerves with no treatment**
**8. Normal control**

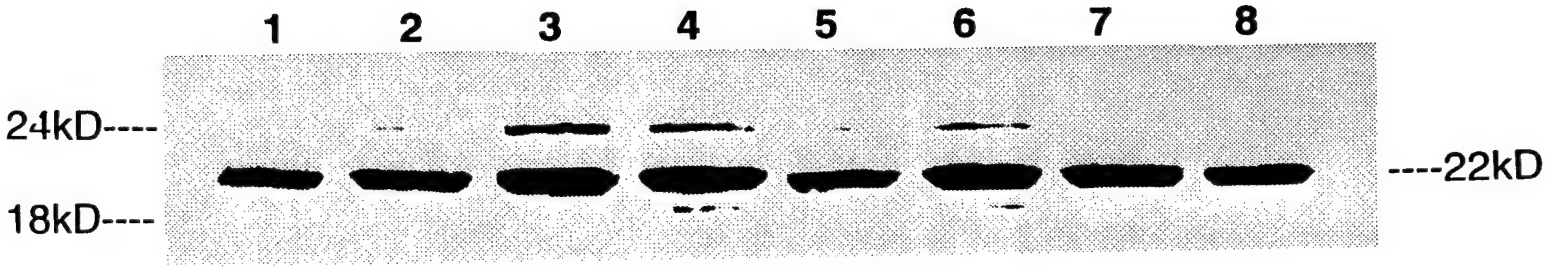


**Fig 4. Western blot of bFGF of the proximal ends of sciati nerves obtained 16 days postoperatively.**

**1. Normal control**
**2. Nerves buried in muscle**
**3. and 6. Nerves with no treatment**
**4. and 7. Nerves tied with #6 suture**
**5. and 8. Nerves sealed with a bipolar coagulator**

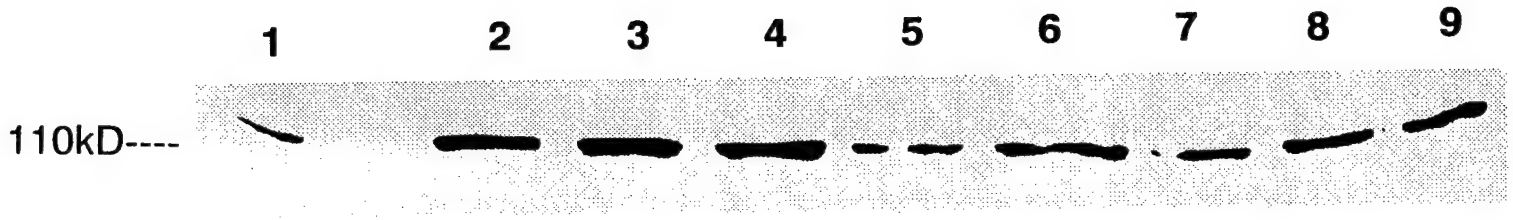


**Fig 5. Western blot of FGFR-1 of the proximal ends of sciatic nerves obtained 16 days postoperatively.**

**1. Normal control**

**2. and 5. Nerves sealed with a bipolar coagulator**

**3. and 6. Nerves tied with #6 suture**

**4. and 9. Nerves with no treatment**

**7. and 8. Nerves buried in muscle**

# V. Neuroma Formation and Fate of the Schwann Cells in the Constriction of Sciatic Nerve and Homograft Nerve Repair


## Summary

A fluorescent dye with high affinity for DNA (DAPI) was used to investigate the origin of the cellular components in the formation of neuroma. In the first experiment, unilateral sciatic nerve of rats was injected with 3 $\mu$l DAPI (20 $\mu$g/ml). Four weeks later, the same rats underwent a 10 mm homograft. A section of contralateral sciatic nerve was used as a homograft and surgically connected to the DAPI injected sciatic nerve. In another animal model, sciatic nerves of five rats were constricted completely with a No. 4 suture. The DAPI was injected into the nerve either proximally or distally to the constriction. The rats were sacrificed at 2, 6, and 10 weeks post-secondary surgery. Grossly, the nerve graft and adjacent proximal sectioned sciatic nerve ends were thickened and the graft was obviously shortened. The nerves were sectioned in a cryostat and used for fluorescent microscopy. In the first group of animals, the thickened tissue, suggesting an early neuroma, did not show many cells crossing the interface between graft and recipient nerve within six weeks, but by ten weeks, an increasing number of cells migrated from recipient nerve to the graft. In the second group of animals, connective tissues were found growing around the constricted site 2 weeks post surgery. Histological examination showed cells with labeled nuclei in the connective tissues which suggest that fibroblasts of epineurium from both proximal and distal epineurium can migrate to the constricted area to form a neuroma.

## Background

In the normal nerve, an important function of Schwann cells and endoneurium is to insulate axons from the surrounding tissues. If this limiting barrier is destroyed, regenerating axons escape into a disorganized mass of fibroblasts and Schwann cells to form a nodule, bulb or neuroma {36}. In the anastomosis area of the homograft nerve repair, the endoneurium and Schwann cells are lesioned. In some cases this promotes the development of the neuroma. A constriction can induce pseudoneuromas by causing proliferation of fibrous tissue of epineurium, perineurium or endoneurium {30, 33}. While Schwann cell migration was proven in developing peripheral nerves {37}, local proliferation is the main source of Schwann cells in the distal segments of cross-anastomosed nerves {34, 27}. 4,6-Diamidino-2-phenylindole hydrochloride (DAPI) is a fluorescent dye with high affinity for DNA. DAPI can be used to supplement cytochemical studies involving cell division in the nervous system {35}. The present study investigates the migration of cellular components in the neuroma formation and homograft nerve repair.

## Methods

Thirteen adult male Sprague-Dawley rats were used in the study. In the first experiment, the unilateral sciatic nerves of six rats were injected with 3 $\mu$l DAPI (20 mg/ml). Four weeks later, the same rats underwent a 10 mm homograft. A nerve section obtained from the contralateral sciatic nerve was used as a homograft surgically connected to the DAPI injected sciatic nerve in three rats (Figure Ia). In another animal model, the sciatic nerves of five rats were constricted completely with No 4 silk suture. The DAPI was injected into the nerves either proximal or distal to the ligation (Figure Ib). The rats were sacrificed at

two weeks, six weeks and ten weeks respectively after surgery. The nerves were fixed overnight in 4% paraformaldehyde and stored in PBS solution. The nerves were sectioned in a cryostat and used for fluorescent microscopy.

## Results and Discussion

The nerve grafts and adjacent proximal sciatic nerve ends were thickened and the graft was obviously shortened. In some cases, the neuroma formed at the anastomosis, especially at six weeks post-operation. Microscopy revealed that at two weeks and six weeks, few cells migrated at the interface between graft and recipient nerve. But in the rats of ten weeks post-operation, the numbers of migrating cells was greatly increased (Figure II). The cell components of the neuroma developed in the anastomosis derived mainly from the proximal ends of the severed sciatic nerve. The histological evidence showed that the cell components in graft are similar to that in the normal nerve trunks, most of these cells migrated from recipient nerve to the graft. The immunocytochemistry showed positive staining for S-100 protein in the graft. In the constricted nerve trunk, at six weeks and ten weeks, the connective tissue grew around the ligature (Figure Va) and the connective tissue contained the nuclei with fluorescent dye (Figure Vb). In the nerve trunk proximal to the ligation, the nerve fibers had normal appearance beyond six weeks post-operation. But in the nerve distal to the ligation, the nerve fibers showed degenerative changes as evidenced by negative staining for S-100 protein. It appeared that after the nerve fibers degenerated, the Schwann cells died in the distal part of the severed sciatic nerve.

In this study, cells originated from proximal ends of severed sciatic nerve migrated to the graft and the neuroma developed at the interface. Most cells migrated after 6 weeks

post-operatively in the current study. It also seems that there was a re-arrangement of the Schwann cells in the graft. In the group with constricted sciatic nerves, the current study showed that the neuroma that develops from epineurium can come from the nerve trunk either proximal or distal to the ligation. This overgrowth of endoneural, perineural, or epineural sheaths is classified as a false neuroma {33, 38}. In the nerve proximal to the ligation, immunocytochemistry showed positivity for S-100 protein, which is consistent with Schwann cell differentiation {38, 28}. However, in the nerve trunk distal to the ligation, the normal appearance of the nerve fibers disappeared and Schwann cells showed degenerative changes as evidenced by negative staining for S-100 protein. These results are consistent with the fact that the proliferation and the fate of the Schwann cells are affected by the nerve fibers {27, 37}. The myelin of Schwann cells can not be retained for a long period after the nerve fibers degenerate.

## References


Aguayo, A.J. and et al. (1976) Multipotentiality of Schwann cells in cross-anastomosed and grafted and unmyelinated nerves: Quantitative microscopy and radioautography. *Brain Res* **104**, 1-20.

Berdon, J.H. and Hess, A.V. (1991) Neuromas. In: Gelberman, R.H. (Ed.) *Operative Nerve Repair and Reconstruction*, pp. 1525-1540. Philadelphia: Lippincott]

Bullitt, E., Lee, C.L., Light, A.R. and Willcockson, H. (1992) The effect of stimulus duration on noxious-stimulus induced *c-fos* expression in the rodent spinal cord. *Brain Res* **580**, 172-179.

Chou, S.M. (1992) Immunohistochemical and ultrastructural classification of peripheral neuropathies with onion-bulbs. *Clin Neuropathol* **11**, 109-114.

Hunt, S.P., Pini, A. and Evan, G. (1987) Induction of *c-fos*-like protein in spinal cord neurons following sensory stimulation. *Nature* **328**, 632-634.

Figures

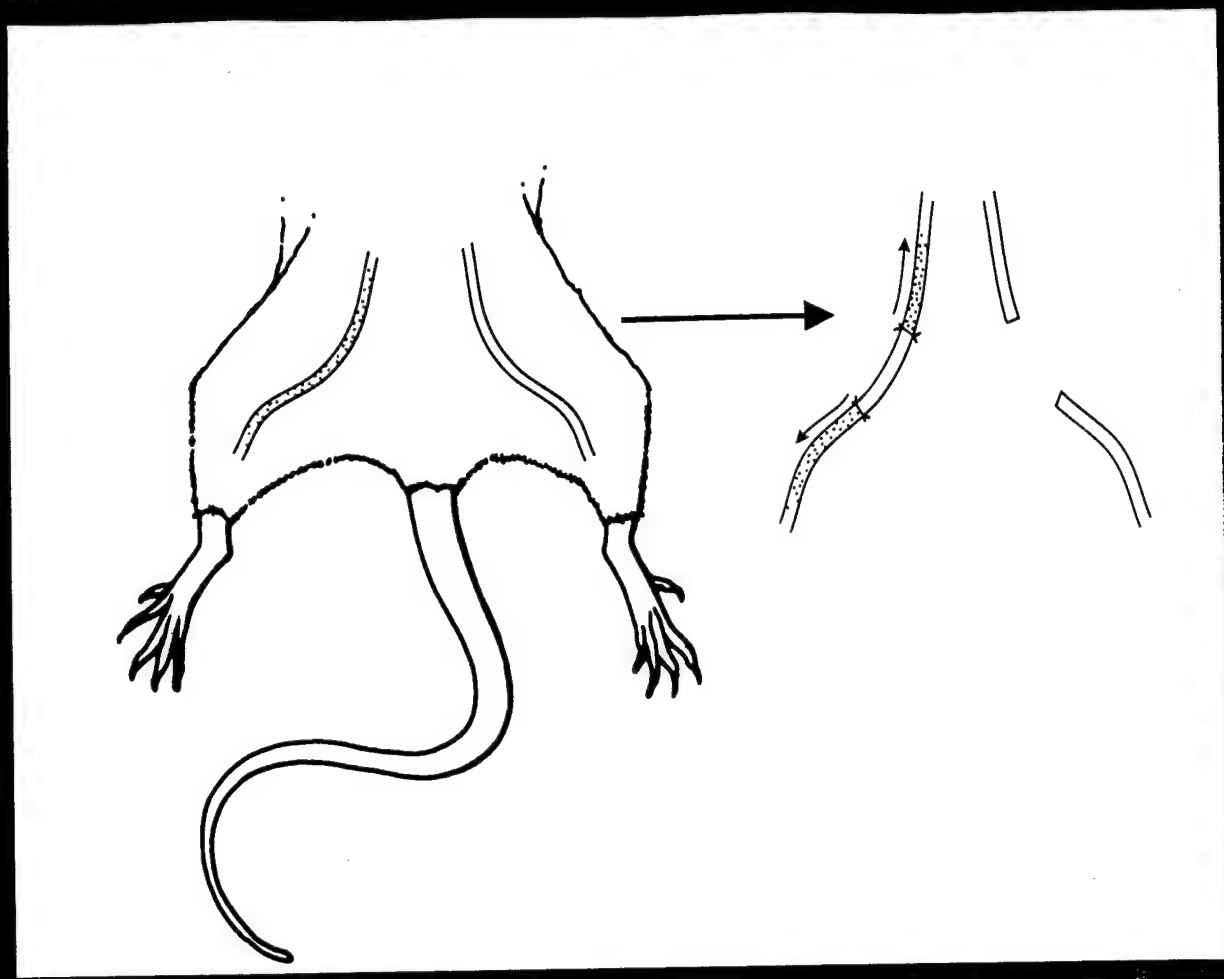

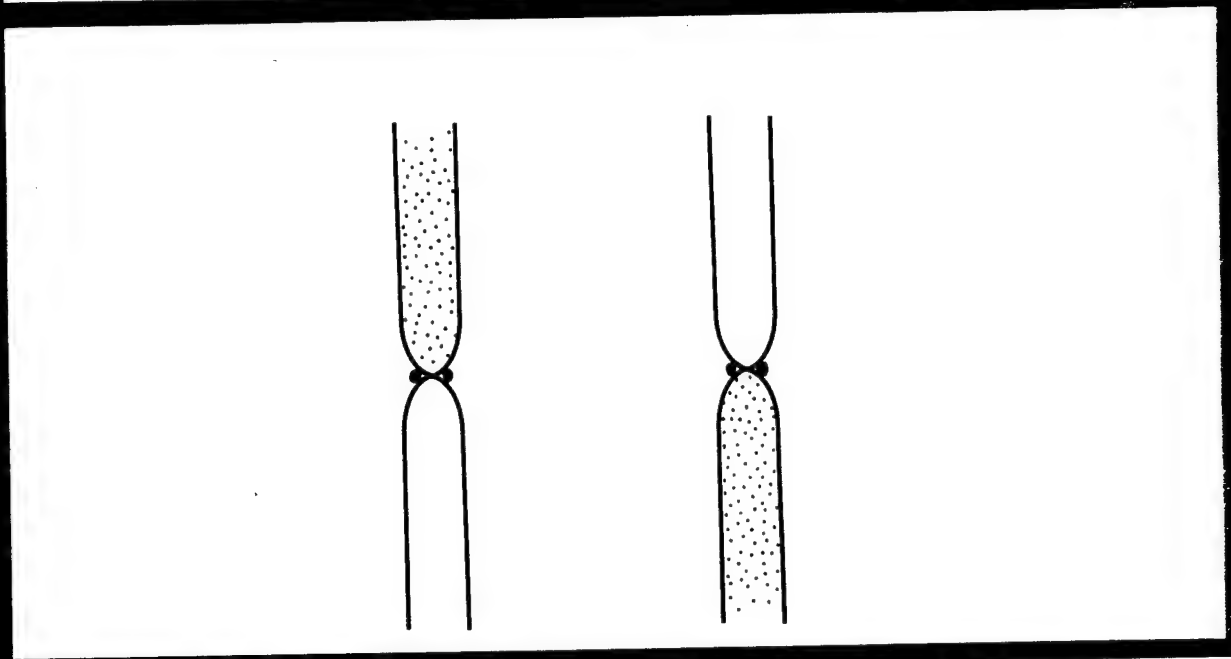

**Fig I. a, The left sciatic nerve of the rat was injected with DAPI. Four weeks later, a section of right sciatic nerve (10 cm) was cut and grafted to the left sciatic nerve. b, bilateral sciatic nerves of rat were constricted completely with No.4 silk suture. The DAPI was injected into the nerves either proximal (on the left) and distal (on the right) to the ligation.**

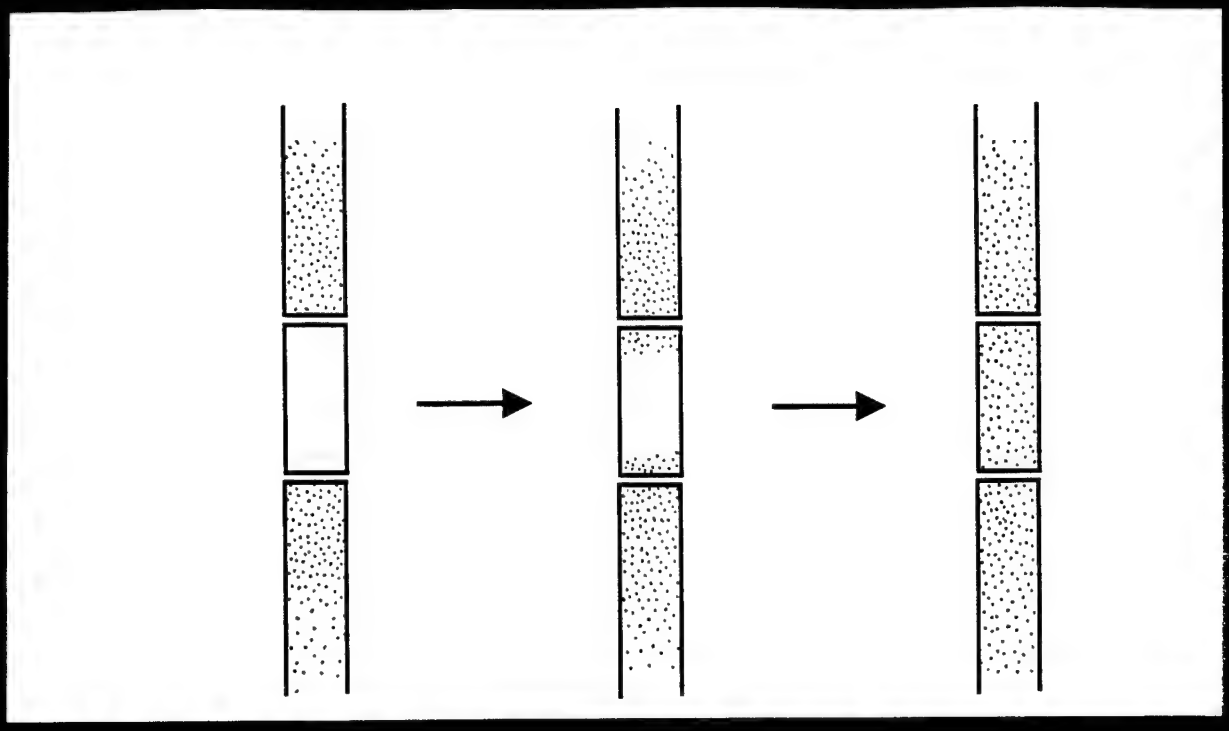

**Fig II. (a) schematic drawing showing the migration of the cells from recipient nerve to the graft at 2 weeks, 6 weeks and 10 weeks post-operatively. (b) A picture showing DAPI positive nuclei in the graft 10 weeks post-operatively.**

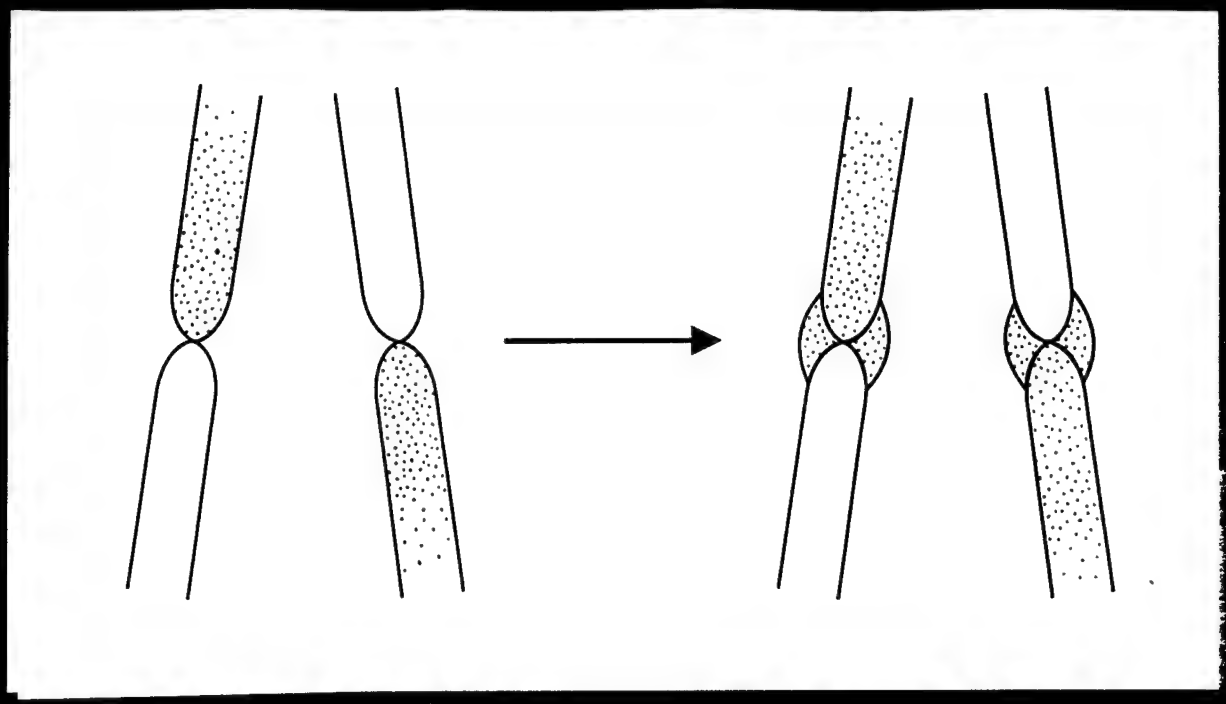

**Fig V. Diagram depicting that in the constricted nerve trunk, the connective tissues grew around the ligature (a). The connective tissues contain the nuclei with fluorescent dye (b).**

# VI. Expression of Immediate Early Gene *c-fos* in Central Nervous System in early Brachial Plexus Injury: A Comparison of Root Avulsion with Distal Transection


## Summary

To simulate accidental injury of the brachial plexus, twenty adult male rats underwent brachial plexus injury. The brachial plexus was lesioned by either root avulsion or transection 1.5 to 2 cm below the dorsal root ganglia under transient anesthesia with halothane inhalation. The rats were permitted to wake for 30, 60 and 120 min prior to sacrifice. Expression of *c-fos* proto-oncogene in the spinal cord and brain was detected by immunocytochemistry to identify the *c-fos* protein product. When both groups of animals were compared to the untransected control animals, an increase in *c-fos* gene expression in both the spinal cord and the brain was detected at 30 min after nerve transection. These levels continued to rise at 60 and 120 min post-nerve injury. While both groups demonstrated greater *c-fos* gene expression than controls, the groups with avulsive injury showed a greater elevation than those with distal transection. Fos-like immunoreactivity (FLI) appeared mainly in the dorsal horn of the spinal cord, somatosensory and pyriform cortex, hippocampus and thalamus of the brain. Our results suggest that stretch nerve injury close to the spinal cord may have distinct and heightened effects on gene expression in the central nervous system when compared to transection more distal to the spinal cord.


## Background

The *c-fos* gene has previously been shown to be induced within minutes in the central nervous system after various types of peripheral nerve stimulation. However, these earlier

studies concentrated on more distal injuries, using the rat sciatic nerve. In contrast, injuries closer to the spinal cord present a more complex neurosurgical problem. Regeneration and functional restoration of the patient differ considerably, depending on the site and nature of the injury. Recent investigations indicate that *c-fos* may serve as an anatomic and functional marker to reflect noxious or non-noxious stimulations. Previous studies have shown that transection as well as electrical stimulation of distal peripheral nerves will induce expression of the *c-fos* proto-oncogene in the spinal cord and higher cultures {2, 3, 7, 9, 16}.

The *c-fos* protein has been proposed to have a regulatory role in the cell and it may be involved in the transcription of genes responding to the events as well as for cellular repair processes {5, 11}. In addition, it has been postulated that the *c-fos* protein is a third messenger in the cellular signaling system. It may link extracellular signals to nuclear events {14}.

The activation of neuronal signaling systems in response to peripheral nerve lesions are not well known. Determining the components of such a signaling pathway is of obvious importance for understanding why some neurons are capable of surviving trauma to their peripheral processes, undergoing successful regeneration, whereas other neurons do not survive and undergo degeneration {8}. In the current study, the brachial plexus (nerves) injury was induced in two different ways: stretch injury at the dorsal ganglion region, or by cutting these nerves 1.5 to 2 cm peripheral to the ganglia. Expression of *c-fos* in the CNS was studied using an immunocytochemical method.

## Methods

Twenty male Sprague-Dawley rats (270-350 g) were anesthetized by halothane

inhalation. Two incisions were made bilaterally, on the midline of the back to expose the C4 to T1 vertebrae and the other from the axilla to the elbow to expose the brachial plexus nerves. The laminectomy was then performed under an operating microscope and the dorsal ganglia of C4 to T1 were exposed. The brachial plexus nerves were also exposed along their way from axilla to elbow. Then the rats were used in the following situations:,

1. The nerves of C4 to T1 were stretched in the dorsal ganglion region.
2. The nerves were cut about 1.5 cm below the dorsal ganglia
3. The nerves were not injured and the animals were used as sham control.

The rats were allowed to wake for 30, 60, or 120 min before sacrifice. A separate group of animals (controls) were not subjected to any of the three procedures described above. The rats were then anesthetized with pentobarbital and perfused intracardiovascularly with 250 ml warm saline, followed by 4% paraformaldehyde (500 ml). The spinal cord of C5 to C8 was post-fixed in the latter solution for 4 hrs and cryoprotected overnight in 30% sucrose in PB buffer. Frozen sections of 40$\mu$m were cut and process for *c-fos* protein-like immunoreactivity by the ABC method. Northern blots were performed according the methods of Chomozynski and Sacchi {#4} and New et al. {#12}.

**Results**

FLI detection showed elevated levels of *c-fos* expression 30 min postoperatively in the nerve-injured animals. These levels continued to rise at 60 and 120 min post-nerve transection. While both experimental groups demonstrated greater *c-fos* gene expression than controls, the animals with root avulsion showed a greater elevation than those with a transection below the ganglia within 120 min postoperatively. Immunocytochemistry

showed that, in the nerve-lesioned animals, the increased *c-fos* protein appears mainly in the dorsal horn of the spinal cord, and FLI neurons appear mostly in the I, II, and III laminae, with some showing in the IV, V, VI, VII, and X. In the ventral horn of the motor area, only a few FLI positive motor neurons could be seen in some cases (Fig. 1). In the brain, it was found that the FLI positive motor neurons appear in large numbers in the somatosensory and pyriform cortex, hippocampus, and thalamus. In all these sturctures, the FLI neurons in the animals with avulsive injury were evidently more abundant than in those animals injured below the ganglia (Figs. 2, 3).

## Discussion

Brachial plexus injuries are commonly found in patients who have experienced trauma to their upper limb(s). The injury usually causes a serious functional problem of the injured upper extremity in the patient's later life. This disability is attributed to the fact that some cells with axotomy do not survive and regenerate. The cellular responses to the axonal lesions are not well known. The proto-oncogenes function in several aspects of signal transduction processes. They may transfer the information between and within cells {11}

Expression of *c-fos* been found in the CNS in response to many kinds of stimulation, such as mechanical, chemical, electrical, thermal, or inflammatory {1, 3, 6, 7, 8, 9, 10}.

Moreover, it has been proven that *c-fos* expression can reflect the types of stimulation administered {7, 9}. Earlier studies were mostly performed on anesthetized animals and some authors have noted that anesthetics and analgesics can affect the *c-fos* expression {9, 13}. Hunt et al. {#7} reported that distribution of FLI neurons in the lamina of spinal cord

was related to the nature of the sensory stimuli.

In the present study, nerve trunks, including all kinds of afferent and efferent nerve fibers, were transected. The transection is a kind of persistent stimulation to the involved neurons {15}. Our results demonstrate that FLI in the nerve transections or avulsion were similar in distribution, but different in the amounts of mRNA or Fos-like proteins. The results suggest that the two-site transections might produce a similar type of stimulation to the CNS; however, the injury in the dorsal ganglion region produces a more intense stimulation than the transection below the ganglia. We investigated early stage changes, including those occurring within 30, 60 and 120 min. Although changes were evident in the dorsal horn of the spinal cord, there was not much change noted in motor neurons in the spinal cord. In order to provide more information to the understanding of regeneration and degeneration of spinal neurons after peripheral nerve injury, further studies are needed correlate *c-fos* expression and neuronal cell death.

## References


Abbadie, C., Lombard, M.-C., Morain, F. and Besson, J.M. (1992) Fos-like immunoreactivity in the rat superficial dorsal horn induced by formalin injection in the forepaw: Effects of dorsal rhizotomies. *Brain Res* **278**, 17-25.

Bullitt, E. (1989) Induction of *c-fos*-like protein within the lumbar spinal cord and thalamus of the rat following peripheral stimulation. *Brain Res* **493**, 391-397.

Bullitt, E., Lee, C.L., Light, A.R. and Willcockson, H. (1992) The effect of stimulus duration on noxious-stimulus induced *c-fos* expression in the rodent spinal cord. *Brain Res* **580**, 172-179.

Chomcaynski, P. and Sacchi, N. (1987) Single-step method of RNA isolation by acid quanidinium thiocyanate-phenol-chloroform extraction. *Anal Biochem* **162**, 156-159.

Curran, T., Miller, A.D., Zokas, L. and Verma, I.M. (1984) Viral and cellular *fos* proteins: A comparative analysis. *Cell* **36**, 259-268.

DeLeo, J.A., Coombs, D.W. and McCarthy, L.E. (1991) Differential *c-fos* protein expression in mechanically versus chemically induced visceral nociception. *Mol Brain Res* **11**, 167-170.

Hunt, S.P., Pini, A. and Evan, G. (1987) Induction of *c-fos*-like protein in spinal cord neurons following sensory stimulation. *Nature* **328**, 632-634.

Jones, K.J. and Evinger, C. (1991) Differential neuronal expression of *c-fos* proto-oncogene following peripheral nerve injury or chemically-induced seizure. *J Neurosci Res* **28**, 291-298.

Menetrey, D., Gannon, A., Levine, J.D. and Basbaum, A.I. (1989) Expression of *c-fos* protein in interneurons and projection neurons of the rat spinal cord in response to noxious somatic, articular, and visceral stimulation. *J Compar Neurol* **285**, 177-195.

Morgan, J.I., Cohen, D.R., Hempstead, J.L. and Curran, T. (1987) Mapping patterns of *c-fos* expression in the central nervous system after seizure. *Science* **237**, 192-197.

Morgan, J.I. and Curran, T. (1991) Stimulus-transcription coupling in the nervous system: Involvement of the inducible proto-oncogenes *fos* and *jun*. *Annu Rev Neurosci* **14**, 21-51.

New, G.A., Hendrickson, B.R. and Jones, K.J. (1989) Induction of heat shock protein 70 mRNA in adult hamster facial nuclear groups following axotomy of the facial nerve. *Metab Brain Dis* **4**, 273-279.

Presley, R.W., Menetrey, D. and Levine, J.D. (1990) Systemic morphine suppresses noxious stimulus-evoked Fos protein-like immunoreactivity in the rat spinal cord. *J Neurosci* **10**, 323-335.

Sagar, S.M., Sharp, F.R. and Curran, T. (1988) Expression of *c-fos* protein in the brains: Metabolic mapping at the cellular level. *Science* **240**, 1328

Sharp, F.R., Griffith, J., Gonzalez, M.F. and Sagar, S.M. (1989) Trigeminal nerve section induces Fos-like immunoreactivity (FLI) in brainstem and decreases FLI in sensory cortex. *Mol Brain Res* **6**, 217-220.

Smith, M.A., Banerjee, S., Gold, P.W. and Glowa, J. (1992) Induction of *c-fos* mRNA in rat brain by conditioned and unconditioned stressors. *Brain Res* **578**, 135-141.

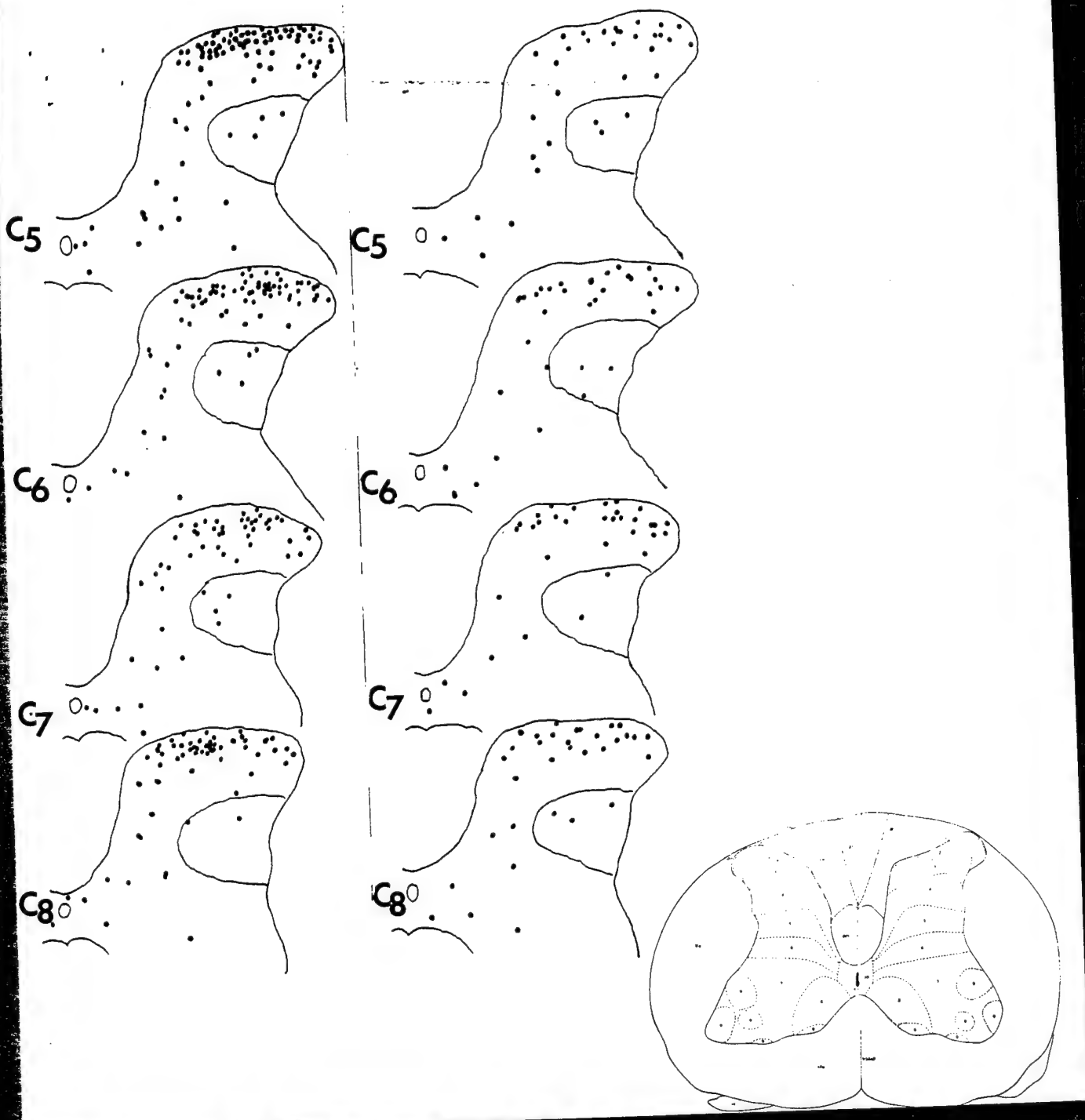


**Fig. 1. Camera lucida drawing showing the Fos-like proteins in the spinal cord of C5 to C8 induced by peripheral nerve injury. Each dot represents one labeled cell. Note that there are more labelled cells in the superficial dorsal horn than in the deeper layers of the spinal gray, and that there are more labelled cells in the animals with injury in the ganglion region (on the left) than those below the ganglia (on the right).**

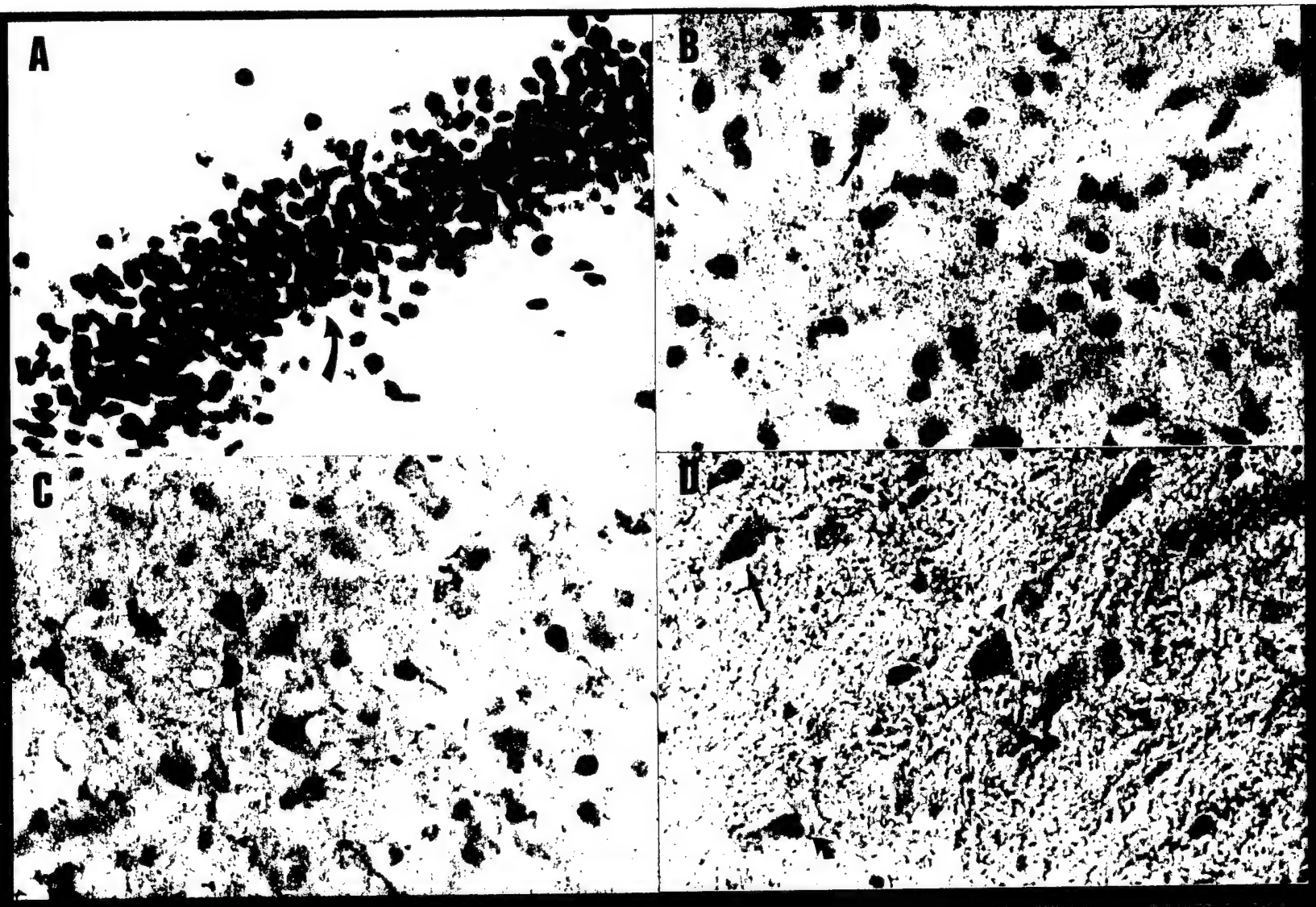


**Fig. 2. Photomicrographs demonstrate FLI neurons in some structures of central nervous system from rats with injury in the dorsal ganglion region. A: Dentate gyrus of hippocampal region (X125). B: Thalamus (X125). C: Layer 5 of somatosensory cortex (X125). D: Ventral horn of spinal cord (X125).**

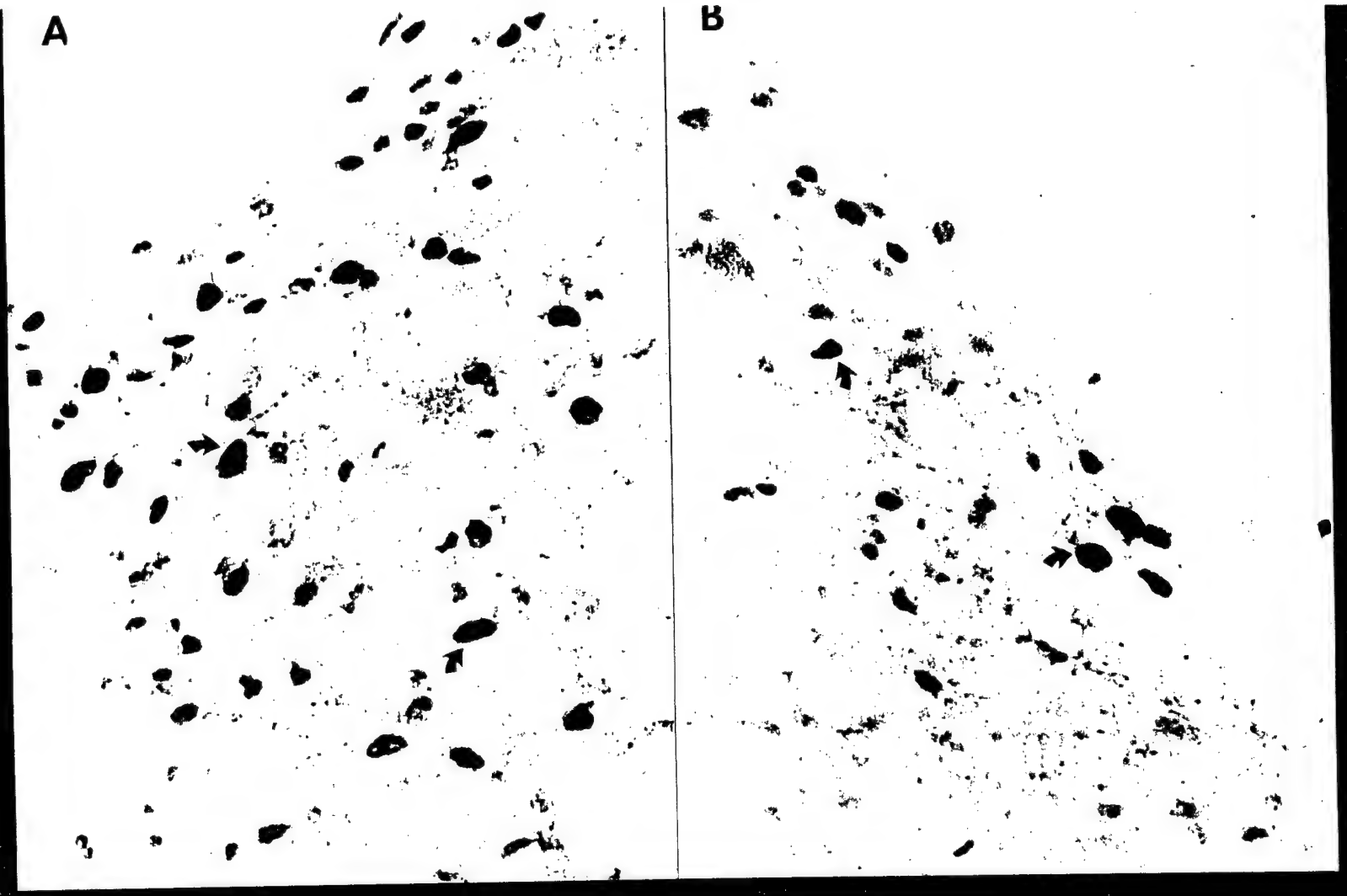




Fig. 3. These photomicrographs illustrate the FLI neurons in spinal cord and brain from the rats 2 hours postoperatively. Note that there are evident differences in the numbers of FLI neurons between the animals with the injury in the dorsal ganglion region and below the ganglia. A: Superficial dorsal horn of C6 from a rat with injury in the ganglion region (X125). B: Equivalent region of A from a rat with the injury below the dorsal ganglia (X125).

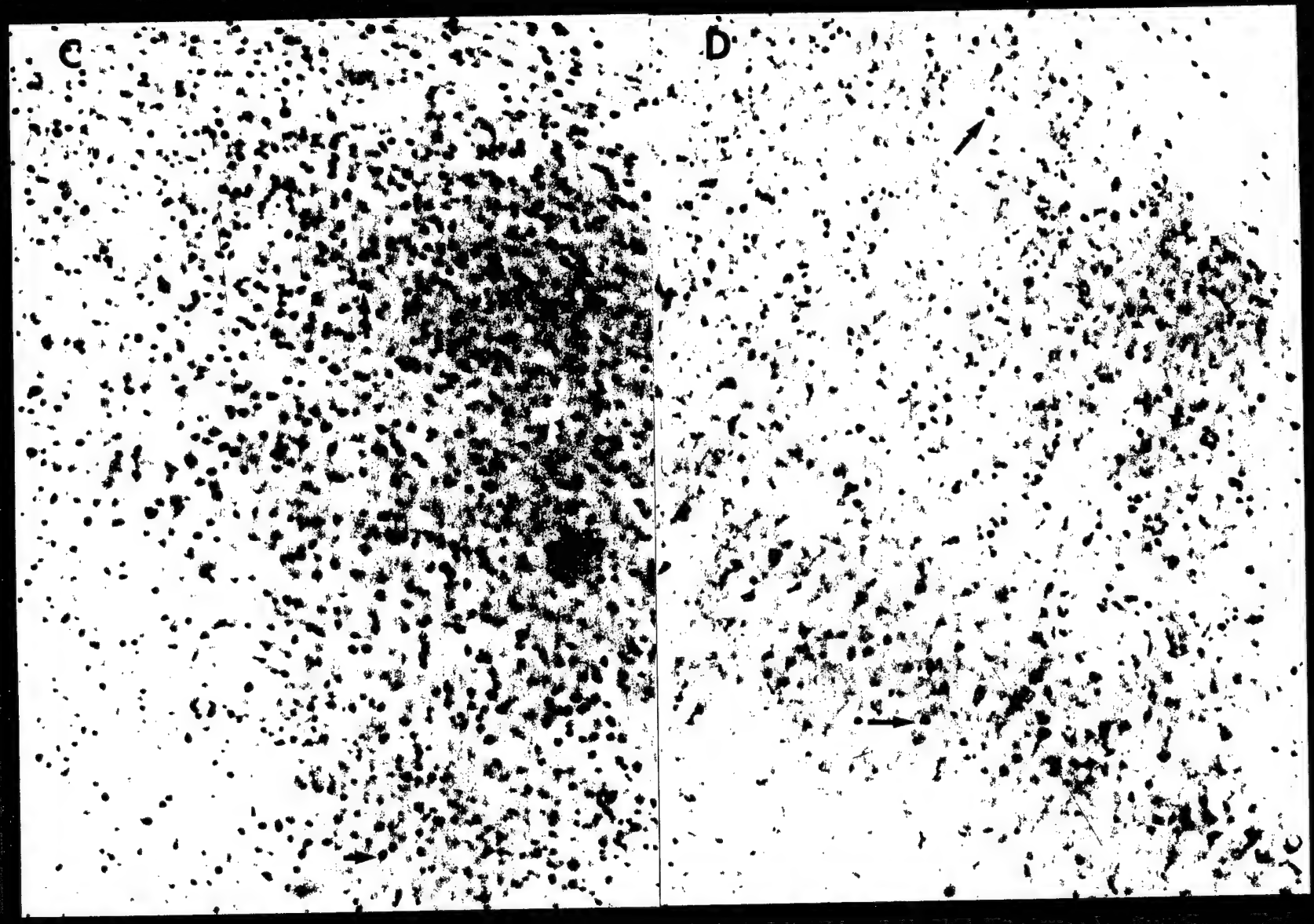


**Fig. 3. C: Somatosensory cotex of a rat with the injury in the dorsal ganglion region (X31). D: An equivalent region from a rat with the injury below the dorsal ganglia (X31).**


**Fig. 3. E and F: Hippocampal regions of the rats with the injury in the dorsal ganglion region and below the ganglia respectively (X31).**

# VII. Detection of MAPK Activation in Fibroblasts Cultured from Human Neuroma Tissues


## Summary

MAPK (Mitogen-activated protein kinase) plays a cardinal role in regulating many cellular processes and is a major currency in signal transduction pathways. MAPK pathways are extensively used for transcytoplasmic signaling to the nucleus, where transcription of specific genes is induced through phosphorylation and activation of transcription factors. MAPK is activated through threonine/tyrosine phosphorylation by a dual specificity protein kinase, known as a MAPK kinase (MAPKK), which, in turn, is activated through serine phosphorylation by a third protein kinase, known as MAPKK kinase (MAPKKK). In the present study, we measured activation of MAPK using TNF- and IL-1- stimulated confluent fibroblasts cultured from human peripheral nerve neuromas. Our data demonstrates that a rapid increase in the activation of MAPK was produced by TNF and IL-1, and we also observed a synergistic effect on MAPK activation. Our study suggests that these cytokines (TNF and IL-1) must, in part, share the same signal transduction pathways proceeding from MAPK kinase to MAPK although the early post-receptor events are unclear. These results suggest that the early inflammatory events associated with nerve injury may increase neuronal fibroblast proliferation.


## Background

TNF and IL-1 are pleiotropic cytokines that posses a wide spectrum of immunologic and nonimmunologic activities. The activities shared by TNF and IL-1 include cytostatic or cytotoxic effects on certain tumor cells, inhibition of lipoprotein lipase, production of

collagenase and prostaglandin $E_2$, induction of $\beta$-interferon and induction of granulocyte macrophage colony-stimulating factor. The effects of TNF and IL-1 on a variety of cells in vitro as well as systemic effects in vivo are often biologically indistinguishable. When two cytokines are used together in experimental studies, the net effect often exceeds the additive effect of each cytokine. This synergism between these two molecules include stimulating fibroblasts to produce $PGE_2$, cytotoxic effect on certain tumor cells, inducing neutrophilic infiltration in acute inflammation and a Shwartzman-like reaction. TNF and IL-1 can respectively stimulate fibroblasts to secrete NGF which is responsible for outgrowth of neurites. Other studies from this laboratory have shown (by immuno-histo-chemical methods) an increase in NGF in the experimental monkey neuroma.

TNF and IL-1 are distinct structurally and bind to different receptors, but produce similar biological activities. Activation of the same transduction pathways leading to synergistic activation of MAPK as shown in the present study may contribute to the biological events mentioned above. We used physiological concentrations of the cytokines to stimulate fibroblasts which increased MAPK levels 3-4-fold when compared to control cells. When TNF$\alpha$ and IL-1 were used together, the activity of MAPK increased dramatically up to 5 to 6-fold over control (Fig. 1). The results show that synergistic action significantly increases MAPK (up 20.05). The concentration of TNF-$\alpha$ and IL-1 were 10 ng/ml, and cells were removed from serum for 24 hrs prior to the 15 min stimulation. The data is presented as mean $\pm$ standard error and represents three replications for each of two different experiments.

Recent studies in fibroblasts have shown that MAPK activity is closely related to early G1 and later G1 phase transition. Our study indicated that TNF and IL-1 also possess

mitogenic effect on neuroma fibroblasts. This suggested that TNF and IL-1 are likely to accelerate fibroblast release from G1 block allowing them to proliferate. Other investigators have found TNF protein localized within nerve fibers in the cerebral infarct at 6 hours after ischemia. TNF and IL-1 were also detected in wound effusion fluid, which suggests that TNF and IL-1 show up early in damaged tissues as a possible consequence of the accumulation of activated macrophages and lymphocytes. In the effected peripheral nerve, accumulation of cells within the restricted volume of the nerve fiber may, in fact, result in locally high concentration of cytokines.

**Protein Kinase Activity in Neuroma Tissues**

Our observations have confirmed that cytokines associated with inflammation can induce activation of MAPK in fibroblasts cultured from neuroma tissues. We infer that the activity of MAPK will be varied at the different stages of neuroma formation because cellular content and the types of cytokines in peripheral nerve tissues are temporally changing during the early phase of the response to injury. The primary study on cells cultured from monkey neuromas compared with cells from segments of normal monkey nerve showed that there were differences in MAPK activity between the normal nerve, and when compared to the proximal part of the neuroma and the middle part of neuroma. MAPK activity in the proximal part is higher than that in the middle part and in normal nerves. Nearly the same level was detected in normal nerve and middle part of neuroma at ten months. The neuroma itself is dense due to the accumulation of collagen, but the proximal part of the neuroma is more cellular and has more neural tissue. In subsequent studies, we will further confirm the relationship between the MAPK activation and neuroma formation. Animal neuroma models will be set up in rats and rabbits after microsurgery. The proximal nerve stumps will be

obtained at different study points, one day, three days, one week, two weeks, one month, two months, three months and six months. Protein extracts will be used as samples for detecting protein kinase activity.

**Technique for Efficient Neuroma Tissue Culture**

Neuroma tissues have a dense collagen matrix and are quite different from other tumors. After being cut apart, many of the small pieces float in the medium; however, cells require a solid substrate upon which to grow so, therefore, the tissues often fail to develop in culture. We have modified older methods, developing a new culture procedure which has made cell culture more than before. A brief description of the method is as follows: Rinse the neuroma tissue extensively with PBS buffer and wash the tissue three times with serum free medium. Move the neuroma tissue onto a 100 mm polystyrene tissue culture dish and cut the tissue into small pieces, about 3 mm in diameter with a number 22 surgical blade. Place 4 or 5 pieces of neuroma tissue into a 25 cm flask and tighten the cap. Let the tissues dry for 15 min while assisting the tissues to attach to the bottom of the flask. Slowly and carefully add 3 ml medium supplemented with 20% fetal bovine serum, 100mg/ml penicillin, and 100 mg/ml streptomycin. Incubate and allow fibroblasts to sprout from tissues at 37°C, 5% $CO_2$ for 5 days while changing the medium (3 ml each time) twice in two day intervals. After fibroblasts sprout from cut tissues, fall on the flask, and begin to grow, gently shake the flask isolating the tissues from the bottom of the flask. Let the tissues move to new places. Allow the tissues to grow for another 4 or 5 days with medium change as before. When the cells grow to confluence, passage or freeze the cells. Now we can supply large numbers of neuroma cells for a variety of studies.

In our studies, we found that after several subpassages the cellular and molecular

character of fibroblasts cultured from neuroma tissues change. We have used factors (TNF$\alpha$, IL-1, PDGF) to stimulate fibroblasts and measure MAPK activation. Passage numbers 2 to 6 have shown a good response to these cell signaling factors at different concentrations. However, after passage 7 the responses of the fibroblasts declined, and at 10 subpassages later the fibroblasts failed to respond with MAPK activation. At present it is not clear at what point in the signaling pathway this occurs, but it is an important cautionary point in these experiments.

**Uncovering the Underlying Factors of Neuroma Formation**

In both the neurosurgical patient population and animal studies, the formation of disorganized, enlarged bulbs are more localized to the proximal nerve stumps after nerve injury. If the damaged stump is part of a large nerve trunk, such as the sciatic nerve, a large neuroma will be formed. We know that both proximal and distal nerve stumps are exposed to vascular cells, particularly those of immune origin, blood clots, damaged and dying cells, extra-cellular fluid, inflammatory cells: macrophages, lymphocytes, neutrophils and the many types of cytokines secreted by the cells or transported from elsewhere.

An interesting question is why neuromas are formed in proximal, but not in distal stumps. The differences between proximal and distal nerve stumps are blood supply and regenerating axons which connect to the central nervous system. After transection injury of nerves, the blood vessels associated with the nerves are usually damaged at the same time. In the distal stump, blood supply is stopped altogether; however, axon and cellular degeneration continues, but in the proximal stump there may well be a continuous blood supply and the initiation of axon regeneration. At the same time the general surrounding environment is quite similar. Spaces and matrix for cell growth and the presence of

inflammatory cells are similar for both proximal and distal stumps. From this it is possible to suggest two key factors which may ultimately determine whether or not a neuroma forms following injury. These factors are: (1) blood supply which is a fundamental condition for tissue repair and cell growth, and (2) the presence of neural tissue as well as the transport of material from the cell body. Fibroblasts are the primary cell type found in the neuroma. Moreover, the characteristics of this pathological state suggest that it may be one of a fibrosed tissue. Fibroblast proliferation in neuroma formation may be a simple response to tissue repair or it may have additional influences.

**Studies in Progress**

**Group I.** Studies have been designed to answer these questions. Microsurgical procedures will be used to ligate the tibial branch of the sciatic nerve in rabbits after careful isolation of epineural blood vessels to maintain the blood supply to the distal stump. It is realized that endoneuronal vessels would be damaged. In this situation, distal and proximal nerve stumps have a similar volume of blood supply in a period of microvascular regeneration. A chemical cuff located closer to the dorsal root ganglia with colchicine will be used to slow axonal transport. Alternatively, location of a thin plastic tube within the nerve which is then connected to an osmotic pump can be used to effect axonal transport at various times after the ligation. A pump is used to continuously transport materials from ganglia to distal stumps. An artificial environment is made in distal stumps which is the same as natural proximal stumps, and proximal stumps is only allowed to have a blood supply without nerve axon regeneration.

**Group II.** In this experiment, the epineural blood supply to the proximal stump will temporarily interfere with using vascular clips. This will be maintained for 2 days to two

weeks after ligation. The two groups of rabbits are kept for one or more months.

The results of these experiments will be important in understanding neuroma formation. A hyperplasia bulb is formed in proximal nerve stumps. The reasons are (1) fibroblast proliferation is only responsible to tissue damages; (2) there are still some survivor axons.

There is a formation of bulb in distal nerve stumps and no bulb in the proximal stumps. This is because the materials transported by the axons contain some factor or factors which are closely associated with neuroma formation.

**Group II.** Neuroma formation is only in proximal stumps and not in distal stumps, which suggests that blood supply is responsible for cell growth and tissue repair. It is a common fundamental factor, not a special factor for neuroma formation.
Neuroma formation happens in both side stumps, which suggests fibroblast proliferation is due to cell response to tissue damage and nerve repairing.

In an additional set of experiments, we will employ the osmotic pump to introduce inhibition of fibroblast proliferation directly to the site of potential neuroma production. Clinically, this approach may be implemented, as the damage has occurred due to surgical manipulation associated with repair. Direct manipulation of the cells responsible for neuroma formation is the most efficient way to encourage regeneration and decrease complications from neuroma.

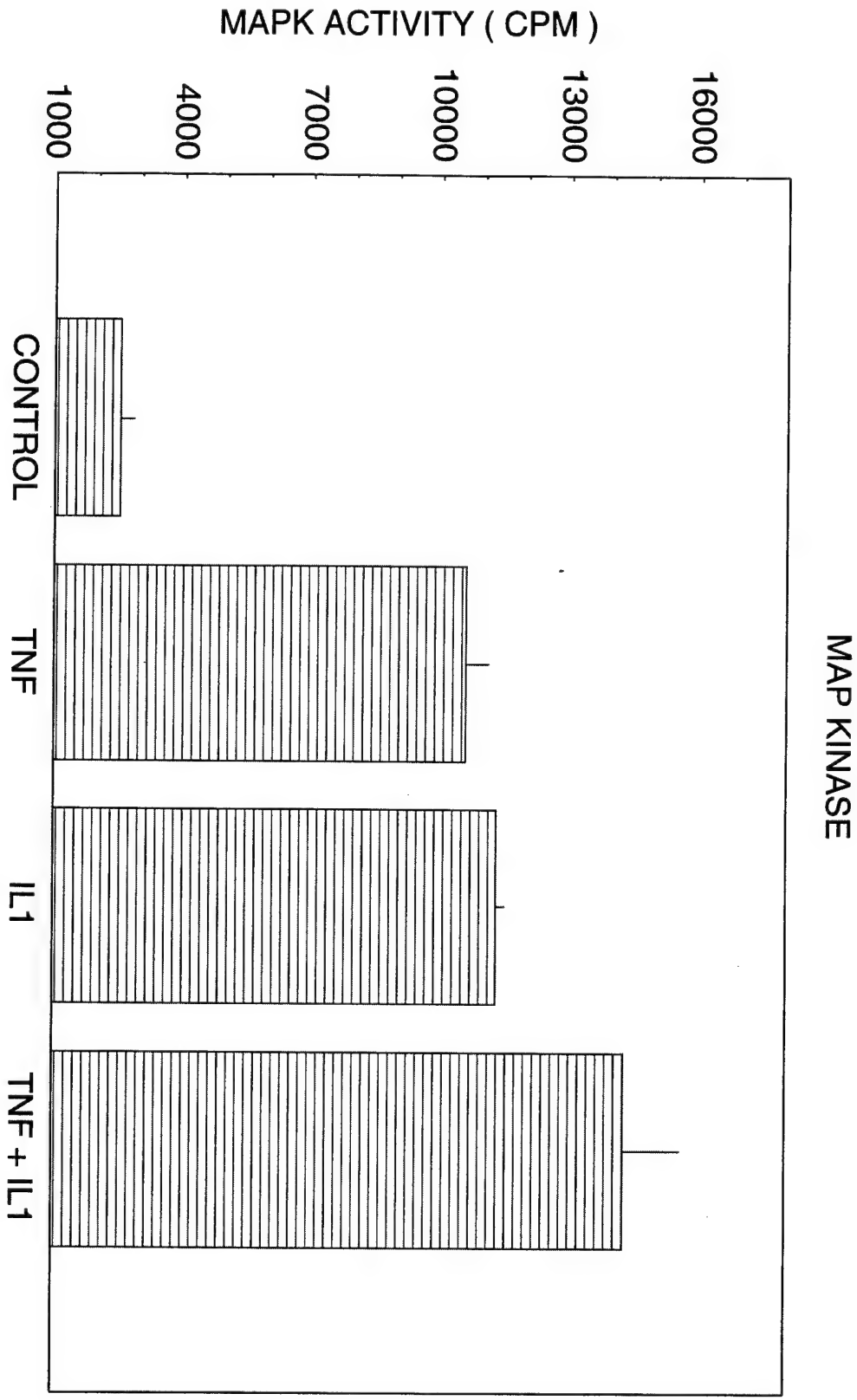
MAPK ACTIVITY ( CPM )
1000
4000
7000
10000
13000
16000
CONTROL
TNF
IL1
TNF + IL1
MAP KINASE

Figure 1

# VIII. Opioid Receptors in Peripheral Nerve

Opioid receptors in the mammalian CNS were originally studied to determine their pharmacological, behavioral, and receptive binding properties. These studies revealed three receptor types: mu, delta, and kappa, each of which responds to different noxious stimuli. Binding sites for these receptors have been found throughout the CNS, as well as peripheral tissues. Recent research has emphasized the role of peripheral opioid receptors and immune system interaction releasing endogenous peptides toward these peripheral receptors. Our goal was to determine if these receptors are found in peripheral neuroma tissue from humans, many of which are extremely painful. In order to distinguish the location of these receptors within the neuroma tissue and peripheral nerve, double labeling with anti-neurofilament protein, which has been shown to bind to differing sensory divisions in nerves, will be used. Quantitative analysis of human nerve, painful neuroma, and non-painful neuroma will be carried out with the mu (MOR1) and delta (DOR1) receptor antibodies (a gift of Dr. Elde at the University of Minnesota) in order to find the difference in proportion of receptors for noxious stimuli in normal, painful and non-painful neuromas.

Human nerve and neuroma tissue were obtained at the time of surgical correction from 3 patients who had peripheral nerve injuries. The patients all had trauma to peripheral nerve sites with neuroma formation occurring subsequent to injury. The surgeries were carried out 8-10 months after injury. Nerve and neuroma sections removed from these patients during their surgical procedures were initially frozen in liquid nitrogen. These sections were then used for cryostat section in the method described below.

To treat both the technique and the antibodies, rat spinal cord samples were used for

immunohistochemistry. Spinal cord sections were dissected, isolated, and fixed with 4% paraformaldehyde in 0.1 M phosphate buffer. Cryostat sections were then incubated with rabbit anti-MOR1 (1:300), rabbit anti-DOR1 (1:300), or mouse anti-Kappa2 opioid receptor (1:300) KOR1 (Calbiochem) for 18-24 hours at 4°C with PBS containing 0.3% Triton-X. The sections were then washed in PBS several times. After washes, the sections were incubated with anti-mouse and rabbit fluorescence and anti-mouse Texas Red second antibody. Controls for human nerve, neuroma, and rat spine were carried out by incubating sections identically, with the exception of using only the primary antibody solvent.

Control sections failed to have any immunoreactivity; however, the possibility exists for cross reactivity with structurally related proteins.

**Double staining for KOR2 and NF200.** The same procedure described above was used for tissue preparation for double labeling. Cryostat sections were incubated for 24 hours at 4°C with a mixture of mouse anti-NF200 (Sigma) and rabbit anti-MOR1 receptor (1:300) monoclonal antibodies. Samples were then incubated with a mixture of Texas Red anti-mouse IgG and fluorescence anti-rabbit IgG. Control experiments showed no cross reaction between primary and secondary antibodies.

In the spinal cord of the rat sectioned at L1-L4, anti-MOR1 and anti-DOR1 reactivity was noted in the superficial dorsal horn. Controls for the serial section of the same tissue sample showed no reaction with anti-MOR1 or anti-DOR1. We noted reaction in the white matter and ventral horn; however, immunofluorescence was much lower in these sections and no areas of dense reaction were noted. The reaction of MOR1 and DOR1 was most notably in Lamina 1 and border Lamina II in the dorsal horn of the spinal cord.

Neuroma tissue sections showed reaction with KOR2, MOR1, DOR1, and NF200.

We took double labeled MOR1 and NF200 sections of the same area of cryostat sections with two different filters. The section revealed no areas of double staining and had distinct reaction areas for both markers. We labeled NF200 with Texas Red, while the second label for the MOR1 was an anti-rabbit fluorescence label. In summary, we did not find conclusive NF200 and MOR1 activity on the same area of neuroma tissue with double labeling, although it was clear that evidence for peripheral opioid receptors was found in human nerve and neuroma. KOR2 immunofluorescence revealed positive reaction in human neuroma tissue.

Previous research on the presence of opioid receptors in peripheral tissue has focused on rat peripheral nerve tissue. In those pervious experiments, neuroanatomical localization of opioid binding sites in the sciatic nerve, peripheral cutaneous nerve fibers, and immune cells in peripheral nerve have been found. Research in this area has also revealed intrinsic modulation of these receptors via opioid-type proteins released by immunocytes in peripheral nerve terminals. These studies have also shown that local inflammation has an up-regulatory effect in the density of binding sites in the nerve and peripheral tissue. The present investigation reveals immunohistochemical proof for the presence of opioid receptor sites in the peripheral nerve and neuroma tissue of humans. Moreover, the difference, both quantitative and qualitative, in the density of binding sites in the tissues, as well as the sensory subtypes of opioid receptors, has been investigated.

In order to visualize the density of opioid receptor subtypes in peripheral tissue, KOR2 (Calbiochem), MOR1 and DOR1 receptor antibodies were used in immunohistochemical assays. The antibodies have high affinity to protein domains in the non-denatured receptors. Rat spine dissected from L1-L4 was used to confirm our findings. Previous studies have shown the presence of both MOR1 and DOR1 in the dorsal horn of the

rat spine. We confirmed these results, and also confirmed the existence of KOR2 receptor in the dorsal horn of rat spine. Our investigation then turned toward the same receptor subtypes present in human peripheral nerve tissue. MOR1, DOR1, and KOR2 receptor binding was noted in neuroma tissue in the human. In our study, both human painful and non-painful neuroma was used. Both tissues revealed density of fluorescence reaction; however, quantifying the difference between the two tissues could not be achieved. Furthermore, although the presence of all three receptor types had been revealed, the exact localization of the receptors cannot be determined. In hopes of addressing the latter issues stated previously, double staining studies with NF200 were carried out. In this section of our investigation we hoped we could localize, with immunofluorescence, areas of binding that would localize to sensory nerve. Our studies revealed that NF200 and all of the opioid receptors, in fact, did not bind to similar areas in the neuroma tissue. Although the results are inconclusive with respect to determining whether these opioid receptors are localized on sensory nerves, or if they are only found on immunocytes in the neuroma tissue, the likelihood that these receptors are on motor sensory fibers is diminished. The reasons include the results of previous experiments which have shown NF200 in higher proportions in motor sensory nerve fibers than in visceral fibers. Thus, the lack of localization of NF200 and opioid receptor antibody in human neuroma suggests one of two possibilities: 1) human neuroma contain mu, kappa, and delta opioid receptor subtypes on immunocytes and fibroblasts found in peripheral nerve tissue and not on the nerve fibers itself, and 2) human neuroma contains opioid receptors on visceral sensory nerve fibers.

The significance of our findings is quite extensive. Endogenous opioid activity in human neuroma can possibly reveal differences between painful and non-painful neuroma.

This can be done by Western blot analysis quantifying the difference in the opioid receptors in these two neuroma tissues. More importantly, the existence of these receptors can support the use of exogenous opioids in the peripheral nerve terminals for antinociceptive effects.

# IX. Sodium Channels in Human Neuromas

## Specific Aims

1. To determine if nerve injury alters the distribution/quantity of sodium channels.

2. To determine whether the sodium channel population is altered in human neuromas.

## Studies and Results

The study of sodium channels in nerve injury has proceeded well. Peripheral nerve fibers of *Carassius auratus* (goldfish) were acutely and focally injured by exposure to the neurotoxic agent, potassium tellurite ($K_2TeO_3$). Using a polyclonal antibody directed against the $\alpha$-subunit of the sodium channel, the injured nerves were examined using immunocytochemical and radioimmunoassay (RIA) methods. Identical studies were performed on contralateral control nerves from the same fish. These studies showed a focal accumulation of sodium channels within the tips of injured axons. The major increase in sodium channel concentration occurred between 7 and 11 days after toxin exposure; however, excess sodium channels persisted chronically in several axonal endings. These studies indicate that nerve injury which is severe enough to cause wallerian axonal degeneration can alter the sodium channel population in the subpopulation of injured axons.

The study of sodium channels within human painful neuromas has also proceeded well. Painful neuromas from 16 patients have now been examined using a site-specific anti-sodium channel antibody. This antibody is directed against an 18-mer peptide which corresponds to a region highly conserved in all known vertebrate sodium channels. Normal

sural nerves from 6 of these patients served as controls. All specimens were examined using the same antibody in both immunocytochemical and radioimmunoassay (RIA) methods. Immunocytochemistry showed abnormal segmental accumulation of sodium channels within many axons in the neuromas. Dense immunolocalization was especially apparent within axonal tips. Contrastingly, in sural nerves focal accumulation of sodium channels was restricted to nodes of Ranvier. RIA confirmed a significantly ($P = 0.0075$) greater sodium channel density in neuromas (median - 28.6; mean $\pm$ SEM = 32.5 $\pm$ 3.7 pM per g) as compared to sural nerves (median = 18.2; mean $\pm$ SEM = 17.1 $\pm$ 2.2 pM per g). These data indicate that sodium channels accumulate abnormally within the axons of human painful neuromas.

**Significance**

Peripheral nerve trauma is often associated with dysesthesias and painful impulses arising from injured axons. This is especially the case with neuromas, which because of their painfulness may cause considerable distress for patients. The complete explanation for the pain of peripheral nerve trauma is not known, but ectopic axonal hyperexcitability is likely a major factor. Since the axolemmal distribution of sodium channels largely determines the regions of electrical excitability in normal axons, an altered distribution or quantity of such channels could cause ectopic impulse generation in injured axons. The accumulation of sodium channels within injured axons is a likely cause of such ectopic axonal hyperexcitability and pain. Modification of sodium channel distribution or function may prove a particularly fruitful approach to the treatment of pain in diseases of the peripheral nervous system.

**Plans**

Over the next year we plan to investigate the functionality of sodium channels within neuromas by utilizing patch-clamp techniques on axonal membrane. Although our studies to date have shown immunological evidence of excess sodium channels within the axons of neuromas, we have no direct evidence of their functional properties. It will be important to demonstrate their electrical properties, density, and ability to generate action potentials. We also plan to extend our immunologic and electrical studies to experimental neuromas developed in monkeys. The monkey neuroma model has been developed by Dr. David Kline in the Department of Neurosurgery and is already underway. Study of these experimental neuromas will allow elucidation of the timing and sequence of the development of sodium channel abnormalities. It will also allow potential therapeutic trials aimed at modifying the sodium channel population and the development of pain.

Finally, we are developing site-specific anti-potassium channel antibodies, which will be useful in exploring the potassium channel population of neuromas. This is important since a down-regulation of the quantity of function of potassium channels could contribute to abnormal axonal excitability.

# X. Central Nervous System Changes Associated with Chronic Pain in Peripheral Nerve Injury


## Summary

Pain affects all human beings and, when acute, serves as one of the alerting mechanisms to protect us from harm. However, when pain becomes chronic, as is often seen after peripheral nerve trauma, it is frequently intractable and detrimental to the quality of life. The neuronal pathways and the mechanisms by which acute pain is converted to chronic pain are unknown.

It is hypothesized that a critical balance exists between tactile and painful input to sensory thalamus. The connections between and within sensory thalamus and cerebral cortex serve to modulate and suppress noxious signals and thus the perception of pain. Moreover, it is suggested that prolonged reduction of the tactile input produces a disruption of this balanced relationship. The imbalance augments the activity in the nociceptive components of the thalamo-cortico-thalamic relationship. The results of prolonged augmentation is suggested to initiate to initiate mechanisms for neuronal plasticity which produce permanent changes in neuronal circuitry and, ultimately, centrally generated pain.

A prime objective of this work has been to identify the anatomical sites and potential mechanisms that underlie the conversion from a state of acute pain to a state of chronic neuropathic pain. Immunocytochemical methods are be employed to identify the alterations in early gene expression using the *c-fos* marker, levels of neuronal oxidative metabolism with cytochrome oxidase and in levels of transmitters (glutamate, GABA, serotonin), modulatory neuropeptides (substance P) and modulators of intracellular calcium (calbindin) in animal models for neuropathic pain after peripheral nerve ligation.

## Background and Significance

Neuropathic pain occurs as a result of injury to a peripheral nerve and its surrounding tissue matrix. The predisposing stimulus may vary but the resulting change in elements of the peripheral nervous system invariably alters the transmission of nociceptive signals. Signal alteration may be achieved by augmentation of the afferent signal as in the case of inflammatory lesions or lesions that produce painful neuromas. Alternatively, the nociceptive signal may be diminished as in the case of amputation or nerve root evulsion. The pain that is similarly described in these conditions has components of dysesthesia, allodynia and hyperpathia often with a lancinating and burning quality within the distribution of one or several peripheral nerves. With time the painful sensation may resolve spontaneously but often spreads (Willis, '92) and becomes chronic and intractable. The chronic, self-perpetuating nature of neuropathic pain is thought to be of central nervous system origin (Levitt, '88) yet the mechanism by which the pain is generated is unclear.

Mechanisms implicating every level of somesthetic processing have been proposed to explain neuropathic pain. One hypothesis purports that there is increased activity in peripheral neurons that convey painful stimuli through sensitization of their peripheral nociceptors (Hanesch et. al., '92; Perl, '92; Walters, '92), either by reducing their stimulus threshold or through the formation of repetitive stimulation loops (Levine et. al., '92; Willis, '92; Perl, '92; Campbell et. al., '92). Although repetitive firing of nociceptive neurons can contribute to inflammatory pain, these factors do not explain similar perceptions of pain associated with nerve root evulsion.

A second and perhaps the most favored hypothesis is that due to the alteration of afferent signals there is a reorganization of the circuitry in the dorsal horn of the spinal cord

or caudal medulla implemented through structural changes that occur as a result of direct neuronal response to transmitter interaction with postsynaptic receptors, as well as the result of indirect action effected through the activation of second messenger systems (Coderre, '93; Coderre et. al., '93, for review; Lipton and Rosenberg, '94, for review).

Although the above hypotheses are likely to contribute significantly to the generation of central pain and indeed may be the basic mechanisms by which all changes in central neuronal circuits are effected, the changes seen in lower level integrative networks produced by cellular and molecular mechanisms are inadequate to explain several aspects of central pain. First, cognitive awareness of a painful stimulus is thought to occur clinically at the level of the thalamus (Albe-Fessard et. al., '85) and is thought to depend on the integrity of the sensory system through the thalamic level. Yet individuals in whom the afferent pathways have been destroyed through disease, trauma or surgical intervention often continue to perceive pain or have only transient relief of their painful symptoms (Bosch, '91). Second, the degree of integration of sensory stimuli that occurs at the spinal level is inconsistent with the complexity of perceived sensation that is described in neuropathic pain. The most dramatic example of neuropathic pain is seen in phantom limb pain. In contrast to the exquisite detail of sensation and structure seen in phantom limb pain, sensations described after nerve blocks have uncertain borders and poorly-defined characteristics, which further supports the contention that centrally generated pain is likely to involve portions of the nervous system that process sensory information at a more complex level such as that seen in the precisely organized maps found in somatosensory cortex and thalamus (Merzenich et.al., '78; Johnson, '90, for review). Third, the latency of the conversion from the state of acute but persistent pain to that of chronic pain is longer than that which would be expected

in responses seen at spinal levels (Lombard et. al., '79). It is therefore the contention of this laboratory and others (Rausell et.al., '92) that the mechanisms primarily responsible for the central generation of chronic neuropathic pain are most likely to be a product of the complex relationship between thalamus and neocortex. We have investigated a hypothetical neuronal circuit that is likely to contribute significantly to establishing and maintaining states of chronic neuropathic pain.

A critical balance is assumed to exist between tactile and painful input to sensory thalamus. Normally, the connections between and within sensory thalamus and cerebral cortex serve to modulate and suppress noxious signals and thus the perception of pain. In cases of prolonged reduction of the tactile input, as in conditions of deafferentation or indirectly through excitotoxic changes in prolonged inflammation, the critical balance between touch and pain is changed. The change enhances activity in the nociceptive components of a thalamo-cortico-thalamic pathway that results in an increased perception of pain. The prolonged augmentation is thought to initiate mechanisms for neuronal plasticity that produce permanent changes in neuronal circuitry and thereby produce centrally generated pain. Clinical observations have supported this suggestion when patients with long histories of phantom limb pain report the resolution of their pain after experiencing a cerebrovascular event that involves the white matter underlying the parietal cortex (Yarnitsky et. al., '88; Bosch, '91).

## Methods

Because neuropathic pain may be generated either through the diminution of a nociceptive signal as in the case of amputation or nerve root evulsion or through the

augmentation of an afferent signal as in the case of inflammatory lesions or lesions that produce painful neuromas, conceptually different animal models thought to be representative of neuropathic pain in the human condition were used in this study. One model, that of deafferentation by dorsal rhizotomy, is employed in earlier portions of this study and initiates chronic pain by the reduction of sensory input. The second model, that of chronic inflammation, initiates chronic pain by augmentation of the sensory input. The third model, that of nerve ligation, initiates chronic pain by altering the quality of the afferent signal by partial nerve destruction and neuroma formation.

Because both excitotoxic and neuroplastic mechanisms are potentially involved in the conversion from a state of acute pain to a state of chronic pain, purported cytochemical participants that are likely contributors in these processes were immunochemically labeled within nuclei of the central nervous system at different times during the development of autonomous behavior. Immunocytochemical methods were employed to identify the alterations in early gene expression of the *c-fos* marker, levels of neuronal oxidative metabolism with cytochrome oxidase and in levels of transmitters (glutamate, GABA, serotonin), modulatory neuropeptides (substance P) and modulators of intracellular calcium (calbindin) at intervals following the presentation of the initiating stimulus. Special attention were directed toward identifying alterations of these cytochemical markers within portions of the proposed neural circuit (RNT, PDC, VB and PDT), as well as in spinal cord and brain stem nuclei. The changes observed in the models were compared to determine regions that may function differently in establishing chronic neuropathic pain due either to sensory deprivation, alteration or augmentation.

For this three groups of 48 Sprague-Dawley rats either underwent dorsal rhizotomy,

receive injections of complete Freund's adjuvant to induce a chronic inflammatory lesion or underwent median nerve ligation. Rats in each group were evaluated at varying times after the initiating procedure to assess the pain threshold. At intervals, rats from each group were euthanized for study using immunocytochemical methods.

For controls, 16 rats received sham operations in which all but transection of the dorsal rootlets (8 rats) or median nerve ligation (8 rats) were performed, eight rats received sterile saline injections into one of the forepaws and eight rats without surgical intervention lived in a comparable environment and underwent similar testing for a period of time equal to the longest survival periods of the experimental groups. The rats were then sacrificed and the tissue processed in a fashion identical to that for the experimental groups.

**Method for Generating a Neuropathic State**

**Dorsal rhizotomy.** A combination of ketamine (60 mg/kg) and xylazine (8 mg/kg) was administered to produce deep level of anesthesia for surgical preparation. Sprague-Dawley rats were placed in a spinal stereotaxic apparatus for immobilization during the procedure. The body temperature was monitored with a rectal probe and was maintained at 37°C. The skin and muscle overlying the cervical vertebrae were incised and a laminectomy performed to expose the dorsal roots from the C4 to T2. The dura was incised and the dorsal rootlets transected unilaterally with iridectomy scissors from levels C4 to T2 under visual guidance to avoid damage to the radicular blood supply. The cut edges of the dura were reapproximated and the incision in the overlying muscle and skin closed. The rats were then allowed to recover from the anesthesia. Local anesthetic ointment, 1% Xylocaine, was applied to the surgical incision twice a day for 3 days to reduce postoperative discomfort. The rats were housed in cages containing soft sawdust bedding to minimize discomfort and

were monitored daily for up to 6 months for signs of autotomy.

**Inflammatory stimulus.** Sprague-Dawley rats were anesthetized with a combination of ketamine (60 mg/kg) and xylazine (8 mg/kg). One forepaw of each rat received a subcutaneous injection of 0.2 ml of complete Freund's adjuvant (CFA; *Mycobacterium tuberculosis*; Sigma) suspended in an oil:saline (1:1) emulsion (0.5mg *Mycobacterium*/ml emulsion) using a sterile tuberculin syringe. The rats were then allowed to recover from anaesthesia. The injections were repeated weekly, when necessary to produce prolonged periods of inflammatory stimulation. The procedure itself is easily controlled and initially no more painful than a subcutaneous injection. Anaesthesia was used, however, during this portion of the procedure to control for the anesthetic variable when comparisons are made between CFA-induced and rhizotomy-induced pain. Routine analgesics were not used subsequent to CFA injection because such medication would mask the effect that is being tested. The subjects were housed, monitored daily for the onset of autotomy and evaluated for alterations in the pain threshold. One additional group of rats was sacrificed one hour after experimental manipulation to assess immediate early changes initiated by the inducing stimuli. These rats had only begun to recover from anaesthesia and thus did not demonstrate behavioral changes or assessable changes in pain thresholds but would be more likely to reveal a changes in *c-fos* activity. Additionally, rats were monitored daily for the presence of infections that may develop in association with the inflammatory lesions. Self-inflicted injury to a limb in the form of lacerations or amputations or purulent ulcerative skin lesions were considered cause for early euthanasia of the subjects in this study.

**Nerve ligation.** Sprague-Dawley rats were anesthetized with a combination of ketamine (60 mg/kg) and xylazine (8 mg/kg). An incision in the skin of the forelimb was

made. The median nerve in the arm was exposed and looped with a loose ligature. The incision was closed and the rats were allowed to recover from anaesthesia. Routine analgesics were not used subsequent to nerve ligation because such medication would mask the effect that is being tested. The subjects were housed, monitored daily for the onset of autotomy and evaluated for alterations in the pain threshold. One additional group of rats were sacrificed one hour after experimental manipulation to assess immediate early changes initiated by the inducing stimuli. These rats had only begun to recover from anaesthesia and thus would not demonstrate behavioral changes or assessable changes in pain thresholds but as in the CFA-model, were be more likely to reveal a changes in *c-fos* activity. Additionally, rats were monitored daily for the presence of infections that may develop in association with the inflammatory lesions. Self-inflicted injury to a limb in the form of lacerations or amputations or purulent ulcerative skin lesions were considered cause for early euthanasia of the subjects in this study.

**Assessment of Neuropathic State**

**Primary behavioral assessment - development of autotomy.** Autotomy is the behavior in animals that is thought to be analogous to neuropathic pain in humans. It is manifested by varying degrees of avoidance of stimulation, licking, scratching and gnawing of the affected limb. It is thought to occur in response to spontaneous neuronal activity within the central nervous system. Assessment of the levels of autotomy can be made visually by the investigator. The severity of autotomy was scored daily and recorded according to a modification of Wall et.al. ('79) in which removal or attack of each claw or phalanx were given a score of 1, for a possible total score of 18. Animals attaining a score of 10 on this scale in the form of lacerations or amputations underwent early euthanasia.

The brains of these animals were processed histologically as described below.

**Determination of pain threshold.** Observations of autonomous behavior can only provide a subjective estimate of the presence of a neuropathic state. Objective measurements of the pain threshold therefore were also obtained in an attempt to quantify further the response to manipulation. The pain threshold of all rats was determined by its response to noxious thermal stimuli according to the protocol of Hargreaves et al. (1988). For this, rats were held under a plastic chamber and placed on an elevated glass surface. The forepaw was radiantly warmed from below through the glass plate. The timer and heat source were turned off automatically when the paw was moved. An upper cutoff latency of 10 seconds was imposed to prevent tissue damage. The rats were evaluated prior to experimental manipulation to provide a baseline of response. After the initiating stimulus, experimental and control rats were reevaluated at intervals of 24 hours, 3 days, 1 week, 4 weeks, 2 months and 6 months, and just prior to sacrifice.

**Histological preparation of tissue for immunoreactivity.** For perfusion, a 120 mg/kg dose of pentobarbital sodium was administered to produce a level of deep anesthesia. Transcardial perfusion of the circulatory system was accomplished by means of a wash of 0.85% saline followed by 3% paraformaldehyde in 0.1M phosphate buffer (pH 7.4). The brain and spinal cord were removed and post-fixed for 2-3 hours in cold fixative. The tissue were transferred to cold 30% sucrose in phosphate buffered saline and stored overnight at 7°C. Forty-micron-thick sections of the brain, brain stem and cervical and lumbar spinal cord were cut,frozen and collected in serial order in 10% sucrose in phosphate buffer. Routinely, sections were processed in series for *Fos*-immunoreactivity (*c-fos*, *fra*, *c-jun*, *jun-b*) and for localization of glutamic acid (GLU), glutamic acid decarboxylase (GAD),

calbindin, sP and serotonin (5-HT) using the peroxidase-antiperoxidase (Vectastain ABC) method. Tissue sections were incubated in the appropriate antiserum for 48 hours at 4°C with gentle agitation, followed by incubation in secondary antiserum (goat anti-rabbit IgG for 60 minutes at 25°C). Following incubation in rabbit ABC for 60 minutes at room temperature the sections were then rinsed in phosphate buffered saline and reacted with 3,3'-diaminobenzidine in the presence of hydrogen peroxide to localize peroxidase activity. Cobalt chloride intensification (Adams, 1977) was used to enhance the visualization of the horseradish peroxidase reaction. Histological control sections were incubated without antiserum or without hydrogen peroxide to determine the specificity of labeled profiles. The sections were mounted onto slides. Selected sections were counterstained with neutral red for identification of cytoarchitectural landmarks.

An additional series of sections were reacted for the presence of cytochrome oxidase activity. For this a series of sections were transferred from 0.1M phosphate buffer (pH 7.4) into a solution of 0.1M Tris buffer, dimethyl sulfoxide (DMSO) and cobalt chloride for 10 minutes. Following this initial incubation and a thorough rinse in phosphate buffer, the sections were transferred into a solution of 3,3'-diaminobenzidine, cytochrome c, DMSO and catalase for incubation at 38°C to produce a color change. The sections were then rinsed, mounted on slides and coverslipped for microscopic evaluation. A final series of sections were mounted and stained with cresyl violet as needed to clarify architectonic complexities. These procedures are routinely used in the laboratories of the PI.

**Table of tissue reactions**. Maximum spacing between sections is 400 $\mu$m, 1 in 10.

| Glutamate | *c-fos/fra* | clabindin | sP | GABA | cytoch ox | 5-HT |
|---|---|---|---|---|---|---|

Samples of dorsal root ganglia and median nerve were removed, cut and processed histochemically to localize and identify changes in the distribution of sodium channels in collaboration with Dr. John England. These results were compared to those observed in similar studies of human neuromas. Selected sections were also processed for routine histological staining to identify morphological characteristics of the median nerve and dorsal root ganglia.

**Data reduction.** Every section was carefully examined for evidence of labeled profiles. Labeled neurons, terminal fields and projection pathways were visualized at high power through the light microscope and charted onto images of each section. The distribution and relative optical density of the labeling as well as counts of labeled profiles were made and reconstructed in relationship to blood vessels, tissue artifacts and architectonic landmarks. Cellular morphology and cell counts were made of the dorsal horn ipsilateral to the site of manipulation and compared to the results of a similar analysis of the contralateral dorsal horn. Representative chartings for each case are traced exactly with pen and ink for publication.

## Results

Three rats that have been subjected to a component of the CFA protocol have been perfused and their brains have been processed for levels of glutamate, calbindin and *c-fos* activity following single injections into the left forepaw. Post-injection survivals for these animals were 24 hours, 1 week and 4 weeks. Analgesiometry was not performed due to lack of equipment. Within 2 hours of administering CFA, the injected forepaw showed marked edema and erythema. Following recovery from anaesthesia, the rats' activity was

subjectively decreased from pre-injection levels and the use of the left forepaw was avoided. The inflammatory process progressed over the next 24 hours producing moderate to severe erythema and edema that approximately doubled the size of the forepaw. The level of inflammation appeared to stabilize after 24 hours and in the longest surviving rat remained at maximum levels for 12-14 days. The edema and erythema thereafter decreased over the next week and use of the paw increased but the forepaw never returned to its pre-injection condition. Autonomous behavior never developed.

Immunocytochemical labeling of intracellular calbindin was found to be increased in cells and axons of the dorsolateral portion of the substantia gelatinosa and the intermediolateral cell column ipsilateral to the injected forepaw when compared to the contralateral counterparts within 24 hours of administration of CFA. Complementary increases in labeling of glutamate were also observed at similar cord levels in the neuropile of the substantia gelatinosa and intermediolateral cell column. Calbindin activity was also increased in the axons of the medial lemniscus contralateral to the injected forepaw within 24 hours of injection. Although calbindin and glutamate labeling also appeared to be increased at this time in the VB contralateral to the injected forepaw, the preliminary results are equivocal. After a 1 week survival, the labeling of calbindin and glutamate both appeared to decrease in the dorsolateral portion of the substantia gelatinosa and the intermediolateral cell column as shown for calbindin. Labeling in the contralateral spinal cord, medical lemniscus and VB was not changed appreciably from the initial labeling pattern seen following 24 hour survival. Following a 4 week survival, the intensity of calbindin labeling was less in VB contralateral to the injected forepaw when compared to the ipsilateral counterpart.

*c-fos* labeling was found only in the rat that survived for 4 weeks. Neurons were

found to be labeled bilaterally, but asymmetrically denser contralateral to the injected forepaw, in the posterior thalamus adjacent to the medial border of the ventral lateral geniculate nucleus and extending into the posterior-most aspect of the lateral portion of the posterior nucleus of the thalamus (Pol). The significance of this labeling is unclear. Because the identical dilution of the same batch of antibody was used to label *c-fos* in all of the tissue, the lack of labeling cannot be explained by non-reactive antibodies. Alternatively, it is possible that the pattern of labeled cells is artifactual since similar patterns of labeling have been observed in relation to components of the circadian cycle (Kurkoff, 1994). All of the rats, however, were sacrificed within 1 hour of each other, demonstrated no apparent difference in behavior and experienced no difference in manipulation prior to or during anaesthesia and perfusion. The asymmetry of the labeling and the fact that the pattern was only observed in the animal that had survived for 4 weeks therefore suggests a need for further study and clarification.

# XI. PUBLICATIONS

Zhang DM, Beuerman RW, Zhao S, Tran H, Kline D, Gould H. Cellular factors involved in neuroma formation. *Soc Neurosci* 21:1798, 1995.

Zhao S, Zhang D, Kline DG, Beuerman RW, Ma Q, Tran H. Increase in sonic fibroblast growth factor and fibroblast growth factor receptor-1 following sciatic nerve injury and neuroma formation. *Soc Neurosci* 21:497, 1995.

Ma Q, Beuerman RW, Zhao S, Pedroza L, Tran H, Nguyen D, Kline D. Immunolocalization and quantitation of fibroblast growth factor receptor-1 in the human peripheral neuroma. *Soc Neurosci* 21:2050, 1995.

Beuerman R, Zhao S, Tran H, Ma Q, Kim D, Kline D. Epidermal growth factor and fibroblast growth factor in human neuroma tissue. *Soc Neurosci* 20:663, 1994.

Zhao S, Beuerman RW, Kim DH, Zhang D, Kline DG. Neuroma formation and fate of the Schwann Cells in the constriction of sciatic nerve and homograft nerve repair. *Soc Neurosci* 20:707, 1995.

England JD, Happel LT, Kline DG, Gamboni F, Thouron C, Liu ZP, Levinson SR. Sodium channel accumulation in human painful neuromas. *Neurology*, in press.

Beuerman RW, Kline DG. Growth factors in the human neuroma. *Sunderland Society Meeting, Zurich, Switzerland*, June, 1995.

England JD, Gamboni F, Ferguson MA, Levinson SR. Sodium channels accumulate at the tips of injured axons. *Muscle Nerve* 17:593-598, 1994.

England JD, Happel LT, Kline DG, Gamboni F, Levinson SR. Sodium channel accumulation in human painful neuromas. *Neurology* 45(4:Suppl):A296, 1995.

England JD, Happel LT, Kline DG, Gamboni F, Levinson SR. Human painful neuromas. *Sunderland Society Meeting, Zurich, Switzerland*, June, 1995.

England JD, Levinson SR, Shranger P. Immunocytochemical investigations of sodium channels along nodal and internodal portions of demyelinated axons. *Microscopy Research Technique*, in press.

England JD. Traumatic nerve injuries and neuromas. *Curr Opin Orthopaedics* 6(6), in press, 1995.

**886.13**

IMMUNOLOCALIZATION AND QUANTITATION OF FIBROBLAST GROWTH FACTOR RECEPTOR-1 IN THE HUMAN PERIPHERAL NEUROMA. Q. Ma, R.W. Bauerman*, S. Zhao, L. Pedroza, H. Tran, D. Nguyen, D.G. Kline. Dept. of Ophthalmology, LSU Eye Center, New Orleans, LA 70112

Immunocytochemical localization of fibroblast growth factor receptor-1 (FGFR-1) was studied in the cultured cells (passage 4 or 5) from human neuroma tissue obtained at the time of surgery. The cultured cells consisted of large numbers of fibroblasts and a few Schwann cells identified by anti-NGF receptor. The results showed that the fibroblasts were positively stained using an immunohistochemical procedure with a monoclonal antibody to recognize FGFR-1. Further, the subcellular location of FGFR-1 in the cells was investigated by electron microscopy using pre-embedding indirect immunogold double labeling. The particles (15 nm gold probe for FGFR-1) were found to be arranged regularly along the cell membranes at an average distance of 1.3±0.5 μm from the receptors, and particles (5 nm gold probe for basic fibroblast growth factor) were also present in the cytoplasm. It is interesting that the numbers of gold particles (for FGF receptor-1) were dramatically reduced after administration of basic fibroblast growth factor in the binding test. FGF membrane receptors were quantitated by flow cytometry using microbeads as the standard. The receptor density was calculated to be about 5600 per cell. The results will be useful for determining the function of FGF receptors in the formation of neuromas. Supported in part by DAMD17-93-V-3013.

**707.14**

CELLULAR FACTORS INVOLVED IN NEUROMA FORMATION. D.M. Zhang, R.W. Beuerman, S. Zhao, H. Tran, D. Kline, H. Gould*. Depts. of Ophthalmology, Neurosurgery, and Neurology, LSU Medical Center, New Orleans, LA 70112.

Nerve growth factor (NGF) and its low-affinity receptor (NGFR) have recently been detected in the distal segment of the sciatic nerve 6 hours to 14 days after transection. We have investigated cellular localization of NGFR, growth associated protein (GAP-43), basic fibroblast growth factor (bFGF), and FGFR1 at 2 weeks to 12 months in a monkey neuroma model and in human neuromas. In the monkey 2 weeks after transection, tibial nerve proximal segment immunoreactivity for NGFR was found in the perineurium and less intensely in endoneurium. In both monkey and human neuroma, intense staining for NGFR was associated with disintegrating fibers. We also found staining of Schwann sheaths surrounding masses of axons. Immunoreactivity for NGFR was more intense in 12-month monkey specimens and in human neuromas than in 2-week monkey neuroma. Proximal segments of the neuroma showed equal axonal staining for GAP-43, whereas very few thin disorganized fibers were stained with GAP-43, and the number of GAP-43-stained fibers decreased with time of neuroma development. Western blot of 3-month monkey neuroma showed a decrease in bFGF and FGFR1, compared with the proximal segments. In conclusion, the increase in NGFR, together with the decrease in GAP-43, bFGF, and FGFR1, may be related to the formation of the neuroma. However, the role of NGFR in the development of the axon mass of the neuroma is not clear. Supported in part by DAMD17-93-V-3013.

**288.17**

INCREASE IN BASIC FIBROBLAST GROWTH FACTOR AND FIBROBLAST GROWTH FACTOR RECEPTOR-1 FOLLOWING SCIATIC NERVE INJURY AND NEUROMA FORMATION. S. Zhao, D. Zhang, D.G. Kline*, R.W. Bauerman, Q. Ma, D. Zhang, H. Tran, Depts. of Neurosurgery and Ophthalmology, LSU Eye Center, New Orleans, LA 70112

Neurosurgical practice has indicated that nerve ends that have the endoneurium and perineurium sealed with a bipolar coagulator or that are buried in the muscle are less likely to produce a neuroma, compared with nerve ends that are ligated or untreated. These experiments were undertaken to investigate the roles of basic fibroblast growth factor (bFGF) and FGF receptor-1 in neuroma development. The sciatic nerves of adult rats were severed below the sciatic nerve notch and the severed ends were treated in one of four ways: 1] buried in the muscles; 2] perineurium and endoneurium sealed with a bipolar coagulator; 3] perineurium tied with #8 suture; and 4] no treatment. The nerves were harvested at 2, 4, 8, and 16 days after surgery. A section (0.5 mm) was removed from the proximal severed end of each nerve and total proteins were extracted. The results of Western blot analysis showed increased amounts of bFGF and FGF receptor-1 beginning 2 days after surgery, compared with normal controls. The nerves that had been treated with the bipolar coagulator or buried in the muscles yielded less bFGF and FGF receptor-1 than the nerves that were ligated or the nerves that were not treated. This study provides evidence that bFGF and FGF receptor-1 play a significant role in neuroma formation from the very early stages of nerve repair after injury. Supported in part by DAMD17-93-V-3013.

**299.13**

NEUROMA FORMATION AND FATE OF THE SCHWANN CELLS IN THE CONSTRICTION OF SCIATIC NERVE AND HOMOGRAFT NERVE REPAIR. S. Zhao, R. W. Bescrman, D. H. Kim, D. Zhang and D. G. Kline*
Dept. of Neurosurgery and Ophthalmology, LSU Medical School, New Orleans, LA 70112.

A fluorescent dye with high affinity for DNA (DAPI) was used to investigate the origin of the cell components in the formation of neuroma. Unilateral sciatic nerve of rats was injected with 3 µl DAPI (20 µg/ml). Four weeks later, the same rats underwent a 10 mm homograft. In the first experiment, a nerve section with DAPI was used as a homograft surgically connected to the contralateral sciatic nerve. In the second experiment, the recipient nerve with DAPI had a homograft not containing DAPI. The rats were sacrificed at two weeks and six weeks respectively after secondary surgery. The nerves with the graft were sectioned in a cryostat and used for fluorescent microscopy. Grossly, the nerve graft and adjacent proximal sectioned sciatic nerve ends were thickened and the graft was obviously shortened. By microscopy the nuclei of the Schwann cells were intact indicating a viable graft, however, there was no fluorescent nuclei in either the graft or in the recipient nerves. The thickened tissue suggesting an early neuroma did not show evidence of cells crossing the interface between graft and recipient nerve. In another animal model, the sciatic nerves of two rats were constricted completely with a No.4 suture. The DAPI was injected into the nerve proximally to the constriction, or distally to the constriction. At two and 4 weeks post-operatively, connective tissues were found growing around the constricted site. Histological examination from these nerves showed cell components in the connective tissues with labeled nuclei. Supported in part by DOD 17-93-V-3013.

**284.5**

EPIDERMAL GROWTH FACTOR AND FIBROBLAST GROWTH FACTOR IN HUMAN NEUROMA TISSUE. R. Beuerman*, S. Zhao, H. Tran, S. Ma, D. Kim, D. Kline. LSU Eye Center and Dept. of Neurosurgery, LSU Neuroscience Center, LSU Medical School, New Orleans, LA 70112

The formation of neuromas after injury or surgical repair of peripheral nerves interferes with the establishment of functional connections by the regenerating axons. The purpose of this study was to determine the types of growth factors and growth factor receptors in human neuroma tissue and in cultured cells from these tissues. Tissues obtained from five patients at the time of surgery performed 8-10 months after trauma to the brachial plexus was frozen in liquid nitrogen and small pieces were used to establish primary cultures. Western blots for EGFR, FGF, and bFGFR were carried out on cells and fresh tissue using antibodies for EGFR (cytoplasmic), bFGF, and FGFR-1. The results showed that EGFR was present in confluent cultured cells but not in the tissue. The 18kD form of bFGF was present in cells and all tissues; the higher molecular weight forms were seen in three of the tissues. FGFR-1 was found in the cultured cells and, less abundantly, in the tissues. The cultured cells stained positively for S-100 protein, suggesting that they were Schwann cells. PDGF-bb was found in the cultured cells but not in any of the tissues. The results suggest that FGF could be acting in an autocrine fashion on cells in neuromas and that this growth factor may have a role in the development of this condition.

*Supported in part by DAMD17-93-V-3013.*

**Sodium Channel Accumulation in Human Painful Neuromas**

J.D. England, M.D., L.T. Happel, Ph.D., D.G. Kline, M.D., F. Gamboni, Ph.D., C. Thouron, Z.P. Liu M.D., S.R. Levinson, Ph.D.

From the Departments of Neurology (Drs. England, Happel, and Liu), Neurosurgery (Dr. Kline), and Anatomy (Ms. Thouron), Louisiana State University School of Medicine, New Orleans, LA; and the Department of Physiology (Drs. Gamboni and Levinson), University of Colorado School of Medicine, Denver, CO.

Presented in part at the 47th Annual Meeting of the American Academy of Neurology, Seattle, WA, May 1995.

Address correspondence and reprint requests to Dr. John D. England, Department of Neurology, Louisiana State University School of Medicine, 1542 Tulane Avenue, New Orleans, LA 70112-2822. Phone 504-568-4090; Fax 504-568-7130.

Acknowledgements: This work was supported by grants from the National Institutes of Health (NS15879 to SRL) and the United States Department of Defense (DAMD 17-93-V-3013 to JDE, LTH, and DGK).

Key Words: sodium channel, nerve injury, ectopic excitability, immunocytochemistry, radioimmunoassay

Running-head title: Sodium channels in neuromas

England

**Abstract-** Neuromas often exhibit ectopic electrical hyperexcitability, which is likely a major cause of neuroma-associated pain. Although the mechanism of this abnormal axonal impulse generation is not known, one possibility is an alteration of sodium channel distribution or quantity. Painful neuromas from 16 patients were examined using site-specific anti-sodium channel antibodies employed in immunocytochemical and radioimmunoassay methods. Normal sural nerves from 6 of these patients served as controls. Immunocytochemistry showed abnormal segmental accumulation of sodium channels within many axons in the neuromas. Dense immunolocalization was especially apparent within axonal tips. Contrastingly, in sural nerves focal accumulation of sodium channels was restricted to nodes of Ranvier. Radioimmunoassay confirmed a significantly greater density of sodium channels in the neuromas as compared to the sural nerves. Thus, sodium channels accumulate abnormally within the axons of human neuromas. This alteration of the sodium channel population may underlie the generation of axonal hyperexcitability and the resulting abnormal sensory phenomena (pain and paresthesias) which frequently occur after peripheral nerve injury.

Peripheral nerve trauma may result in the formation of a neuroma, a tangled mass of regenerating axons embedded within the connective tissue of a nerve trunk.[1] The axons within a neuroma not only fail to reinnervate their original targets, but may also develop abnormal electrical hyperexcitability.[2-5]

In human neuromas, the development of ectopic hyperexcitability within sensory axons is likely a major cause of neuroma-associated pain and dysesthesias. Clinical evaluation of patients with painful neuromas and routine histological analysis of excised neuromas have not identified the factors responsible for this painfulness. Since the ability of an axon to generate an action potential depends ultimately upon the distribution and properties of voltage-gated ion channels, especially voltage-gated sodium channels, a potential cause of ectopic axonal hyperexcitability could be an abnormal redistribution of ion channels within injured axons. A particularly attractive hypothesis is that aberrant axonal electrical hyperexcitability is, in part, caused by an abnormal accumulation of sodium channels along injured or regenerating axons.[5-8]

The present report describes the changes in the sodium channel population which characterize human painful neuromas. These findings are correlated with what is known regarding the remodelling of axonal membranes within neuromas.

**Methods.** *Subjects.* The study group consisted of 16 subjects with painful traumatic neuromas selected from a large population of patients with peripheral nerve injuries seen at the Louisiana State University School of Medicine in New Orleans. Each patient was evaluated clinically and electrophysiologically (EMG/NCS) by a team of neurologists and

neurosurgeons. The painfulness of each patient's nerve injury was graded subjectively on a scale from 1+ to 4 + (see Table for details). For each of the 16 patients in this study, surgical treatment of the neuroma was believed to offer the best chance for pain relief or nerve regeneration. Thus, each subject underwent surgical excision of the neuroma. In some cases sural nerve autografts were interposed within the resected nerve segment.

*Preparation of anti-sodium channel antibody.* Site-directed polyclonal antibodies were raised to an 18-mer peptide (EOIII) corresponding to a region highly conserved in all known vertebrate sodium channels. This segment (TEEQKKYYNAMKKLGSKK) resides in a putative intracellular loop connecting domains III and IV in the α-subunit of the sodium channel.[9] The peptide EOIII was synthesized with the addition of a carboxy terminal cysteine by conventional solid phase methods. Following purification by reverse-phase HPLC, EOIII was conjugated to maleimide-activated keyhole limpet hemocyanin (KLH) using the Imject kit from Pierce. Antisera to EOIII-KLH conjugates were raised by immunizing rabbits at 4 week intervals. One of these antisera, designated 2944, exhibited very high titers to purified eel electroplax sodium channels in a sensitive radioimmunoassay.[10] The radioimmunoassay signal was also diminished by pure EOIII peptide in the same manner as equivalent mole amounts of pure sodium channel. Conditions for preadsorbed controls could thus be established for immunocytochemistry (described below), and anti-EOIII concentrations in whole sera were estimated to be 1-3 mg/ml for various bleeds. Finally, 2944 antibodies were purified from antisera via affinity chromatography on an EOIII-coupled column (ImmunoPure Ag/Ab Immobilization Kit #2, Pierce); the resultant antibody fractions had anti-EOIII titers approximately one-half that of the original antisera. These affinity purified antibodies were

England

used in all subsequent immunocytochemical and radioimmunoassay experiments described below. The antibodies also have been used in previous immunocytochemical studies in rat sciatic nerve.[11]

*Immunocytochemistry.* Immunocytochemical methods were performed with minor modification of described procedures.[8,12,13] Briefly, freshly excised neuroma specimens or sural nerve specimens were delivered to the laboratory in Ringer's lactate solution. Specimens were cut into several pieces, several of which were frozen at -70$^0$C for subsequent radioimmunoassay analysis (described in next section); the remainder of the specimens were prepared for immunocytochemistry by fixation in 4% paraformaldehyde/0.1 mol/L phosphate-buffered saline (PBS) for 1 hour at room temperature. Nerves were teased apart using dissecting needles and fixed upon poly-L-lysine coated slides with 4% paraformaldehyde/0.1 mol/L PBS for 15 min. After rinsing in 0.1 mol/L PBS three times, the slides were immersed in 0.1 mol/L PBS/0.3% Triton X-100 (Sigma)/10% normal goat serum for a minimum of 1 hour. For sodium channel labeling, specimens were incubated overnight at room temperature with the primary anti-sodium channel antibody (2944) diluted 1:50 in 0.1mol/L PBS/0.3% Triton /10% normal goat serum. For controls, the primary anti-sodium channel antibody was preblocked with the peptide antigen (1 µl of peptide/2 µl of antibody overnight at 4$^0$C). After incubation with the pure or preblocked primary antibody, sections were rinsed three times in 0.1 mol/L PBS and then incubated for at least 1 hour at room temperature with lissamine rhodamine-labeled goat antirabbit IgG diluted 1:50 in 0.1 mol/L PBS/0.3% Triton/10% normal goat serum. Sections were then rinsed in 0.1 mol/L PBS three times, dried, coverslipped with 0.05 mol/L PBS/glycerine mixture, and examined with either an Olympus BH2

England

epifluorescence microscope or a Leica laser scanning confocal microscope.

*Radioimmunoassay.* Neuroma or sural nerve specimens were weighed and then homogenized in 1% Lubrol PX and centrifuged at 45,700 g for 25 minutes. The supernatants were diluted in 0.1 mol/L sodium phosphate buffer, pH 7.5/1% bovine serum albumin/0.1% Lubrol/0.021% egg phosphatidylcholine (Sigma, grade V) to a concentration of <10 mg wet tissue/100 µl. Samples (100 µl per tube) were incubated with the anti-sodium channel antibody (2944) diluted 1:2000 for 1 hour at room temperature. Twenty microliters of $^{125}$I-labeled purified eel sodium channel (17fmol or 30,000 cpm; specific activity = 1.06 mCi/nmol; 1 Ci = 37 Gbq) was then added to each tube and incubated another 2 hour at room temperature. Antibody-antigen complexes were solid phase precipitated by adding 100 µl of Tachisorb-R (Calbiochem # 575544) and incubating with gentle shaking for 2 hour at room temperature. Samples were washed with 0.1 mol/L sodium phosphate buffer/1% bovine serum albumin/0.1% Lubrol/0.02% egg phosphatidylcholine (Sigma, grade V) (1.25 ml per tube) and then centrifuged at 3700 g for 5 minutes. Pellets were resuspended in the same buffer and recentrifuged at 3700 g for another 5 minutes. The supernatants were discarded, and the radioactivity of the pellets was determined with a gamma counter. Concentrations of sodium channels were calculated with reference to a standard curve determined by using known quantities of highly purified eel sodium channel. Except for the particular primary antibody and the type of experimental nerve preparations, these procedures are the same as those described previously.[8,10]

**Results.** *Immunocytochemistry.* Seventeen neuromas from 16 subjects (one specimen from each of 15 subjects and two specimens from one subject) and six sural nerves from six of these subjects were examined immunocytochemically.

In the sural nerves, sodium channel-specific immunoreactivity (IR) was seen only at nodes of Ranvier. Acutely mechanically desheathed myelinated axons exhibited no specific immunoreactivity along internodal axolemma. Unmyelinated axons exhibited no specific immunoreactivity anywhere along their axolemma. These results in human sural nerve are identical to those found with similar immunohistochemical studies in fish posterior lateral line nerve[8,12,13] and rat sciatic nerve.[11] Although electrophysiologic and biochemical studies demonstrate some voltage-gated sodium channels along unmyelinated and internodal axolemma,[14-19] their density is too low to be visualized immunocytochemically with our anti-sodium channel antibodies.[8,12,13,20]

All neuromas showed abnormally intense sodium channel-specific immunoreactivity (IR) within many axons. This immunoreactivity was seen in large diameter (>1 μm) and small diameter (<1 μm) axons although larger axons with dense IR were more frequently encountered. The IR was always nonuniform in distribution, occurring in patches of variable density along the axons. Of special note, this dense specific IR usually appeared along demyelinated or unmyelinated segments of axolemma. When myelinated fibers were seen, focal accumulation of sodium channels was observed only at normal nodes of Ranvier. Some of the most intense immunolabeling was seen at neurite tips ,and these axonal endings were always devoid of a myelin sheath. Within neuromas there was considerable individual axon variability of IR with some axons showing many patches of intense IR and other axons

(even neighbors) showing no IR. Even in the most intensely labeled neuromas, no more than 30-40% of all axons showed sodium channel-specific IR. Although all neuromas exhibited abnormal sodium channel- specific IR within many axons, there was considerable variability in terms of the number and intensity of axons stained within individual neuromas. Only minimal nonspecific immunofluorescence was seen when the primary anti-sodium channel antibody was preblocked with peptide, confirming the specificity of the above-noted IR. Figure 1 provides examples of these immunocytochemical observations.

*Radioimmunoassay (RIA).* Sixteen neuromas from 15 of the subjects (one specimen from each of 14 subjects and two specimens from one subject) and six sural nerves were examined by RIA. Portions of all of these specimens had been examined immunocytochemically (see above). For each specimen the concentration of sodium channels was calculated and expressed as pM per g wet weight. The Mann-Whitney U test was used for statistical analysis of the two populations. RIA data demonstrated a significantly ($P = 0.0075$) greater sodium channel density in neuromas (median = 28.6; mean $\pm$ SEM = 32.5 $\pm$ 3.7 pM per g) as compared to sural nerves (median = 18.2; mean $\pm$ SEM = 17.1 $\pm$ 2.2 pM per g). The true density of axonal sodium channels within these neuromas is probably even greater since neuromas contain far more nonneural tissue than normal nerve. Figure 2 graphically illustrates the sodium channel density for each specimen. Matched pairs of specimens were available from 5 subjects (ie, neuroma and sural nerve from the same subject). In each case the neuroma contained a significantly greater density of sodium channels than the sural nerve. The Table provides these data for all patients and also ranks the pain associated with each neuroma. There was a trend in the direction of greater

painfulness for neuromas with greater concentrations of sodium channels except for one specimen - the neuroma with the highest density of sodium channels (74.2 pM per g) was only mildly painful. It is clear that more data are needed to determine if there is a positive correlation between the density of sodium channels within neuromas and their degree of painfulness.

**Discussion.** This study shows that sodium channels accumulate abnormally within some axons of human painful neuromas. This conclusion was reached using two different but complementary methods (immunocytochemistry and radioimmunoassay). The sodium channel accumulation in axons of neuromas was unique in several aspects. First, it was nonuniform throughout the axons, occurring in a segmental fashion. Typically, single axons contained multiple distinct, physically separable regions of sodium channel staining. Second, it occurred in demyelinated or unmyelinated axons. Normal myelinated fibers within the neuromas showed focal high intensity labeling of sodium channels only at the nodes of Ranvier. Third, many neurite or axonal tips contained a high concentration of sodium channels. Fourth, there was variability in the magnitude of sodium channel accumulation among the different neuromas.

Several previous studies of nerve injury in fish and neuromas in rats are especially relevant to the present study of human neuromas. Immunocytochemical analysis of neuromas of the lateral line nerve of the fish, *Apteronotus* [6] and focally injured nerve fibers of the lateral line nerve of *Carassius auratus (*goldfish) [8] have shown sodium channel accumulation at the endings of injured axons . These studies of injured lateral line nerves in

fishes used a fish-specific anti-sodium channel antibody directed against the entire α- subunit of the channel, an antibody entirely different than the one used in the present study.[10,12,20,21] Devor, et al immunolocalized sodium channels at the electron-microscopic (EM) level in neuromas produced in rats.[7] Sodium channel accumulation occurred in preterminal axolemma which was either demyelinated or unmyelinated as well as in neuroma end bulbs. The large diameter (>1 μm) axons within the neuromas acquired excess sodium channels only after myelin was stripped from their internodal axolemma. Many of these axons contained distinct patches of heavy sodium channel immunolabeling. These findings are concordant with our observations in human neuromas and, thus, may be a general feature of neuromas.

The accumulation of sodium channels within the axons of neuromas may be due to several factors. Sodium channels are synthesized in neuron cell bodies and transported down axons by microtubule-based fast axoplasmic transport.[22,23] When the cell bodies of the squid giant fiber lobe are dissociated from their giant axons and maintained in culture, sodium channels amass within the somata.[22] This observation suggests that axonal membrane normally serves as a sink for sodium channels synthesized within the cell body and that its removal by axotomy causes sodium channels to accumulate in the remaining viable membrane. After injury to axons, sodium channels, which are continuously transported down axons, would be expected to accumulate at the nerve fibers' distal segments. Concordant with this hypothesis are studies which demonstrated that block of fast axoplasmic transport decreases ectopic electrical activity in injured peripheral nerves.[24] Colchicine and vinblastine applied to nerves decreased the incidence of spontaneous and epinephrine-evoked ectopic discharges in experimental neuromas distal to the site of drug application. The application of

these drugs (presumably by blocking anterograde fast axoplasmic transport) prevented new neuromas from developing ectopic discharge and decreased discharges in neuromas which had already become active, suggesting that blockade of fast axoplasmic transport prevented the accumulation of sodium channels at the distal ends of the traumatized axons, thus reducing their electrical excitability.

Local demyelination of axons within neuromas may be another factor that permits focal accumulation of sodium channels. In the present and previous studies [6-8] of traumatic nerve injury, when sodium channels were found in large axons (>1 μm diameter), the axolemma was devoid of myelin. Demyelination of axons, even when not accompanied by axotomy, permits the insertion of sodium channels along previously internodal axolemma.[10,12,19,25] Since the quantity of sodium channels in demyelinated nerves is three to fourfold greater than normal nerve, demyelination may trigger an upregulation in the neuronal synthesis of sodium channels.[10] Taken together, these observations indicate that changes of the regional axonal environment at the site of injury may act to change the distribution of sodium channels.

An important question regarding the accumulation of sodium channels within neuromas is whether this is relevant to the pathophysiology of pain associated with neuromas. Neuromas certainly may serve as a generator of painful impulses.[26] Wall and Gutnick were the first to demonstrate that some afferent fibers originating in a neuroma develop spontaneous electrical hyperexcitability.[2] This axonal spontaneous hyperexcitability and the sensitivity of neuromas to mechanical and chemical stimuli are now indisputable facts.[3-5,27] The prevalence of such ectopic axonal hyperexcitability varies with nerve fiber type and with

the time since nerve injury, but it is nearly always present. At peak activity, an average of 28% of all injured fibers fire spontaneously and an even higher percentage exhibit abnormal mechanosensitivity.[3,4] Most of the fibers with ongoing abnormal activity are afferent fibers, mostly A-fibers and a smaller number of C-fibers.[3-5] Motor fibers rarely develop spontaneous activity although they do occasionally develop mechanosensitivity.[2,4] Since the axolemmal distribution of sodium channels largely determines the regions of electrical excitability in normal axons, an altered distribution or quantity of such channels is a likely cause of ectopic impulse generation in injured axons.[5-8]

Besides the immunologic evidence supporting abnormal accumulation of sodium channels within neuromas, pharmacological and mathematical models support this concept. Local anesthetics such as lidocaine and mexiletine, which selectively block sodium channels, have been studied in animals and humans with peripheral nerve injury. In humans with neuromas, pain can be decreased by local infiltration of lidocaine into the subcutaneous tissues surrounding the neuroma.[28] In rats with experimental neuromas, intravenous infusion of both lidocaine and mexiletine can abolish completely the spontaneous afferent activity arising within neuromas without blocking nerve conduction itself.[29] Mexiletine given orally to humans can decrease pain associated with peripheral nerve injury.[30] Matzner and Devor showed that the sodium channel blockers tetrodotoxin and lidocaine stop neuroma firing by suppressing the process of impulse initiation without blocking impulse propagation. In contrast, veratridine, which increases sodium conductance, accelerates ectopic firing. Calcium channel blockers have no significant effect on ectopic impulse generation.[31] Taken together, these pharmacological studies provide strong evidence that the generator potential associated

with ectopic neuroma firing sites is encoded into an impulse train by a process that depends on voltage-sensitive sodium channels. Mathematical models suggest that excess membrane sodium conductance plays a major role in promoting axonal hyperexcitability. The Hodgkin-Huxley equation was used to predict the effects of altering maximal sodium conductance ($g_{Na+max}$) on the process of repetitive neuronal firing[32]. This model shows that increasing $g_{Na+max}$ ,without changing any other membrane parameter, decreases the threshold current necessary to evoke repetitive firing. This change in membrane properties renders the membrane hyperexcitable. Although changes in other membrane properties may occur in the axons within neuromas, these data indicate that accumulation of excess sodium channels is sufficient to cause ectopic axonal hyperexcitability.

The accumulation of sodium channels within injured axons may be a feature common to all varieties of peripheral nerve trauma, especially those which give rise to neuromas. It is likely to be a major cause of ectopic axonal hyperexcitability. When injured sensory fibers develop hyperexcitability, the perception of pain and paresthesias likely occurs;[33] however, the entire explanation for neuroma-associated pain is, undoubtedly, more complicated than this. The membrane remodeling that allows a redistribution of sodium channels probably causes changes in other membrane-associated proteins as well. In particular, other ion channels may undergo changes in distribution, quantity, or function. If alterations of voltage-sensitive potassium channels or calcium channels occur, axonal membrane electrical properties could be affected in a complex manner. Peripheral nerve injury should also trigger changes in the central nervous system such as postsynaptic amplification of afferent barrages and central sensitization, in which normally nonpainful afferent input is perceived as painful.[34-37] These

other factors notwithstanding, further investigation of ion channel distribution and function within damaged axons should provide a better understanding of the basis for the abnormal electrical excitability that frequently develops after peripheral nerve trauma. Modification of ion channel distribution or function may prove a particularly fruitful approach to the treatment of pain in diseases of the peripheral nervous system.

England

## References


1. Sunderland S. Consequences of disruption of the endoneurium and perineurium. Neuroma formation. Fibre interaction and the artificial synapse. In: Sunderland S. Nerves and nerve injuries. 2nd ed. Edinburgh: Churchill Livingstone, 1978:188-200.
2. Wall PD, Gutnick M. Properties of afferent nerve impulses originating from a neuroma. Nature 1974;248:740-743.
3. Govrin-Lippmann R, Devor M. Ongoing activity in severed nerves: source and variation with time. Brain Res 1978;159:406-410.
4. Scadding JW. Development of ongoing activity, mechanosensitivity, and adrenaline sensitivity in severed peripheral nerve axons. Exp Neurol 1981;73:345-364.
5. Devor M, Lomazov P, Matzner O. Sodium channel accumulation in injured axons as a substrate for neuropathic pain. In: Boivie J, Hansson P, Lindblom U, eds. Touch, temperature, and pain in health and disease: mechanisms and assessments, progress in pain research and management. vol 3. Seattle: IASP Press, 1994:207-230.
6. Devor M, Keller CH, Deerinck TJ, Levinson SR, Ellisman MH. $Na^+$ channel accumulation on axolemma of afferent endings in nerve end neuromas in Apteronotus. Neurosci Lett 1989;102:149-154.
7. Devor M, Govrin-Lippmann R, Angelides K. $Na^+$ channel immunolocalization in peripheral mammalian axons and changes following nerve injury and neuroma formation. J Neurosci 1993;13(5):1976-1992.

8. England JD, Gamboni F, Ferguson MA, Levinson SR. Sodium channels accumulate at the tips of injured axons. Muscle Nerve 1994;17:593-598.

9. Vassilev PM, Scheuer T, Catterall WA. Identification of an intracellular peptide segment involved in sodium channel inactivation. Science 1988;241:1658-1661.

10. England JD, Gamboni F, Levinson SR. Increased numbers of sodium channels form along demyelinated axons. Brain Res 1991;548:334-337.

11. Dugandzija-Novakovic S, Koszowski AG, Levinson SR, Shrager P. Clustering of $Na^+$ channels and node of Ranvier formation in remyelinating axons. J Neurosci 1995;15:492-503.

12. England JD, Gamboni F, Levinson SR, Finger TE. Changed distribution of sodium channels along demyelinated axons. Proc Natl Acad Sci 1990;87:6777-6780.

13. England JD, Levinson SR, Shrager P. Immunocytochemical investigations of sodium channels along nodal and internodal portions of demyelinated axons. Microscopy Research Technique In press.

14. Chiu SY. Asymmetry currents in the mammalian myelinated nerve. J Physiol 1980;309:499-519.

15. Chiu SY. Sodium and potassium currents in acutely demyelinated internodes of rabbit sciatic nerves. J Physiol 1987;391:631-649.

16. Neumcke B, Stampfli R. Sodium currents and sodium-current fluctuations in the rat myelinated nerve fibers. J Physiol 1982;329:163-184.

England

17. Ritchie JM, Rogart RB. Density of sodium channels in mammalian myelinated nerve fibers and nature of the axonal membrane under the myelin sheath. Proc Natl Acad Sci 1977;74:211-215.

18. Shrager P. Sodium channels in single demyelinated mammalian axons. Brain Res 1989;483:149-154.

19. Waxman SG, Ritchie JM. Molecular dissection of the myelinated axon. Ann Neurol 1993;33:121-136.

20. Ellisman MH, Levinson SR. Immunocytochemical localization of sodium channel distributions in the excitable membranes of Electrophorus electricus. Proc Natl Acad Sci 1982;79:6707-6711.

21. Thornhill WB, Levinson SR. Biosynthesis of electroplax sodium channels in Electrophorus electrocytes and Xenopus oocytes. Biochemistry 1987;26:4381-4388.

22. Brismar T, Gilly WF. Synthesis of sodium channels in the cell bodies of squid giant axons. Proc Natl Acad Sci 1987;84:1459-1463.

23. Lombet A, Laduron P, Mourre C, Jacomet Y, Lazdunski M. Axonal transport of the voltage-dependent $Na^+$ channel protein identified by its tetrodotoxin binding site in rat sciatic nerves. Brain Res 1985;345:153-158.

24. Devor M, Govrin- Lippmann R. Axoplasmic transport block reduces ectopic impulse generation in injured peripheral nerves. Pain 1983;16:73-85.

25. Black JA, Felts P, Smith KJ, Kocsis JD, Waxman SG. Distribution of sodium channels in chronically demyelinated spinal cord axons: immuno-ultrastructural localization and electrophysiological observations. Brain Res 1991;544:59-70.

England

26. Chabal C. Membrane stabilizing agents and experimental neuromas. In: Fields HL, Liebeskind, JC, eds. Progress in pain research and management. Vol 1. Seattle:IASP Press, 1994:205-210.

27. Koschorke GM, Meyer RA, Tillman DB, Campbell JN. Ectopic excitability of injured nerves in monkeys: entrained responses to vibratory stimuli. J Neurophysiol 1991;65:693-701.

28. Chabal C, Jacobson L, Russell LC, Burchiel KJ. Pain responses to perineuromal injection of normal saline, gallamine, and lidocaine in humans. Pain 1989;36:321-325.

29. Chabal C, Russell LC, Burchiel KJ. The effect of intravenous lidocaine, tocainide, and mexiletine on spontaneously active fibers originating in rat sciatic neuromas. Pain 1989;38:333-338.

30. Chabal C, Jacobson L, Mariano A, Chaney E, Britell CW. The use of mexiletine for the treatment of pain after peripheral nerve injury. Anesthesiology 1992;76:513-517.

31. Matzner O, Devor M. Hyperexcitability at sites of nerve injury depends on voltage-sensitive $Na^+$ channels. J Neurophysiol 1994;72:349-359.

32. Matzner O, Devor M. $Na^+$ conductance and the threshold for repetitive neuronal firing. Brain Res 1992;597:92-98.

33. Nordin M, Nystrom B, Wallin U, Hagbarth K-E. Ectopic sensory discharges and paresthesias in patients with disorders of peripheral nerves, dorsal roots and dorsal columns. Pain 1984;20:231-245.

34. Campbell JN, Raja SN, Meyer RA, MacKinnon SE. Myelinated afferents signal the hyperalgesia associated with nerve injury. Pain 1988;32:89-94.

England

35. Cook AJ, Woolf CJ, Wall PD, McMahon SB. Dynamic receptive field plasticity in rat spinal cord dorsal horn following C-primary afferent input. Nature 1987;325:151-153.

36. Gracely RH, Lynch SA, Bennett GJ. Painful neuropathy: altered central processing maintained dynamically by peripheral input. Pain 1992;51:175-194.

37. Sheen K, Chung JM. Signs of neuropathic pain depend on signals from injured nerve fibers in a rat model. Brain Res 1993;610:62-68.

England

**Table. Sodium channel density and painfulness of neuromas.**

| Patient | Specimen | [Na Ch] | Pain |
|---|---|---|---|
| 1. | C5 neuroma | 23.5 | + |
| 2. | Normal nerve | 23.7 | - |
| 3. | Middle trunk neuroma | 25.8 | + |
| 4. | C5-upper trunk neuroma | 26.3 | + |
| 5. | Femoral neuroma | 28.6 | + |
| | Normal nerve | 9.6 | - |
| 6. | Upper trunk neuroma | 30.1 | + |
| 7. | Axillary neuroma | 30.6 | + |
| 8. | C6 neuroma | 31.0 | + |
| 9. | C5 neuroma | 31.0 | ++ |
| 10. | C7 neuroma | 31.2 | + |
| 11. | Superficial radial neuroma | 32.7 | ++ |
| 12. | Brachial plexus neuroma | 32.9 | +++ |
| 13. | Medial cord neuroma | 48.3 | ++ |
| | Normal nerve | 20.4 | - |
| 14. | Sural neuroma | 48.3 | +++ |
| 15. | Sciatic neuroma (d) | 67.2 | ++++ |
| | Sciatic neuroma (p) | 25.4 | ++++ |
| | Normal nerve | 16.2 | - |
| 16. | Sciatic neuroma | 74.2 | + |
| | Normal nerve | 20.1 | - |

| | |
|---|---|
| [Na Ch] | Sodium channel density in pM per g wet weight |
| (d) | distal segment |
| (p) | proximal segment |
| - | no pain |
| + | mild pain |
| ++ | moderate pain |
| +++ | severe pain |
| ++++ | very severe pain |

Figure 1a

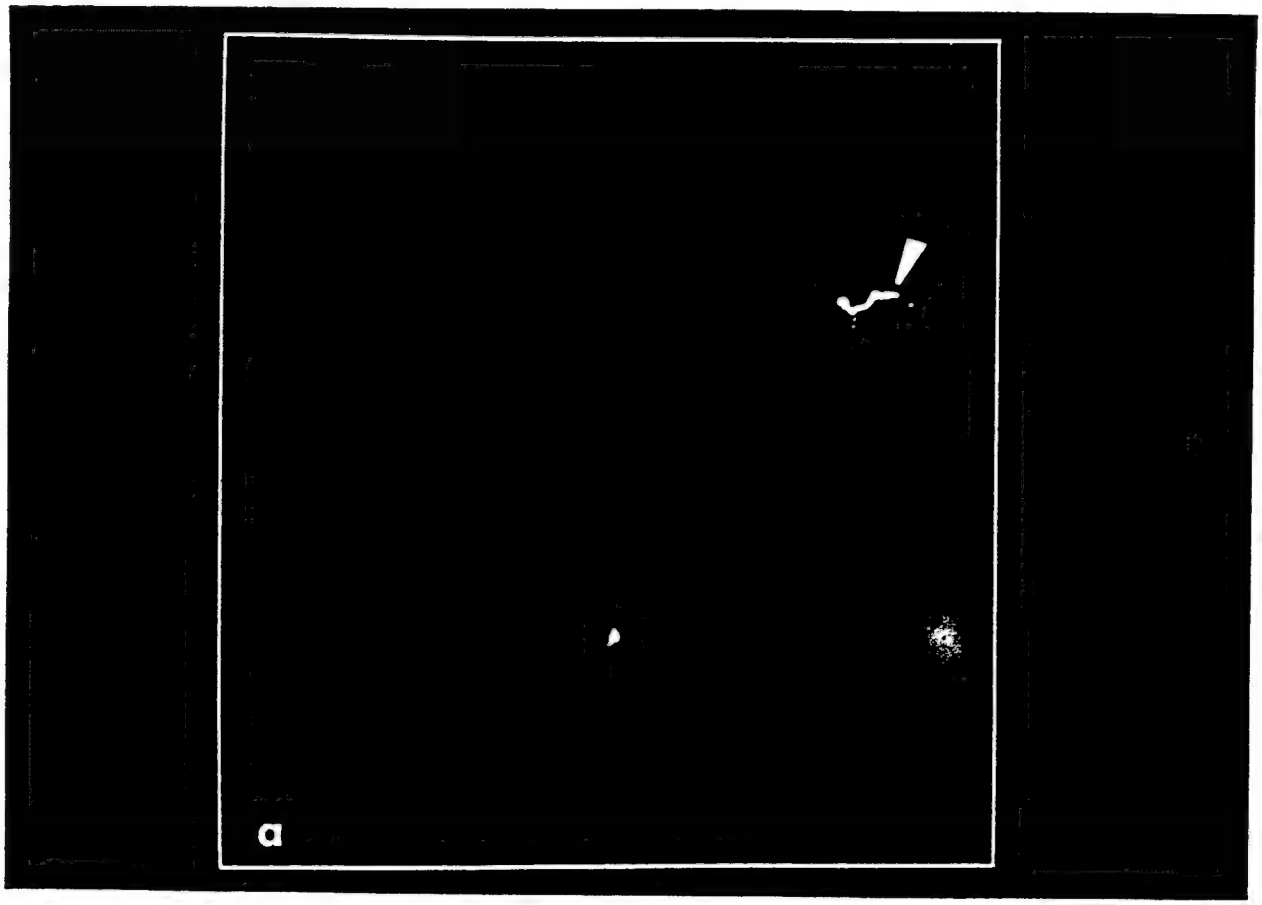

Figure 1b

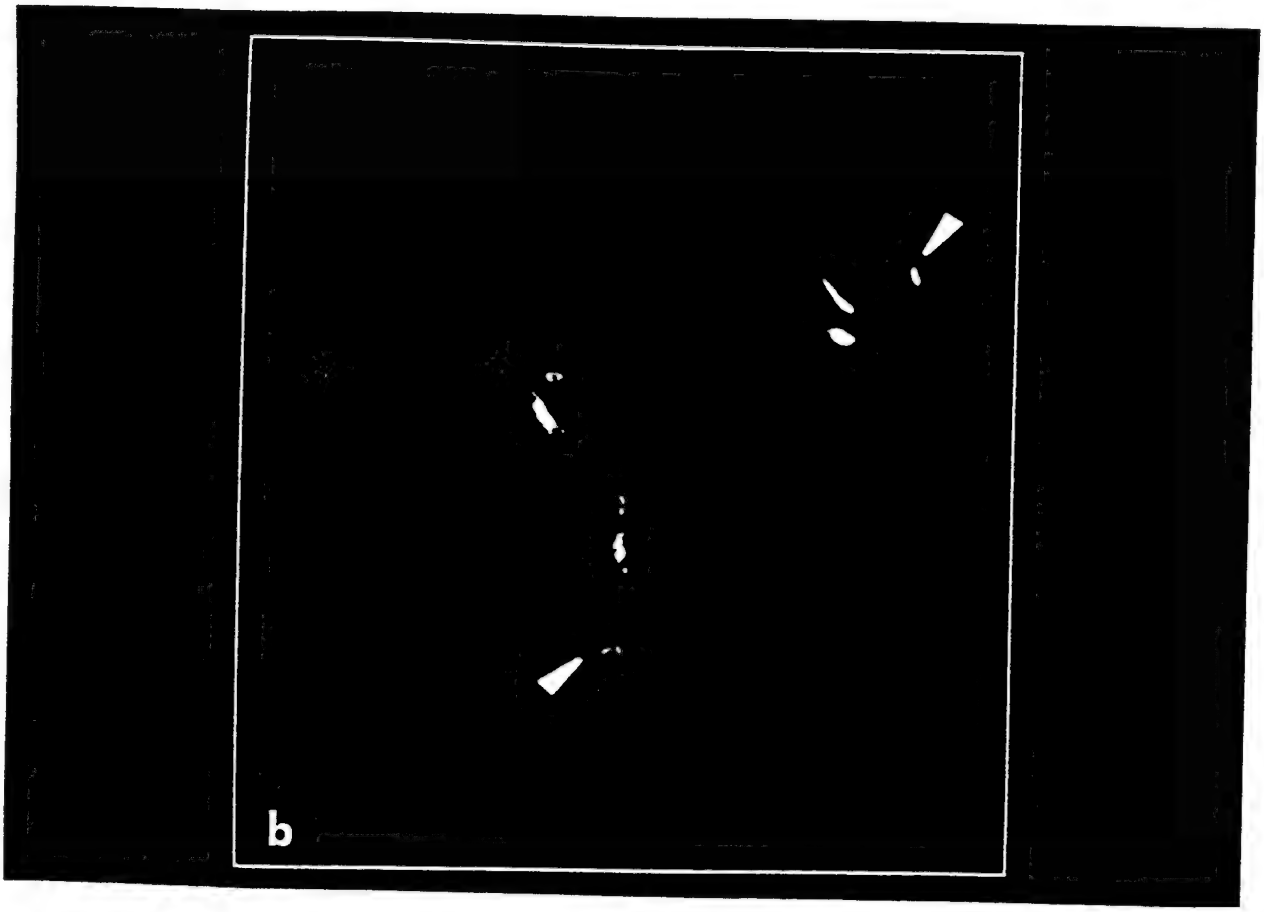

Figure 1c

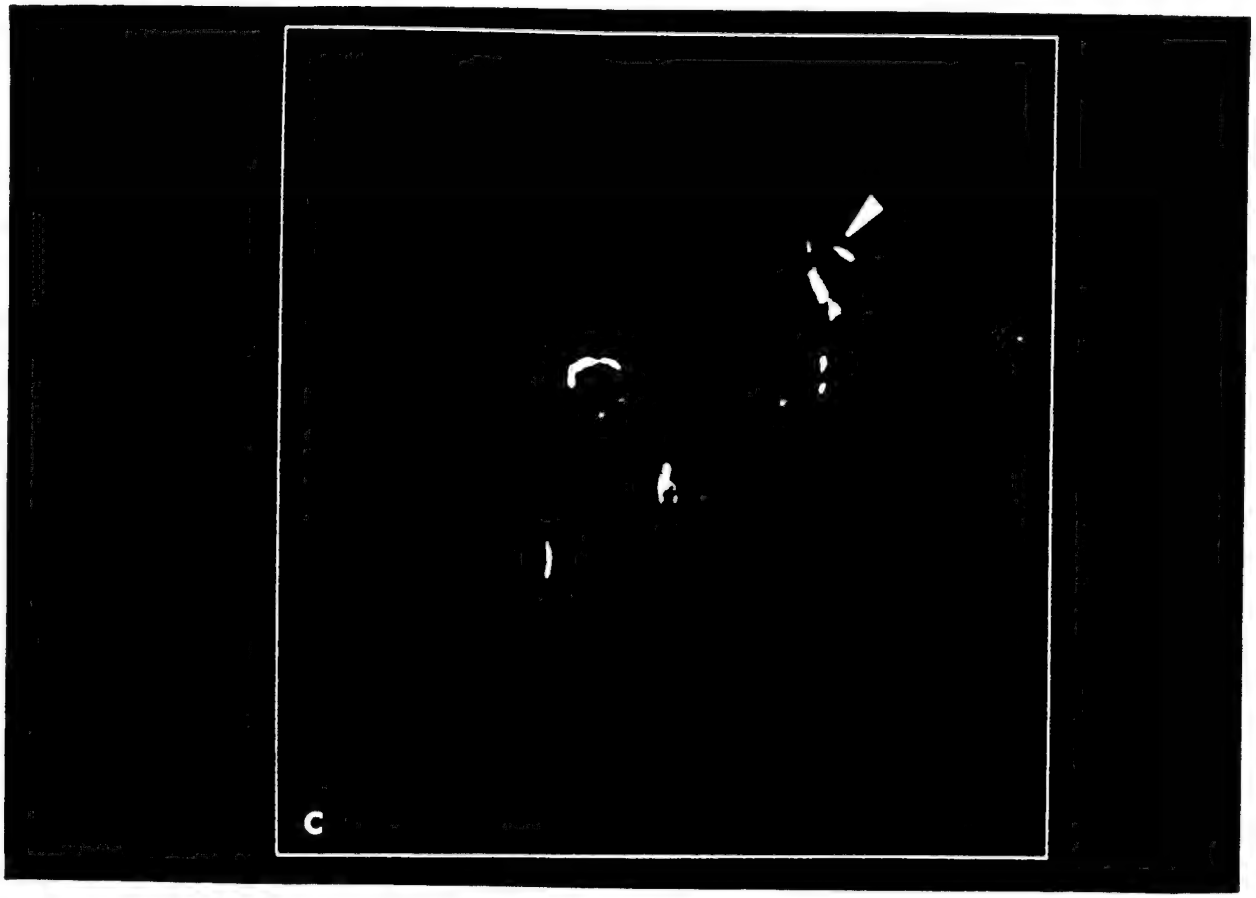

Figure 1d

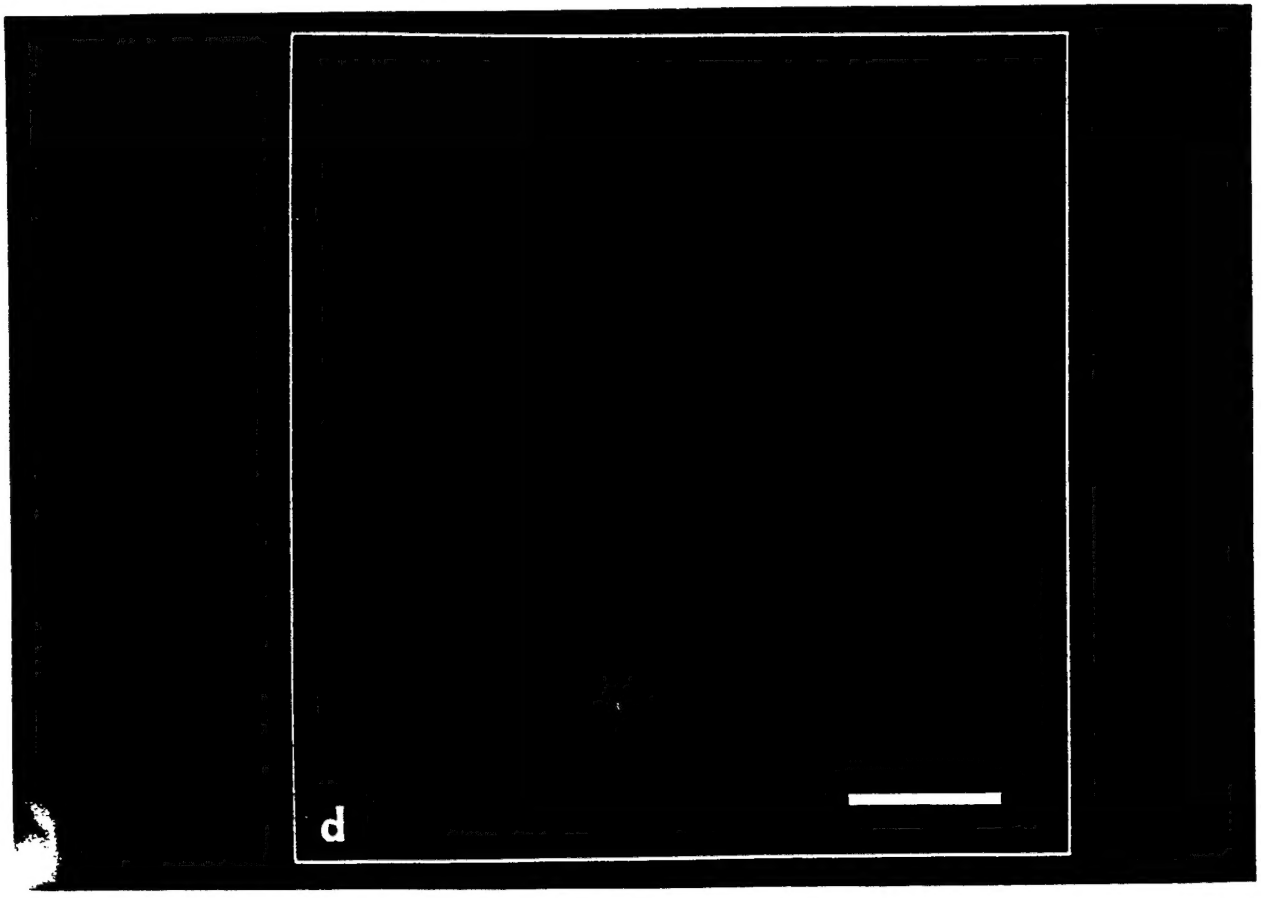

Figure 2

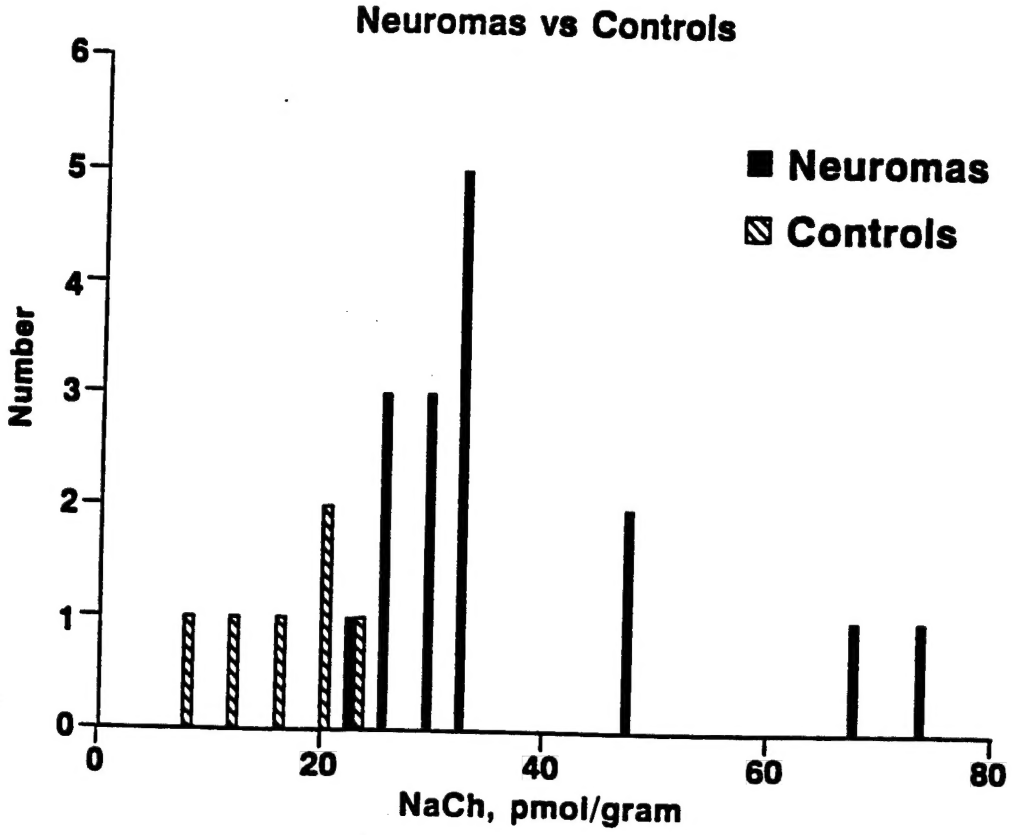
Neuromas vs Controls
Neuromas
Controls
Number
0
1
2
3
4
5
6
0
20
40
60
80
NaCh, pmol/gram

## Legends for Illustrations

**Figure 1.** Sodium channel immunocytochemistry of neuromas. There are distinct segments of sodium channel-specific immunoreactivity throughout the axons of these neuromas (panels a, b, c). Note also the intense immunoreactivity which is present in several axonal tips (arrowheads). Panel d is a control showing the nonspecific immunofluorescence which occurs when the primary anti-sodium channel antibody is preblocked with peptide. Scale bar = 10 μm.

**Figure 2.** Frequency histogram of the sodium channel density in neuromas and control nerves. Note that the neuromas, as a group, have a significantly greater concentration of sodium channels as compared to the control nerves.

## PUBLICATIONS

Zhang DM, Beuerman RW, Zhao S, Tran H, Kline D, Gould H: Cellular factors involved in neuroma formation. Soc Neurosci 21:1798, 1995.

Zhao S, Zhang D, Kline DG, Beuerman RW, Ma Q, Tran H: Increase in basic fibroblast growth factor and fibroblast growth factor receptor-1 following sciatic nerve injury and neuroma formation. Soc Neurosci 21:497, 1995.

Ma Q, Beuerman RW, Zhao S, Pedroza L, Tran H, Nguyen D, Kline D: Immunolocalization and quantitation of fibroblast growth factor receptor-1 in the human peripheral neuroma. Soc Neurosci 21:2050, 1995.

Beuerman R, Zhao S, Tran H, Ma Q, Kim D, Kline D: Epidermal growth factor and fibroblast growth factor in human neuroma tissue. Soc Neurosci 20:663, 1994.

Zhao S, Beuerman RW, Kim DH, Zhang D, Kline DG: Neuroma formation and fate of the Schwann cells in the constriction of sciatic nerve and homograft nerve repair. Soc Neurosci 20:707, 1995.

Beuerman RW, Kline DG: Growth factor in the human neuroma. Sunderland Society Meeting, Zurich, Switzerland, June 1995.